NOTICE

The quality of this microform is heavily dependent upon the quality of the original thesis submitted for microfilming. Every effort has been made to ensure the highest quality of reproduction possible.

If pages are missing, contact the university which granted the degree.

Some pages may have indistinct print especially if the original pages were typed with a poor typewriter ribbon or if the university sent us an inferior photocopy.

Reproduction in full or in part of this microform is governed by the Canadian Copyright Act, R.S.C. 1970, c. C-30, and subsequent amendments.

AVIS

La qualité de cette microforme dépend grandement de la qualité de la thèse soumise au microfilmage. Nous avons tout fait pour assurer une qualité supérieure de reproduction.

S'il manque des pages, veuillez communiquer avec l'université qui a conféré le grade.

La qualité d'impression de certaines pages peut laisser à désirer, surtout si les pages originales ont été dactylographiées à l'aide d'un ruban usé ou si l'université nous a fait parvenir une photocopie de qualité inférieure.

La reproduction, même partielle, de cette microforme est soumise à la Loi canadienne sur le droit d'auteur, SRC 1970, c. C-30, et ses amendements subséquents.

Canada

Computed Torque Control of a Differentially Driven Automated Guided Vehicle

Nael Barakat

A Thesis

in

The Department

of

Mechanical Engineering

Presented in Partial Fulfilment of the Requirements

for the Degree of Master of Applied Science at

Concordia University

Montreal, Quebec, Canada

January 1996

ISBN 0-612-10823-6

ABSTRACT

Computed Torque Control of a Differentially

Driven Automated Guided Vehicle

Nael A. Barakat

This thesis studies the need and applicability of the Computed Torque Control (CTC) scheme for Automated Guided Vehicles (AGVs). Computed Torque Control has been dealt with extensively in the literature for stationary robot arms. An inverse dynamic model of the electro-mechanical system is needed to implement the CTC scheme. In this thesis it is demonstrated that such a model exists for a differentially driven vehicle. Modelling, simulation and experimental studies have been carried out for the differentially driven CONCIC II AGV. A motor-test-rig consisting of a motor has been designed and developed to study the suitability of the CTC scheme for electro-mechanical systems.

The forward and inverse dynamic models of the AGV and the motor-test-rig have been developed to design the CTC scheme for the systems mentioned above. The AGV and the motor-test-rig are tested in the presence of significant changes in the dynamics of the vehicle and operating environment while operating under the influence of the CTC scheme and a kinematics-based Velocity Control (VC) scheme. Both control schemes operate in the cartesian level.

Experimental results for the test rig show that the CTC scheme offers the desired response compared to a velocity control scheme. Simulation studies carried out using the dynamic model of the CONCIC II AGV illustrate that the CTC scheme performs well in the

presence of changes in the dynamic parameters of the vehicle and the operating environment without having to change the filter gains and / or the acceleration values.

Experimental results using the prototype CONCIC II AGV illustrate that the vehicle maintains the desired velocity while climbing a ramp while the velocity control scheme fails to achieve the same.

بسم الله الرحمن الرحيم

To My Parents

Acknowledgment

I would like to extend my sincere gratitude and appreciation to my thesis supervisor Dr. Ramesh Rajagopalan for his time, effort, insightful guidance, and moral and financial support throughout the course of this research. Thanks are due also to Dr. R.M.H. Cheng, Director, Centre for Industrial Control (CIC), for his help, useful suggestions, and guidance to achieve this work. I extend my thanks to him for providing a prototype vehicle to carry out tests.

Thanks and gratitude are also due to Mr. Gilles Huard for constructing the electronics part of the projects and for his technical and moral support; Mr. Michael Oligario for his time and contribution in developing and carrying out experimental work on the vehicle and the data acquisition system; my colleagues and the staff in CIC, for the constructive discussions and for making my stay at Concordia University pleasant and useful; the technical staff in the machine shop for their efforts in building the experimental motor-test-rig, and Concordia security staff for allowing us to use the building space to carry out experimental work during the holiday period.

This work was made possible with the financial assistance of FCAR Master degree scholarship awarded to me for the summer of 1995 and the NSERC research grant (RA20N445) and FRDP grant (RO-20-I891) both awarded to my supervisor Dr. Rajagopalan.

Finally, I would like to thank my family, especially my sister, my friends, Mr. Belgaid Abdulhamid, the Hammad brothers, Mr. Altai Wihel, the Qashoa family for their time and support in all forms.

Last but not least, the author wishes to aknowledge the contribution of the past and the present faculty, staff and students whose work at the centre has directly or indirectly contributed to this thesis.

Table of Contents

List of Figures

List of Tables

Nomenclature

$\beta_{f,r}$ The directional angle of the side friction forces at the castors (angle between the side friction force at the castor and the longitudinal axis of the AGV)

$\delta_{f,r}$ The directional angle of rolling resistance at the castors (angle between castor travel and the longitudinal axis of the AGV)

θ_r The rotational angle of the vehicle about its centre of mass which coicides with the geometric centre.

$\dot{\theta}$ motor speed in revolution per second (rev/s)

$\ddot{\theta}$ motor acceleration in revolution per second per second (rev/s^2)

Ω_z Angular velocity of the AGV around the Z-axis

$\dot{\Omega}_Z$ AGV angular acceleration about the Z-axis

ω_{x1}, ω_{x2} The speed of left and right driving wheels respectively.

a_y Acceleration of the AGV in the Y - axis

g acceleration of gravity

k_1, k_2 Coefficient of rolling resistance of the driving wheels

$k_{p,i,d}$ Proportional, Integral, and derivative gains for the PID filter

m Total mass of the vehicle

n Gear ratio at the driving motor

r_d Driving wheel radius

D Viscous Damping Constant of the Driving Motor (Nms/red)

DAC Digital to Analog Convertor

F_{ij}	External Forces of the AGV, Where	i = 1 for left motorized wheel
		i = 2 for right motorized wheel
		i = f for front castor
		i = r for rear castor
		j = t for tractive forces
		j = f for rolling resistance
		j = c for cornering forces
		j = n for side-friction forces
F'_{ij}	Reaction Forces from castors	i = f for frot castor
		i = r for rear castor
		j = x for the vector along the X-axis
		j = y for the vector along the Y-axis

F_y The force acting in the Y - axis

I_z Moment of inertia of the AGV about the Z-axis

I_1, I_2 Current of the left and right motors respectively

$J_{1,2}$ Jacobian matrices

J_m motor inertia (Nms^2)

K_{DAC} Gain of the DAC

K_e Voltage constant of the motor or the motor speed constant

K_t Torque constant of the driving motor

L Wheel Span of the CONCIC II AGV

L_1, L_2 One half of the wheel span.

L_{ae} Effective wheel base

M_z Moment around the Z-axiz of the AGV

N Normal reaction

N_d Normal reaction at the wheels

R Electric resistance of the driving motor

R_d Radius of Curvature of the track

R^2 the accuracy of the fitted curve in relation to the data points used

T_f Friction torque of the motor

T_l Torque of the load on the motor (Nm)

T_m Torque generated by the motor

V_{rx} The forward linear velocity of the vehicle.

Vy The forward velocity along the Y-axis

$\dot{V}_y$ The linear acceleration of the AGV = a_y

CHAPTER 1 INTRODUCTION

1.1 Introduction

Global competition among modern industries has focused attention on the development of cost-effective and intelligent methods of production. These methods have to increase productivity while remaining rapid and responsive to market changes. To most industries, a distinct concern in this competition is to reduce operating cost. Material handling contributes to a great extent to this cost, whether it is in warehousing, assembly or component manufacturing. Other industrial concerns include factors such as labour cost reduction and productivity improvement. These factors have directed industries to automate material handling stages as part of the full automation process. Automation proved to be a successful solution and therefore, Automated Guided Vehicles (AGVs) came into the picture. AGVs are defined as " *driverless transportation systems capable of intelligent motion and actions while allowing a great deal of maneuverability* [1] ". The use of AGVs provides many industrial benefits. Examples of which are the greater routing flexibility, less product damage and the ability to operate in hazardous environments.

AGVs are part of the electro-mechanical systems domain. AGVs are also referred in the literature as wheeled mobile robots [1]. To achieve the desired function, robots and AGVs require a control scheme to carry out their assigned tasks. The control scheme is chosen based on different criteria. Some of which are their ability to reduce trajectory tracking error and ease in computational burden. Researchers have been investigating a variety of control schemes for robots. Making a stationary robot arm or an AGV perform

a certain task or motion in the working space as close to the desired one as possible, following a certain trajectory and overcoming different types of disturbance, is the issue that directs research in developing control methods for robot manipulators and AGVs. Manipulator joints and AGV wheels are powered by actuators which output a torque or force at the joints or point of contact of wheels. This requires a control system to compute appropriate actuator commands which will achieve the desired motion. There are two types of control schemes, cartesian control and low level servo control. The former is to position the vehicle or the end effector along the desired trajectory. The later is to assure accurate trajectory tracking at the joint or motor level.

Conventional schemes for controlling electro mechanical systems are mostly based on the kinematics of the system. These schemes perform well in situations where no significant real-time changes in dynamics of the system are encountered [1-4]. They might also perform well at very low operating speeds [3]. The dynamic parameters that change in real-time depend on the type of the vehicle or robot, the operating speed and the task carried out by it. For Automated Guided Vehicles (AGVs) used in industrial environments to transport materials from machine to machine or from the warehouse to the shop and vice versa, the dynamic parameter that need to be considered mostly is the payload change or distribution. The vehicle acceleration has to be adjusted according to changes in the payload. For instance, if vehicles with zero payload to full payload travel with the same set of gains and acceleration settings, the tracking performance will deteriorate [2]. In this respect, one may have to modify either the acceleration or the gains. The acceleration of the vehicle can be controlled by limiting the current for less payloads and more for full payload. In order to

carry out this, the mass change need to be sensed with the help of load cells located in each wheel [4]. Further, while climbing slopes more current is needed to overcome the gravitational effects. This can be accomplished by either providing the slope information and its location to the vehicle ahead of time or measuring the slope in real-time using an instrument such as an inclinometer. In these two situations, an inverse dynamic model of the vehicular system is needed to compute the current requirement by taking into account the changes in payload and/or gradient. For automated vehicles operating outdoor, the dynamic parameters that affect the performance of the vehicle in road following are:

- Payload increase or decrease.
- Distribution of the payload.
- Lane changing.
- Negotiating a road with curved and straight segments.
- Going uphill or downhill.
- Terrain characteristics (coefficient of friction between the terrain and the wheels).

In order to account for these changes in the operating environment and / or condition of the vehicle a control scheme is needed to compute the actuators (motors) torque required. This scheme includes the inverse dynamic model of the system, and is called the "Computed Torque Control" in the literature. Computed Torque Control (CTC) for stationary robot arms has been the subject of interest for nearly 15 years, and more recently extensive experimental studies have been reported [5-9]. Implementing a model based controller highlights the need for accurate control of joint torque, accurate joint position and velocity sensing [10]. It has

been reported in the literature that there is a significant reduction in the trajectory tracking errors as the dynamics are included in the control loop [11]. There is ample material in the literature on CTC scheme for robot arms and the same is not true for the automated vehicles [1, 2].

1.2 AGVs Vs Robots

Robots can be divided into two different categories. This division is based upon the structure, design and modelling of the robot. The first category includes conventional stationary robot arms / manipulators. These are open-chain mechanisms. The second category includes AGVs which are closed chain mechanisms [12, 13]. This makes the modelling and control of AGVs different from that of robots. As a main difference, in the case of stationary robot manipulators the friction force is almost neglected compared to inertial and gravitational forces and torques. Whereas in the case of wheeled mobile robots friction dissipates the majority of the energy produced by the actuator. This is due to the fact that in the absence of frictional force, slippage would result.

Another essential difference is that all stationary manipulator joints are lower - pairs which allow surface contact. On the other hand, AGVs have higher pairs which allow only line / point contacts. Although the tires make surface contact due to deformation in the case of rubber tires, AGVs normally employ moulded rubber tires which undergo little or no deformation. To control the motion of an open chain mechanism all joints have to be actuated and sensed, while for closed chains mechanisms some of the joints can be left unactuated and unsensed [1, 3].

Dynamic modelling of stationary robots or open-chain mechanisms can be achieved using the Newton-Euler iterative method or the Lagrangians energy method. On the other hand, these methods are not suitable for closed-chain robots or higher pair mechanisms. The difficulty in using these methods arises from the fact that they are recursive in procedure while dynamics of mobile robots need to be computed in parallel. Further, in Newton - Euler or Lagrange methods the friction forces are not accounted for. Frictional forces are added separately to the actuator torque expression. Moreover, both methods can not account for dry friction resulting from unactuated or unsensed joints. For these reasons, the conventional methods of modelling the dynamics of robot arms can not be applied to model AGVs [1].

1.3 History and Background of AGVs

The common characteristics of AGVs are the following : they are driverless, battery powered and automatically guided. Beyond these characteristics AGVs have substantial variations in their functions, forms, and their control scheme. Guidance systems can also be a basis for differences among AGVs.

AGVs were first introduced in the 1950s. One of the first AGVs was developed in the USA in 1954 [1]. The controller of this vehicle was based on vacuum tubes technology. In the decade that followed and with the advancement of electronics, controllers were built using the transistor technology. Later in the 1970s integrated circuits came into the picture and following that microprocessors were incorporated into the controllers. Software used with microprocessors made the vehicles integration into manufacturing environment easier

and led to the concept of work cells. Later on, enhanced system control options were made possible by using advanced control capabilities such as real-time communication and performance monitoring and correction. Nowadays, hybrids of AGVs with robots are developed for Flexible Manufacturing Systems and employed in electronic industries [1, 3, 14].

1.4 Applications of AGVs

AGVs can be found in a wide range of applications. Material handling in industrial shop floors is a typical application where AGVs transport components from one machine to the other, from the warehouse to the shop floor and vice versa. This forms an important part of the automation process. AGVs increase the flexibility of the factory in general. In assembly lines AGVs introduce a safer and higher job quality compared to conventional means like manually operated fork lift trucks. Drastic increase in the uptime is achieved by AGVs since they allow assembly lines to work in parallel. In addition to parts handling, AGVs are used in the automotive industry in motor assembly, body assembly, welding stations and painting. Clean environment operations which is a requirement in the electronics industry need effective transportation means as AGVs. Many other industries are increasingly using AGVs like aerospace, paper, textile and pharmaceuticals [1].

In the literature faster AGVs are called Automated Transit Vehicles or Autonomous Transit Vehicles (ATVs). A mathematical relation is provided by Mehrabi [3] to distinguishes these vehicles from AGVs based on the characteristics of the vehicular system and the speed of operation. Automated Transit Vehicles (ATVs) find applications in the

development of an Intelligent Vehicle Highway System (IVHS) also known as the Intelligent Transport Systems (ITS) [4], which aims at developing vehicles that can function autonomously in structured and unstructured environments with the help of intelligent guidance systems and control schemes. This would alleviate the problem of traffic congestion on heavily travelled highways, if adaptive cruising and steering is provided [1, 2, 4, 15]. In environments other than industry, AGVs can be useful and effective. Examples include mail distribution and handling between offices, assisting in hospitals supplies transfer, and agricultural environments. Moreover, AGVs can be used as intelligent means of transportation for the disabled. To enhance the AGV and allow it to perform the required application, it can be fitted with extra fixtures. Examples of these fixtures are robotic arms and cranes. Many scientific applications employ AGVs. Land exploration and underwater investigations are examples of this. In environments that are considered dangerous to human beings, AGVs stand as the best candidates to perform the task. Examples of which is nuclear and explosive material handling. It can also be used in space exploration and remote repair and maintenance on space laboratories or stations. With the rapid developments in AGVs and their capabilities, different markets are expected to open or expand.

1.5 Development of In-House AGVs

Many prototype AGVs have been developed in the Centre for Industrial Control (CIC), Department of Mechanical Engineering, at Concordia University. The first generation AGV was developed during the period 1983-1986 and designated as CONCIC I [16]. This vehicle has a tricycle configuration and is guided by a binary digitizing camera.

The controller includes three microprocessors executing specific operations. The second generation AGV was designed and developed during the period 1988-1991. It was designated as CONCIC II [1, 14]. This vehicle has a diamond shaped wheel-base with a differential wheel configuration comprising two driving wheels and a castor in the front as well as one in the back. The modular design of the vehicle offers flexibility in re-configuring the wheel-base. A binary digitizing camera is mounted on the front of the vehicle that feeds back the location of the vehicle relative to a track with suitable contrast prepared on the floor, ceiling or walls. The vehicle has many safety features including ultrasonic sensors for obstacle avoidance. CONCIC II is controlled by an on-board (80286-12) pc. The control scheme used to drive the vehicle is a conventional kinematic-based controller. CONCIC II is the AGV chosen to carry out the experimentation and development aspects of this thesis. The third generation of AGVs in CIC is designated as CONCIC III and was developed in 1993 [3]. This vehicle is equipped with two integral driving units in the front and also at the rear and has two castors on both sides of the geometric centre. This vehicle uses the dead-reckoning control scheme for guidance in conjunction with a dynamic model of the vehicle.

Dynamic modelling of the CONCIC II AGV has been derived by Huang [14]. Further, she developed a simulation package for the vehicle using its forward dynamic model.

Fourth generation AGV (known as ATV) has been built recently and is under testing. This vehicle is comparatively larger than the older generations and is expected to operate at higher speeds. The main testing that is being carried out on this vehicle is the

implementation of a CCD camera vision based guidance scheme and the C40 parallel processor based vehicle controller. The C40 is used to acquire and analyse the vision system inputs using a Charged Coupled Devices (CCD) camera and then to control and guide the vehicle. The development of these generations of vehicles has provided the necessary platforms for experimental research to back up theoretical development and simulation findings.

1.6 Control of AGVs

Different control schemes have been used or suggested to improve the performance of electro-mechanical systems in general and AGVs in particular. In order to ensure accurate track following of the AGV a control scheme need to be implemented. Most control schemes available are feedback control schemes in which the error happens first and the corrective action takes place after. A better control can be achieved by introducing a feed forward controller which works as a predictor. Some control schemes provided in the literature have investigated this concept for stationary robot arms [10]. Among which is the Computed Torque Control (CTC) scheme. CTC is a dynamics - model based control scheme. Nevertheless, the majority of electro-mechanical systems available in the market are controlled by kinematics based schemes. This is due to many reasons where part of which is the modelling related issues and computational burden in using dynamics based control schemes. The CTC scheme provides better control in the following situations [2, 4, 17, 18]:

1. When moving at high speeds in the case of Automated Transit Vehicles (ATVs).
2. For AGVs and ATVs when the load distribution changes. For example, AGVs

carrying a suspended load or with tanks with semi-filled liquids. When the vehicle negotiates a curve at a reasonable velocity, the shift in the load position will lead to side slip if the dynamics of the load are not taken into account in the control loop. One examples for this is the AGVs used in the General Motors factory in Oshawa Ontario. These AGVs carry assembled engines hanging from a hanger rigidly attached to the AGV. The side motion of the payload causes a disturbance to the AGV motion that can not be accommodated unless the velocity and acceleration of the AGV are reduced significantly.

3. In the presence of external disturbances and interactions with the environment, for example, when an AGV climbs a ramp or when loaded or unloaded while in motion.
4. In the case of lane changing.

1.7 Summary

This chapter discussed the history and background of AGVs as part of modern industry. It also presented the importance of AGVs in the process of industrial automation. Many applications of AGVs are presented in this Chapter. Higher productivity, uptime and flexibility are achieved by employing AGVs in industry. Other uses of AGVs are also identified. The differences between AGVs, ATVs and robot arms have been enumerated.

Control scheme for AGVs are mentioned in general and the need for the CTC scheme for AGVs is detailed in particular. A control scheme that can overcome tracking errors and assure the required performance of the vehicle is needed. Conventional control schemes that are kinematics-based perform well in dynamically stable environments or at low speeds.

Higher speeds of operation and changes in dynamic parameters require a feed forward dynamics based controller to achieve proper track following.

Development of AGV technologies in CIC is also summarized and the different generations are listed.

CHAPTER 2 LITERATURE REVIEW AND PROBLEM DEFINITION

2.1 Introduction

AGVs, which are also referred to as mobile robots in the literature, differ from robot manipulators in terms of the function that they perform and in their design. They are being used increasingly in different applications. Therefore, the choice of a control scheme suitable to run AGVs and achieve the desired performance is an important issue to researchers. Since AGVs also work in a dynamically changing environment, attention is directed by some researchers [2, 3] to use a dynamics-based scheme for control. Motivated by this, and the fact that introduction of dynamic terms to the control loop remarkably improves the system performance for robot manipulators as was reported by leahy [11], attention is focused on the Computed Torque Control (CTC) scheme [10]. The concept of CTC scheme is well established in the field of control of robot arms. This chapter introduces the literature available on the CTC scheme and identifies the need for such a control scheme for AGVs. Further, attention is focused on studying the suitability of these schemes for AGVs.

This chapter also presents a survey of the various kinematic and dynamic modelling techniques. The scope and objective of the thesis are explained in Section 2.4. A definition of the problem is given in this chapter in addition to a brief description of the thesis organization in Section 2.5.

2.2 Review of Control Schemes

A control scheme is necessary to achieve the desired performance of a robot manipulator or an AGV. Control schemes can be (I) at the higher level (Cartesian control); (ii) at the lower level (servo control). Cartesian level control can make use of the kinematics of the system and can also make use of the dynamics of the vehicle or robot. Both cartesian and servo level control can be designed to assure accurate (I) velocity or position control; (ii) current or torque control.

Trajectory planning is mostly performed in the joint space and not in the task space. This leads to ignoring the interaction between joints paths to produce a task path. In general, task space schemes have some advantages over joint space schemes. Task space planning schemes are more general in theoretical development. They are also easier in nature due to their direct interaction with the task planner, but computationally demanding as transformations have to be carried out between task and joint spaces. In addition they deal with the task performed by the robot by dealing directly with the task space and as reported by Tarn [19]. These schemes present a step towards intelligent control. Bejczy et al [7] tested the nonlinear feed back controller as one type of control schemes that interacts directly with the task planner. From the implementation point of view, different approaches are suggested in the literature to perform the task of structuring the accurate controller for robots. In order to achieve best tracking performance, a hierarchical control structure is used for AGVs and stationary manipulators. The hierarchical computer control can have different stages depending on the type of application. The overall control of the robot can be assigned to the host computer while at the joint level separate controllers are used [1,11,17]. This

decentralization of tasks reduces the cycle time and therefore improves the tracking performance of the robot or vehicle. In this same direction of structured control of robots, a study by Simmons [20] on Autonomous vehicles control concludes that structured control as task control architecture should be used for the robot to succeed in uncertain and dynamic environments.

Since the research community has spent considerable amount of time in developing a variety of control schemes for robot manipulators, the following paragraphs will focus on the summary of some of those schemes and their suitability for AGVs. In Section 2.2.2., discussion on the existing control schemes for AGVs is elaborated. A need for Computed Torque Control for AGVs is presented in Section 2.2.3.

2.2.1. Control Schemes for Robot Manipulators

The literature presents many control schemes to follow the desired trajectory or provide a precise contact between the robot arm and the environment. Some schemes provide compensation for the effect of dynamics on the tracking performance of the robot. Other schemes provide an adaptive approach to over come the changes in system dynamics and achieve proper trajectory tracking. Many ideas for trajectory tracking can be found in the literature [7, 11, 12, 17]. Some examples of control schemes implemented on robotic arms are listed by Craig [12]. Craig [12] presents the classical kinematics based control schemes, as well as, the basic hybrid control as a scheme to combine both position and force control in robot arms. This scheme had the problem of neglecting the dynamic coupling effects among individual robot axes [8]. Moreover, simultaneous position and force

precision control have been tested by Jankowsky et al [8]. A comparison between different controllers has been done by An et al [17] and by Bejczy et al [7]. Other examples of control schemes include passive compliance which has been used in the early stages of robotics employment in production lines [12]. Use of optimal control for robots can be found in the literature [3, 21].

A nonlinear feed back controller is reported in [7,19] in addition to a comparison of tracking performance among four different control schemes. Some researchers went into adaptive control investigation as a tool which offers better control over the robot motion [22].

Model based control schemes is a class of advanced control strategies. When applied to achieve proper trajectory tracking, these schemes are based on both the kinematic and dynamic models of the robot [23]. The Computed Torque Control (CTC) scheme belongs to this group of control schemes. In order to understand the properties of the CTC scheme a general idea about model based control schemes properties is presented here.

Model based control schemes are defined by Khosla [24] as the schemes which include the dynamic model of the manipulator to be controlled in their feed-back loop. These schemes could also include an inverse dynamic model in their feed forward loop.

Although the literature reports extensively on the modelling and simulation studies of CTC for robot arms, there have been few experimental evaluations of the performance of these controllers. Firstly, commercial robots do not allow the control of joint torque, which is required in many of the proposed controllers [11, 17]. Further, there are the problems such as high gear ratio as in the PUMA robot, substantial joint friction, limited computational

capabilities of the robot controller, and limited operating speed as in the case of the ASEA robot. Sahba et al [25] suggested the use of algorithms to reduce the torque controllers equations into sets of linear decoupled second - order systems with nonlinear state constraints.

The use of inverse dynamics models in the feed forward path of the control system is discussed in [2, 4, 8, 10]. Feed forward addition to the control loop by introducing inverse dynamics improves the performance of the robotic system [8]. The need for a dynamic model in the control loop and the discussion of the need for inverse dynamics in the feed forward part of the controller have been addressed widely in the literature [2, 8, 9, 26, 27, 28]. The problem of obtaining an inverse dynamics model is presented as an optimal control problem by some researchers as Hatawal et al. [21]. It has been reported in the literature that a model based control scheme outperforms a conventional kinematics based control scheme. The addition of inverse dynamics to the control loop works as a predictor for the controller. This will help the controller start with commands in the range of proper values of signals to what is really needed by the robot [7, 27, 29]. Experimental evaluations are reported in the literature to prove this fact [30].

An et al [17] used the MIT serial link direct drive arm for experimental comparison of various controllers. They observed that trajectory tracking errors decreased as more dynamic compensation terms were incorporated.

Leahy [11] demonstrated the feasibility of implementing a model based control law on the hierarchical control structure of existing industrial manipulators. Leahy work studies three critical issues :

1. The impact of stiffer PD loops on the performance of model based controllers with incomplete dynamic compensation in the feed forward loop.

2. The performance degradation produced by asynchronous calculation of feed forward and feed back compensation torques.

3. The PD loop gain payload adaption requirements.

Leahy concluded that a constant gain PD feed-back loop with torques from a feed forward compensation algorithm that modelled the full inertial dynamics, still outperforms conventional controllers and could be implemented on existing control structures without hardware modifications.

Uebel et al [31] introduced simpler forms of computed torque control scheme applied to industrial stationary robots. They also compared the proposed control scheme to a conventional PD controller and showed through simulation and experiments that the CTC scheme leads to an improved tracking performance [10].

Hashimoto [32] suggested a scheme employing sensors to measure the torque at the joints of the robot arm directly. Some research is directed into sensor development as reported by [32].

Bejczy et al [7] showed that the CTC is a special case of the nonlinear feed-back control scheme. Knowing that the later is a scheme which interacts directly with the task space (Cartesian space) instead of joint space and all its other properties one more advantage is added in favour of the CTC scheme.

CTC scheme application to the Puma 560 robotic manipulator has been addressed by Zhao Fujun [10]. He has also demonstrated the suitability of CTC for a motor-setup and

then for the Puma 560 robot manipulator [10].

2.2.2. Control schemes for AGVs

The objective of the AGV control is to assure accurate track following of the vehicle and ascertain that the vehicle reaches the destination within the stipulated travelling time.

Cartesian level feedback for AGVs is achieved with a variety of guidance schemes. Examples are wire guidance, optical means, infra red sensing, laser range finding and ultrasonic sensing. This feedback information is used to steer the vehicle in the proper direction and to reduce tracking errors to minimum. Feedback information from the wheel sensors (encoders or tachometers) is used in conjunction with a kinematic or dynamic model of the vehicle to compute the cartesian velocity and position of the vehicle. This information will then be used to achieve desired linear and angular velocities of the vehicle with the help of a cartesian controller.

A controller based on the vehicle dynamics can be used to achieve velocity and torque control. In order to control the torque output, an inverse dynamic model is needed. This model computes the wheel actuator torque based on the various dynamic parameters that influence the motion of the vehicle. These parameters can be payload change or distribution, lane changing, negotiating a curve of the track or going uphill or downhill. In this approach the control is performed to maintain the acceleration of the vehicle at the desired value instead of the velocity.

Most schemes of control for AGVs mentioned in the literature are kinematics based.

Examples of such control schemes currently implemented on AGVs are, the kinematics based controller used by Rajagopalan [1] and the dead reckoning method using the forward dynamics of the vehicle used by Mehrabi [3]. Further, commercial AGVs are mostly kinematically controlled [1, 3, 14, 33]. This means that they are controlled by wheel position or velocity only. This kind of controllers lacks the ability to overcome a sudden payload change or uphill movement in addition to all other kinds of dynamic changes the vehicle experiences while moving [2, 4]. The reason for using these kinematic control schemes as the literature reveals is due to the high nonlinearity, complexity, modelling assumptions and computational burden involved with forward and inverse dynamics models which are necessary when using any kind of a dynamic controller.

Studies of motion planning and feed back control of mobile robot systems from a control theory and stability point of view are presented by [3]. It is stated that mobile robot systems are controllable under normal working conditions [34]. Samson [35] concluded that in specific cases a set of smooth time varying feed backs can be used to stabilize a class of wheeled, mobile, car-like systems.

Applicability studies of CTC to AGVs are very scarce in the literature. The CTC scheme for AGVs deals with the power limitations that are imposed on the actuators and organizes the relation between the maximum velocity that can be obtained in relation to the torque required by the actuator [2, 4].

The great majority of researchers agree that a model based controller or a feed forward addition to the control loop of inverse dynamics improves the performance of the AGV dramatically [9, 26, 27]. Canudas et al [9] reported that a major limitation to

controlling an AGV kinematically and achieving the desired tracking accuracy is motor torque limitations. They suggested new constraints to monitor the motor torque limits when reached and replan the path. Sarkar et al [27] present an analysis of the control system stability, controllability and linearizability. They derive a non - linear feed back for wheeled mobile platforms that guarantees input - output stability and Lagrange stability for the overall system. They also investigate the importance of the choice of the output variables in the dynamic model of the system to be controlled.

The advantages of using the CTC scheme for AGVs are summarized by Rajagopalan et al [2, 4] as follows :

1. Performance of the controller is dramatically improved when moving at high speed or handling a heavy load, change of load, curves on the road, going uphill or changing a lane since the dynamics of the vehicle are incorporated in the controller design.
2. Dynamics prediction by introducing the inverse dynamics model to the feed forward path cancel the real time computation for the dynamic compensation and the controller regular delays.
3. Robustness of the controller is achieved for unexpected external disturbance.

It is suggested by Rajagopalan et al [2, 4] that when the CTC scheme is to be applied to autonomous vehicles it should involve the model - based scheme in addition to the use of sensors to provide real-time information on the dynamic changes of the vehicular system. This is to insure a better control and trajectory tracking

In conclusion, a model - based controller combined with feed back sensors of

position and / or velocity provides better performance compared to other kinematic based control schemes.

The concept of computed torque has also been discussed by Tzenov and Cheng [60]. They have addressed the computed torque principle from a dynamic analysis point of view. They have estimated how much torque is needed or should be distributed to utilize the available frictional resources of a multi-wheeled vehicle in a dynamically changing environment.

2.2.3. The Need of CTC for AGVs

Mobile robots or Automated Guided Vehicles (AGVs) are the perfect candidates for tasks related to space exploration, nuclear industry, mining, mobilizing disabled people, and other applications. Mounting a robot manipulator on an AGV would even further enhance its utilization in industry [36, 37]. Thomas et al [38] expected that automation of driving tasks should reduce fuel consumption, provide less wear, less unnecessary milage on the vehicles and more efficient service. In addition Thomas et al [38] discussed the requirement of automated driving and transportation systems as a whole. They concentrated mainly on safety and reliability in addition to payload constraints which are not properly taken care of if the control system is purely kinematic. In addition, they identify speed restrictions as a dominant factor in determining the throughput of a system. Efficiency and robustness are the factors mainly looked at when a controller is designed for an AGV. In this sense Simmons [20] suggested the development of a task control architecture to support the structured control approach of an AGV. Layering reactive behaviour into deliberative

components is the main theme of this work [20]. The deliberative components are supposed to handle normal situations while exceptional situations are handled by the reactive components which are explicitly constrained as to the activation requirements. In general it was concluded that a comoination of deliberative (feed forward) and reactive (feed backward) behaviour is needed to deal with complex and dynamic domains similar to the AGV environment. Moreover for general purpose robots working in uncertain and rich environments a well structured control of planning perception and action is necessary [20].

In the case of AGVs, interactions with the environment that could indicate the great need for CTC replacing regular kinematic control schemes, are the movements of an AGV while climbing a hill or the sudden large change of mass carried by the AGV in a factory or work shop. This is because position and velocity controllers for AGVs would accumulate large errors in cases like those mentioned above and push more on the actuators or motors by increasing the voltage given to them. The motors will draw the required current directly from the amplifier. Since the total output power is limited, the current output becomes limited. As a consequence the motors will draw high energy but the required movement will not be achieved and so more error will accumulate.

Rajagopalan et al [2, 4] stated that conventional control schemes of electro - mechanical systems are based on the information of position and / or velocity. These schemes can perform well in situations during which the effect of dynamic or load disturbances are insignificant. In situations where significant dynamic changes occur, a dynamics based controller will be necessary to achieve the desired AGV performance.

2.3 Models Used in Control

Modelling is known as the presentation of systems using mathematical formulations [39]. These systems could be any electro-mechanical systems under study. More specifically, the robot or AGV system representation in mathematical formulation is the model of that system. Models represent mathematically a relation between the inputs and outputs of the system. Models can be kinematic or dynamic depending on the type of relation that they represent and the input and output variables considered. To determine a suitable model requires the ability to observe the physical situation and to describe it first in qualitative terms. The accurate modelling of the plant or system to be controlled is the first step in any control design [40]. Since it is known that no robot is ever manufactured perfectly, and so the majority of other systems, models provide a qualitative testing of the system necessary to observe the system behaviour well before the quantitative production of that system.

2.3.1 The Kinematic Models

A kinematic model provides the equation of motion to compute the motion parameters of the AGV corresponding to the motion parameters of the wheels. In this sense, a kinematic model can be defined as the relation between the joint space parameters as inputs and the Cartesian space parameters as outputs [12]. A Jacobian matrix [J] relates those two sets of motion parameters. The motion parameters of the AGV are the linear and angular velocities, and those of the wheels are the wheels speed [1]. The other parameters considered in the case of steerable wheels are, the steering angles and the steering rates [1,

3]. The process of computing the vehicle motion parameters from those of the wheels is called the forward kinematic analysis.

The inverse kinematic model is the opposite of the forward kinematic model that was mentioned above. The inverse kinematic analysis computes the wheel motion parameters or joint space parameters as output from those of the AGV parameters or Cartesian space parameters as input. To obtain the inverse kinematic model the Jacobian matrix must be invertible [1]. The Jacobian matrix is a function of the vehicles geometric parameters and so the kinematic models. Rajagopalan [1] states that since the inverse kinematic model is vital to the AGV control, especially using the method of dead-reckoning, It becomes mandatory to determine whether the kinematic model of the vehicle is invertible or not well ahead of time. " A vehicle is said to be Path-Controllable if there exists a unique solution for the motion parameters of the wheels corresponding to the linear and angular velocities of the vehicle" [1]. It was mentioned in the previous chapter that AGVs differ from stationary robots in many aspects [1]. These include the fact that AGVs are closed chain mechanisms and that they form higher pair mechanisms. Therefore AGVs can not be modeled using the Denavit-Hartenberg formulations [1, 12] which is commonly used to model robot arms. For this purpose the Sheith-Uicker formulation was adopted by Muir and Neuman [41] for kinematic models of AGVs. This approach provides the ability to generalize into any kind of wheelbase configuration [1]. This is regardless of the number of wheels or the combinations of driving / driven or steerable / non-steerable wheels.

2.3.2 The Dynamic Models

Accurate modelling of the system is extremely important for the process of its control [40]. Modelling of the system is complete only with the kinematic and dynamic models being available. A dynamic model describes the relationship between the motion parameters of the vehicle (acceleration and velocity) as outputs and the forces and torques affecting the vehicle as inputs. Dynamic modelling can be accomplished using the classical techniques based on D'Alembert's principle used to model road and off-road vehicle dynamics [42, 43], the extended form of Lagrangian and Newton-Euler formulations or the Newtonian dynamics with the transformation approach for kinematic modelling by Muir and Newman [1, 41]. An example that makes use of D'Alembert's principle can be found in Huang [14] where a simulation package employing a dynamic model based on the classical method is provided. Forward dynamic modelling of different robots can be found in the literature [1, 2, 3, 4, 10, 14, 27, 41].

An inverse dynamic model is the opposite analysis of the forward dynamic model mentioned above. Inverse dynamics model can be described as a mathematical relation between the vehicle parameters of operation as inputs and the required forces and torques to be exerted at the actuators as outputs. Inverse dynamic models are useful in the design of controllers.

2.4 Scope of Thesis and Problem Definition

Based on the findings previously mentioned in the literature review, research can be directed towards developing and implementing a model based control scheme for AGVs. Since it has been emphasized in the literature that dynamics based control schemes of robot manipulators outperforms the conventional kinematics based control schemes, study and experimentation can be accomplished to prove that a dynamics based controller like the CTC outperforms the conventional kinematic controllers available for AGVs. The Centre for Industrial Control (CIC) at Concordia University has developed generations of AGVs where CONCIC II AGV is one of them. This AGV is used as a platform to conduct experimental studies and verify the findings of a simulation study carried out in this thesis regarding the applicability and results of using the CTC scheme of control. In order to develop the CTC scheme controller, an inverse dynamic model of the vehicle is needed. A derivation of the inverse dynamic model of the CONCIC II AGV and an analytical study of the dynamic model are carried out. This thesis presents a simulation study of the CONCIC II AGV performance under the effect of the CTC scheme compared to the conventional kinematics based control while operating in a dynamically changing environment. The concept of the CTC scheme application to an electro-mechanical system is also studied experimentally where a test setup is designed and built for this purpose. Control of the motor is accomplished through the PC and the performance is monitored under the effect of CTC scheme in comparison to the performance under the effect of a velocity control scheme. Finally experimentation is carried out using the real prototype vehicle.

2.5 Thesis Layout

This thesis is divided into four sections in addition to Chapters 1 and 2 where general principles and background are presented. The first section contains the mathematical formulations of the models used to simulate or to control the vehicle. This is presented in Chapter 3. The second section includes a discussion of the control strategy suggested to perform the study and the control loops in detail. It presents the principles and details of control schemes and analogies applied in both simulation and experimental studies. This is presented in Chapter 4. The third section presented in Chapter 5 presents the simulation study of the vehicular system performing under the CTC scheme and a conventional scheme of control in a dynamically changing environment.

Section four is included in Chapter 6 where experimental work is presented. This section is subdivided into two parts. The first part includes the experiments carried out on the motor-test-rig designed and built for this purpose. The second part presents results of experimentation carried out using the CONCIC II AGV.

Conclusions and future work recommendations are presented in chapter 7. There are two appendices and they include A. Specifications of the driving motor and B. Details of the motor-test-rig.

2.6 Summary

This chapter discussed the literature available on control schemes for robotic systems in general. It also presented the literature available on the application of the CTC scheme specifically to robotic systems as a whole and to AGVs as a part of those systems. It also

included the discussion of modelling and the use of models. The problem definition and the scope of thesis were also presented in this Chapter. The scope of the thesis includes the implementation issues of the CTC scheme for CONCIC II AGV.

CHAPTER 3 Mathematical Formulations

3.1 Introduction

The literature provides many studies of Computed Torque Control (CTC) applications [2, 40], particularly for robotic arms. It also provides some research on the control of Automated Guided Vehicles (AGVs) [1, 14]. On the other hand, it is very rare to find a combination of both. In other words, CTC application to AGVs is new and therefore rare in the literature.

AGVs operate in dynamically changing environments and have motors which are limited in their power consumption. In addition, AGVs experience un-modeled changes which would require a better control system to overcome them to assure accurate track following. This explains the need for CTC as a scheme capable of handling changes in dynamic parameters of the vehicle and the environment in which it operates.

Chapter 5 presents the simulation studies carried out to compare the performance of the proposed CTC scheme with that of the conventional velocity control scheme in the presence of changes in the dynamics of the operating environment and the load carried by the vehicle. To carry out these simulations a differentially driven vehicle is chosen. CONCIC II AGV at the Centre for Industrial Control (CIC) has such configuration [2]. Hence the forward dynamic model of the vehicle developed by Huang [14] has been used in this study and is summarized in the current chapter.

In addition to a forward dynamic model to simulate the movement of the vehicle, for control purposes, an inverse dynamic model, forward and inverse kinematic formulations are

required. An inverse dynamic model for the chosen differentially driven vehicle is developed in this thesis. A complete analysis has been carried out in this thesis on the development of this inverse dynamic model and is presented in Section 3.4. Kinematic formulations developed by Rajagopalan [2] and Cheng and Rajagopalan [15] have been used in this study and are summarized in Section 3.3.

Experimental validation of the proposed scheme is carried out in two stages. The first stage of experimental study is using an experimental motor-test-rig designed and developed for this thesis and is shown in Fig. 3.1. This setup makes use of a dc permanent magnet based motor set (motor-in-wheel drive unit) that is similar to the ones used in the prototype CONCIC II AGV as the driving wheels. It also includes a loading roller on top of the motor wheel attached to a loading arm to modify the loading torque on the motor wheel by way of changing the weight suspended at the end of the loading arm. Control signal to the amplifier is provided through an interface card designed and built in CIC, and which resides in a pc. Motor response is monitored through a shaft encoder attached to the motor and read by the pc through an LM628 motion controller chip on-board the interface card. For the CTC scheme implementations the LM628 is used as a decoder to count the pulses from the encoder for which the position and the velocity of the motor can be obtained from the LM628. This stage is carried out for acquiring experience in the communication procedure and setup of the different parts of the system. In addition, the same motor is used in the prototype vehicles and so the characteristics of it can be studied and obtained. Detailed schematics of the motor-test-rig are shown in Fig. 3.2.

The second stage of experimentation is carried out using the prototype CONCIC II

AGV Figure 3.3 shows a picture of the CONCIC II AGV. The CONCIC II AGV is a

Figure 3.1 Photograph of the Experimental Motor Rig

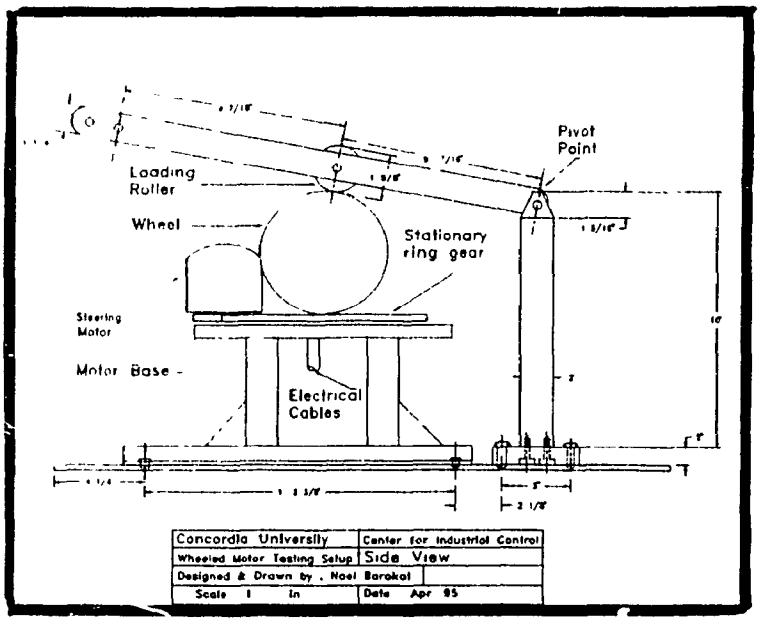

Figure 3.2 Schematics of the Experimental Motor Rig

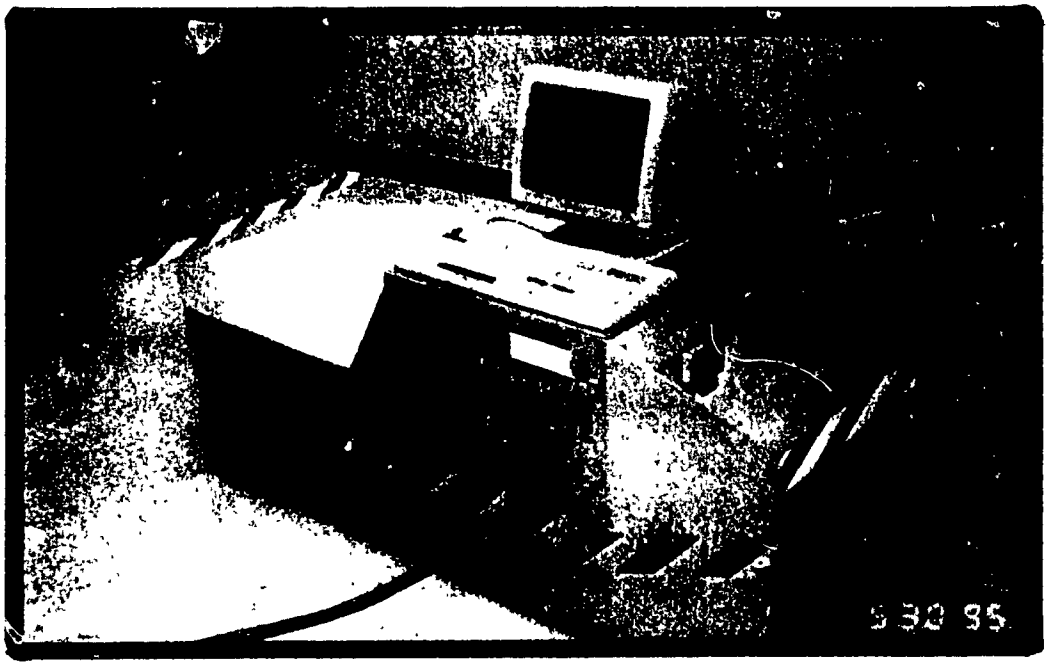

Figure 3.3 Photograph of the CONCIC II AGV

Figure 3.4 Details of the CONCIC II AGV Components

differentially driven vehicle with two motor sets driving at the sides halfway from both front and rear ends of the vehicle. It has also two supporting castors located at the front and rear. The vehicle has a binary digitizing camera and is driven through a pc on-board the vehicle. Figure 3.4 shows a detailed picture of the CONCIC II AGV components.

3.2 Dynamic Models of The Experimental Motor-Test-Rig Setup

For real time control, the motor model includes normally the motor and amplifier in addition to the properties of the drive train. This reduces the motor model to a single input and single output form.

Figure 3.5 shows a photograph of the motor experimental motor-test-rig that has been designed and developed for this thesis. The derivation of the models has been carried out and is presented below.

The equation representing the motor dynamics can be written in the form :

$$T_m = n\ (\ k_t I_1 - J\ddot{\theta} - D\dot{\theta} - T_f\ ) \tag{3.1}$$

Which can be rewritten as follows :

$$T_m = nk_t\ I_1 - nJ\ddot{\theta} - nD\dot{\theta} - nT_f \tag{3.2}$$

$$nJ\ddot{\theta} = nk_t I_1 - nD\dot{\theta} - nT_f - T_m \tag{3.3}$$

$$\ddot{\theta} = \frac{k_t}{J} I_1 - \frac{D}{J}\dot{\theta} - \frac{T_f}{J} - \frac{T_m}{nJ} \qquad (3.4)$$

$$\alpha = \frac{k_t}{J} I_1 - \frac{D}{J}\omega - \frac{T_f}{J} - \frac{T_m}{nJ} \qquad (3.5)$$

In equation (3.5), α is the motor angular acceleration and ω is the motor angular velocity

3.2.1. Forward Dynamic Model

The general form of the forward dynamic model of a motor is represented by equation (3.6) which is a reproduction of equation (3.4) as follows .

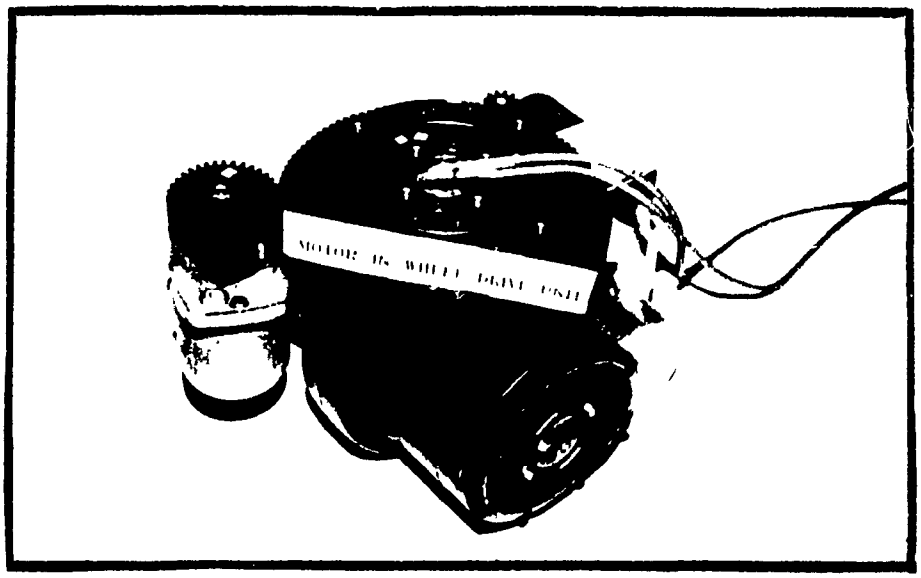

Figure 3.5 Photograph of the Wheel - in - Motor Setup

$$\ddot{\theta} = \frac{K_t}{J} I_1 - \frac{D}{J}\dot{\theta} - \frac{T_f}{J} - \frac{T_L}{nJ} \tag{3.6}$$

where :

$\ddot{\theta}$ = motor acceleration in revolution per second per second (rev/s^2).

$\dot{\theta}$ = motor speed in revolution per second (rev/s).

T_L = load torque in Newton Meter (Nm).

n = gear ratio.

D = motor damping (Nms/rad).

J = motor inertia (Nms^2).

k_t = torque constant of the motor (Nm/A).

I_1 = current of the motor

The values for the constants in equation (3.6) have been substituted for by the parameters of a permanent magnet motor that is being used as an actuator for the CONCIC II AGV. Equation (3.7) has been obtained by this substitution as follows :

$$\ddot{\theta} = 45.6 I_1 - 0.04\dot{\theta} - 40.3226 T_L - 400 T_f \tag{3.7}$$

T_L and T_f are load torque and friction torque of the motor respectively.

3.2.2. Inverse Dynamic Model

Inverse dynamic models are useful in designing controllers. The motor inverse dynamic model is presented in equation (3.8) as :

$$I = \frac{J}{K_t}\ddot{\theta} + \frac{D}{K_t}\dot{\theta} + \frac{T_f}{K_t} + \frac{T_L}{nK_t} \tag{3.8}$$

Again substituting for the variables by the AGV motor parameters, an equation for the motor current is obtained as :

$$I = 0.0219\ddot{\theta} + 0.000877190\dot{\theta} + 0.8861T_L + 8.772T_f \tag{3.9}$$

This equation will be used as the feed-forward controller. The motor characteristic curve and calculations related can be found in Appendix-A.

3.3 Kinematics of CONCIC II AGV

As mentioned in the previous chapter, a kinematic model provides motion equations to compute the motion parameters of the AGV that corresponds to the motion parameters of the wheels. A Jacobian matrix [J] relates these two sets of parameters. For the CONCIC II AGV the derivation of the motion equations can be found in detail in [1]. The assumptions used to formulate the kinematic model of the AGV are the following :

- The vehicle has no slipping at the contact points of the wheels or castors neither laterally nor longitudinally.
- The contact between the tire and the ground is a point rather than a surface. This assumption is valid as the tires are made of hard moulded rubber.
- The change in the orientation angle is very small for the sampling interval considered.

- Wheel alignment errors are ignored since they are very small.

3.3.1 Forward Kinematic Model

A systematic transformation approach is used by Rajagopalan [1] to obtain the kinematic model of a differentially driven vehicle. The kinematic model can be represented in its final form as follows:

$$\begin{bmatrix} V_{rx} \\ \dot{\theta}_r \end{bmatrix} = \frac{r}{L_1 + L_2} \begin{bmatrix} L_1 & L_2 \\ 1 & -1 \end{bmatrix} \begin{bmatrix} \omega_{x1} \\ \omega_{x2} \end{bmatrix} \tag{3.10}$$

$$\begin{bmatrix} V_{rx} \\ \dot{\theta}_r \end{bmatrix} = \frac{r}{L_1 + L_2} [J] \begin{bmatrix} \omega_{x1} \\ \omega_{x2} \end{bmatrix} \tag{3.11}$$

Where V_{rx} is the forward linear velocity of the vehicle and $\dot{\theta}_r$ is the rotational velocity of the vehicle about its centre of mass which coincides with the geometric centre. The wheel radius is represented by r. L_1 and L_2 are one half of the wheel span. The terms ω_{x1}, ω_{x2} are the speeds of left and right driving wheels respectively. It is to be noticed that for all non-zero positive values of L_1 and L_2 the determinant of the Jacobian matrix [J] is never zero and so the Jacobian is invertible. This means that the wheel motion parameters ω_{x1}, ω_{x2} can be obtained for all operating speeds $V_{rx}, \dot{\theta}_r$ of the vehicle [1, 14]. Figure 3.4 shows the layout of CONCIC II AGV.

3.3.2 Inverse Kinematic Model

The inverse kinematic model is obtained by inverting equation (3.10) representing the forward kinematic model. It is given by the form:

$$\begin{bmatrix} \omega_{x1} \\ \omega_{x2} \end{bmatrix} = \frac{1}{r} \begin{bmatrix} -1 & -L_2 \\ -1 & L_1 \end{bmatrix} \begin{bmatrix} V_{rx} \\ \dot{\theta}_r \end{bmatrix} \tag{3.12}$$

From the discussions presented above, it can be inferred that for a differentially driven vehicle the motion parameters of the wheels (ω_{x1},ω_{x2}) can be computed for all values of motion parameters of the vehicle (V , $\dot{\theta}$). This gives one of the advantages of choosing such vehicles. The other advantage to be mentioned is the fact that the forward and inverse kinematic models of differentially driven vehicles are by far simpler than other vehicle configurations. This leads to fewer computational requirements and less computational error due to inaccuracies in evaluated parameters of the vehicle.

Additional advantages to be mentioned in differentially driven AGVs compared to other AGV configurations are the following [1]:

- Differentially driven vehicles can spin around the geometric centre at a minimum radius which is equal to one half of the wheel span, i.e. they are able to "turn on a dime".
- The vehicle can travel in the forward and reverse direction.
- Differential drive provides two degrees of freedom to the vehicle with two actuators and hence has no redundant actuators.
- The inverse dynamic model is easy to obtain and is presented in Section 3.4.6.

Further, the inverse dynamic model provides a unique set of current values (I_1 , I_2) for all operating conditions of the vehicle.

The above mentioned advantages, in addition to the availability of such a vehicle prototype as a platform in the CIC, makes the CONCIC II AGV a perfect candidate for use in experimentation.

3.4. Dynamic Models of CONCIC II AGV

The Computed Torque Control (CTC) scheme is based on the dynamic model of the system to be controlled. As mentioned in Section 3.1, dynamic models of the vehicle are required as a basis for this type of controllers [2].

A dynamic model is a useful tool to study the response of the vehicle and also to design controllers. There are two types of models, one is the forward or direct and the other is the inverse. The forward dynamic model is useful to carry out simulation studies as this model represents the vehicle. In this model, the desired torque is the input while the output is the acceleration. The velocity and position are obtained by integrating the output acceleration [2]. The inverse dynamic model is useful in the design of vehicle controller. The desires acceleration and velocity are the input while the torque or (current) is the output.

3.4.1 Components of The Dynamic Model

The dynamic formulations of the vehicle take into account the effects of

- Inertial and normal forces due to dead weight and payload carried by the vehicle.
- Side forces due to operational speed and path followed (lane changing).

- Centrifugal and gyroscopic forces while negotiating curves and steering.
- Tires characteristics.
- Road conditions. Examples are uphill or downhill, unevenness of the terrain and the friction coefficient between the tire and the terrain.

3.4.2 Assumptions Related to The Dynamic Model

The dynamic model of CONCIC II vehicular system was derived by Huang [14] with the following assumptions :

- The vehicle body is considered to be a two degrees of freedom system.
- The vehicle has a symmetrical structure about the fore-and-after plane of the vehicle.
- The location of the centre of mass of the vehicle coincides with the location of the geometric centre of the vehicle.
- The weight of the vehicle is equally distributed on all the wheels and castors.
- The wheels and castors roll without longitudinal or side slip.
- The castors include about 1% of the total vehicular system mass. Therefore, their mass is negligible.
- The bearings of the castors are assumed to experience no friction.
- Both castors are assumed to have similar characteristics.
- The two motors and their wheels and servo sets are considered to be identical.

3.4.3 Forward Dynamic Model

A force analysis and a dynamic model has been developed for the CONCIC II AGV

by Huang [14]. Figure 3.6 shows the schematics of the AGV and the external forces interacting with it. Some of the relevant equations are given below. The complete model and the derivation of the equations can be found in [2, 14].

The vehicle has two degrees of freedom, a forward motion and a yaw motion. The forces acting on the vehicle body along the direction of travel of the vehicle (Y-axis) are summed and the summation is given by

$$\Sigma F_y = m\dot{V}_y = F_{1t}+F_{2t}-F_{1f}-F_{2f}+\acute{F}_{fy}+\acute{F}_{ry} \tag{3.13}$$

where F_y is the force, $\dot{V}_y$ is the linear acceleration, V_y is the forward velocity along the Y-axis, F_{1t} is the tractive force at the motorized wheel-1 (left side wheel) and F_{2t} is the tractive force at the other motorized wheel. F'_{fy} represents the other forces acting at the contact points of the castors and motorized wheels (the cornering and normal forces). The subscripts f and r are used to represent the front and rear castors respectively.

The rotational movement of the vehicle takes place about the Z-axis. The summation of moments about this axis is written as

$$\Sigma M_z = I_z\dot{\Omega}_z = (F_{2t}-F_{1t})L + (F_{1f}-F_{2f})L + (\acute{F}_{fy}-\acute{F}_{fx})L_{ae} \tag{3.14}$$

The tractive force at the first wheel is given by

$$F_{1t}=\frac{n}{r_d}\left(K_t I_1-\frac{Jn}{r_d}\left(\dot{V}_y-L\frac{\dot{\Omega}}{2} \right) - \frac{Dn}{r_d}\left(V_y-L\frac{\Omega}{2} \right) - T_f \right) \tag{3.15}$$

The tractive force for the second wheel can be computed from

$$F_{2t} = \frac{n}{r_d}\left(K_t I_2 - \frac{Jn}{r_d}\left(\dot{V}_y + L\frac{\dot{\Omega}}{2} \right) - \frac{Dn}{r_d}\left(V_y + L\frac{\Omega}{2} \right) - T_f \right) \quad (3.16)$$

The equations representing the forward dynamics of the vehicle are obtained as

$$\begin{aligned}(m + 2n^2\frac{J}{r_d^2})\dot{V}_y = \frac{nK_t}{r_d}(I_1 + I_2) - (2n^2\frac{D}{r_d^2} + 2K_1K_2N_d)V_y - 2K_1N_d - 2\frac{nT_f}{r_d} \\ -F_{ff}\cos(\delta_f) + F_{fn}\cos(\beta_f) - F_{rf}\cos(\delta_r) + F_{rn}\cos(\beta_r)\end{aligned} \quad (3.17)$$

$$\begin{aligned}(I_z + \frac{2n^2L^2}{r_d^2})\dot{\Omega}_z = \frac{LnK_t}{r_d}(I_2 - I_1) - (\frac{2n^2D}{r_d^2} + 2K_1K_2N_d)L^2\Omega_z \\ + L_{ae}(F_{rn}\sin(\beta_r) - F_{rf}\sin(\delta_r) - F_{fn}\sin(\beta_f) + F_{ff}\sin(\delta_f))\end{aligned} \quad (3.18)$$

3.4.4 Models Effective Terms Investigation

A study of the effect of the different terms in the dynamics equations is presented in this section. The dynamic model equations can be re-written in terms of various forces and/or moments acting on the system as follows :

$$
\begin{aligned}
term\ 1 &= \frac{nk_t(I_1+I_2)}{r_d} = f\,(I_1+I_2) = f\,(R_d,V_y) \quad (N)\\
term\ 2 &= 2(\frac{n^2D}{r_d^2}+k_1k_2N_d)V_y = g\,(V_y) \quad (N)\\
term\ 3 &= 2K_1N_d = Constant \quad (N)\\
term\ 4 &= \frac{-2nT_f}{r_d} = Constant \quad (N)\\
term\ 5 &= C_{fy} = F\,(V_y,\Omega_z,R_d) \quad (N)
\end{aligned}
\tag{3.19}
$$

$$
\begin{aligned}
term\ 6 &= \frac{LnK_t(I_1-I_2)}{r_d} = f(I_1,I_2) = r\,(R_d,\Omega_z)\ (N.m)\\
term\ 7 &= 2(\frac{n^2D}{r_d^2}+K_1K_2N_d)L^2\Omega = p\,(\Omega_z)\ (N.m)\\
term\ 8 &= kC_{fz} = G\,(R_d,V_y,\Omega_z)\ (N.m)
\end{aligned}
\tag{3.20}
$$

$$
\begin{aligned}
C_{fy} &= -F_{ff}\cos(\delta_f)+F_{fn}\cos(\beta_f)-F_{rf}\cos(\delta_r)+F_{rn}\cos(\beta_r) \quad (N)\\
C_{fz} &= F_{rn}\sin(\beta_r)-F_{rf}\sin(\delta_r)-F_{fn}\sin(\beta_f)+F_{ff}\sin(\delta_f) \quad (N)
\end{aligned}
\tag{3.21}
$$

Terms 5 and 8 include all the castor forces that are shown as trigonometric functions in the dynamic model [equation (3.21)]. R_d is the radius of curvature of the track the vehicle is following. The contribution of force value within the operating velocity range of CONCIC II is computed. Figures 3.7 and 3.8 show the results of these computations as function of linear and angular velocities. In addition, the effect of these velocities on current values are taken into consideration in order to complete the analysis. For a linear velocity range of 0 to 5 m/s and an angular velocity range of 0 to 1 rad/s, variable terms are plotted. From

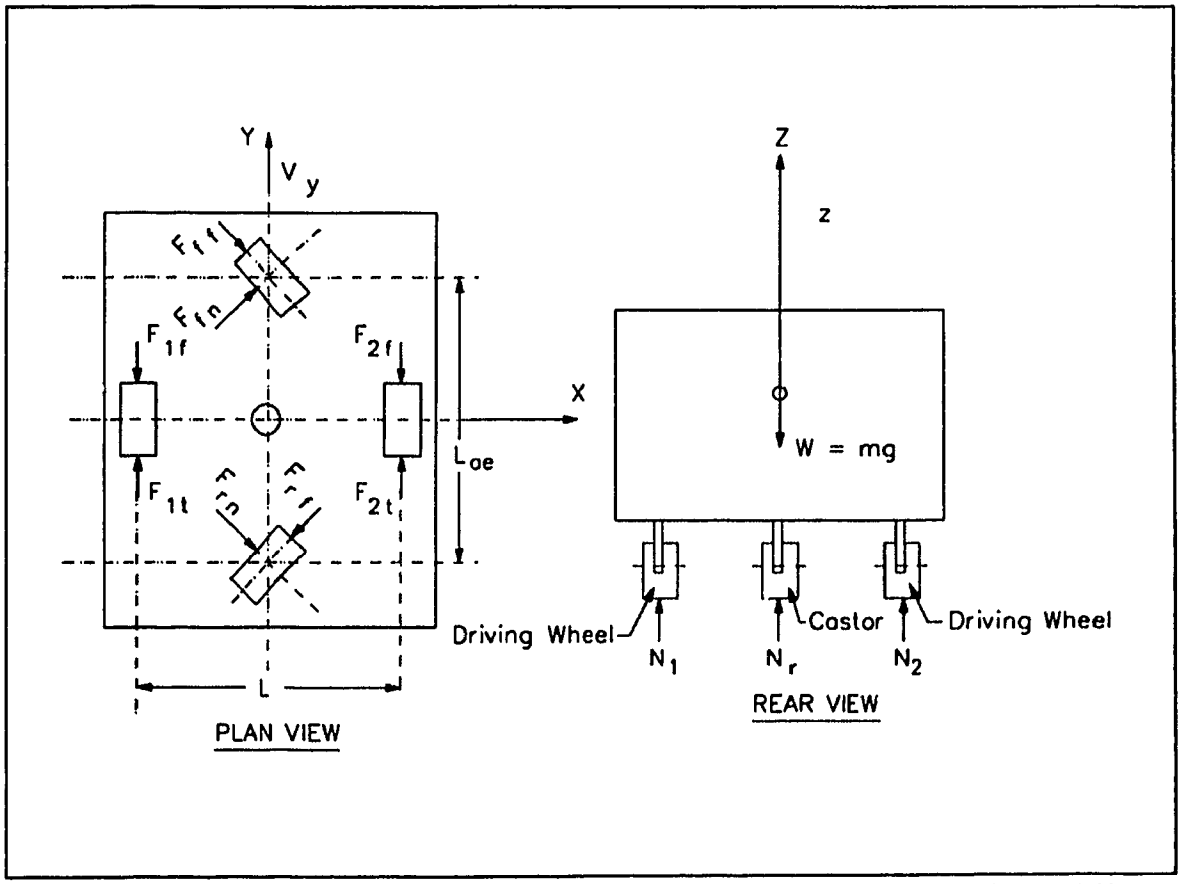

Figure 3.6 Schematic of CONCIC II AGV and the External Forces [1, 4, 14].

Figure 3.7, it can be seen that term 1 of equation (3.19) contributes 220 to 250 N force for the chosen linear velocity range. This is because this term includes the forcing function or the input to the system, which is the actuators current values I_1 and I_2. Knowing that the current value is a function of both the velocity and acceleration of the system, a value for term 1 of equation (3.19) is found even at zero velocity as long as there is acceleration.

It can be seen from Figure 3.7 that the contribution of the terms 2 and 5 of equation (3.19) is in a range of 0 to 30 N force. This is nearly 3 % of the force due to term 1.

From Figure 3.8, it is evident that the contributions of terms 7 and 8 are nearly less than 2% of the force due to term 6. Term 6 contributes by a value of - 480 Nm torque when the angular velocity component is present. The constant terms (terms 3 and 4) contribute only by less than 2% to the total force over the velocity range studied. However, in this thesis, the simulations are carried out using the full form of the dynamic model given by equations (3.17) and (3.18). The simplification was done to arrive at the simplified inverse dynamic model first then incorporate the minor contributing terms afterwords.

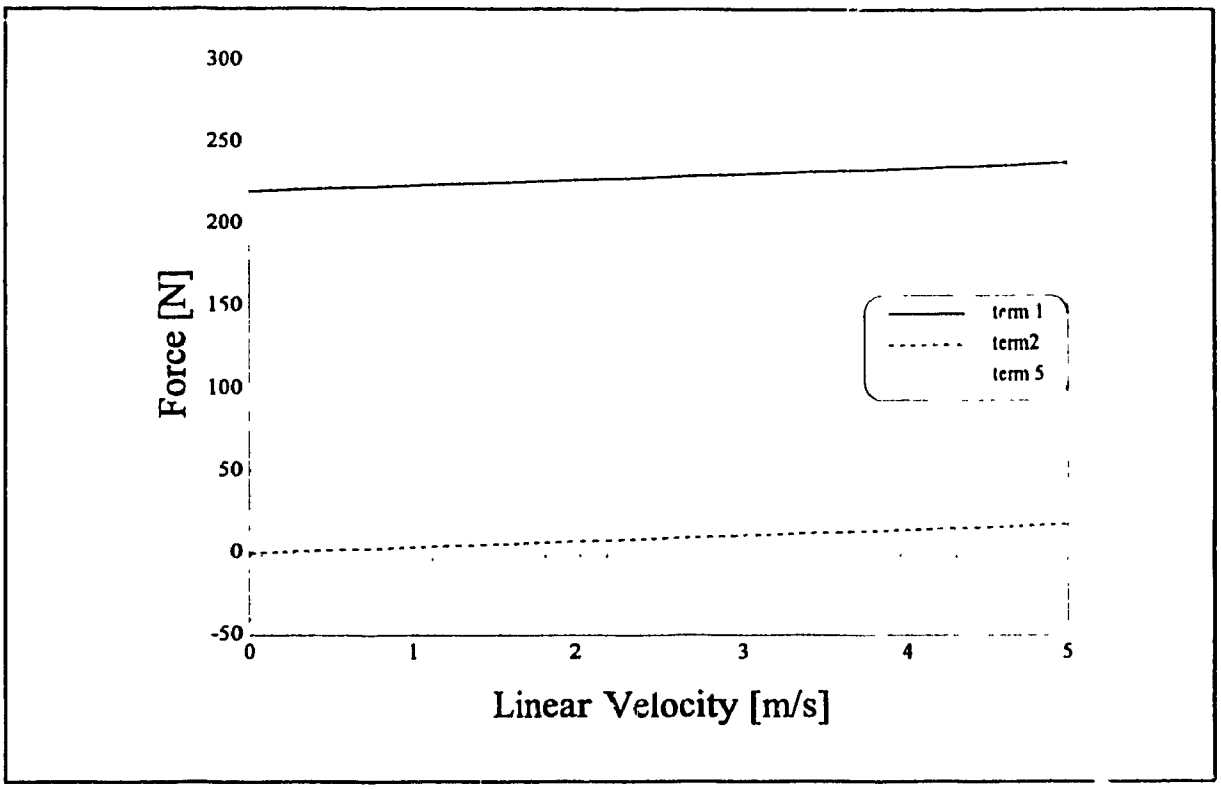

Figure 3.7 Effective Terms which are Functions of Linear Velocity of the AGV

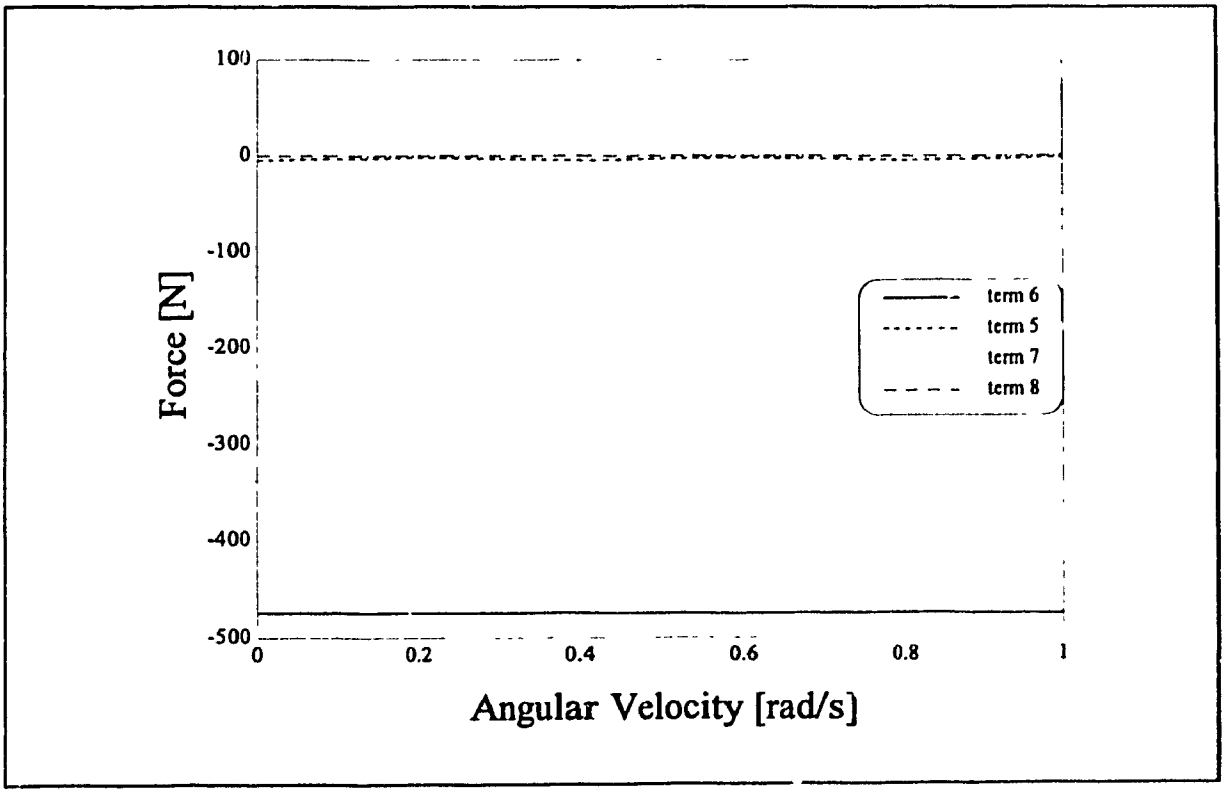

Figure 3.8 Effective Terms which are Functions of Angular Velocity of the AGV

The same argument can be used to compare the effects in the moment equation of the dynamic model which has been divided into terms 6, 7 and 8. From Figures 3.7 and 3.8, it is clear that the contribution of both terms 7 and 8 is nearly less than 2% of the force due to term 6. It is to be mentioned that these last 3 terms (i.e. terms 6, 7 and 8) are not zero only when there is a rotational (angular) acceleration and velocity.

Equations (3.17) and (3.18) are simplified to visualize the parameters that significantly affect the performance of the vehicle. The terms containing the cornering forces and other frictional effects in equations (3.17) and (3.18) can be omitted as they contribute only to less than 4% of the total forces and moments acting on the vehicle when operating at linear velocity of 0 to 5 m/s. This greatly simplifies the forward dynamic model. This form of the equations is useful to study the effect of payload and inertia on the performance of the vehicle as well as the interaction between the vehicle speed and acceleration. The simpler forms are given as :

$$(m+2n^2\frac{J}{r_d^2})\dot{V}_y = \frac{nK_t}{r_d}(I_1+I_2)-(2n^2\frac{D}{r_d^2}+2K_1K_2N_d)V_y \qquad (3.22)$$

$$(I_z+\frac{2n^2L^2}{r_d^2})\dot{\Omega}_Z = \frac{nLK_t}{r_d}(I_2-I_1)-2(\frac{n^2D}{r_d^2}+K_1K_2N_d)L^2\Omega_z \qquad (3.23)$$

equation (3.22) can be re-written in the following form

$$a_y = \dot{V}_y = \frac{F}{M}(I_1 + I_2) - \frac{B}{M}V_y \qquad (3.24)$$

where $F = n K_t/r_d$, $M = m + 2 n^2 J/r_d^2$, $B = (2 n^2 D/r_d^2)L^2 + 2K_1K_2N_d$, which are constants whose values depend on the characteristics of the vehicle and the motors used. Equation (3.23) can be simplified along the same lines and the final simplified form is given by

$$\dot{\Omega}_z = \frac{LF}{I}(I_1 - I_2) - \frac{B}{I}\Omega_z \qquad (3.25)$$

Where $I = I_Z + 2 L^2 n^2 / r_d^2$, which is a constant whose value depends on the characteristics of the vehicle and the motors used.

3.4.5 Invertibility Investigation

Equations (3.24) and (3.25) can also be expressed in a matrix form. This results in the following equation

$$\begin{bmatrix} \dot{V}_y \\ \dot{\Omega}_z \end{bmatrix} = \begin{bmatrix} \frac{F}{M} & \frac{F}{M} \\ \frac{LF}{I} & -\frac{LF}{I} \end{bmatrix} \begin{bmatrix} I_1 \\ I_2 \end{bmatrix} - \begin{bmatrix} \frac{B}{M} & 0 \\ 0 & \frac{BL^2}{I} \end{bmatrix} \begin{bmatrix} V_{ya} \\ \Omega_{za} \end{bmatrix} \qquad (3.26)$$

Equation (3.26) is in conventional forward dynamics form showing the input-output relationship and the contribution by various components. Using this equation the desired motion parameters of the vehicle (linear and angular accelerations) can be computed using

the wheel parameters (current I_1 and I_2) and actual values of linear and angular velocities of the vehicle. Further reorganization of equation (3.26), the following result is obtained :

$$\begin{bmatrix} \dot{V}_y \\ \dot{\Omega}_z \end{bmatrix} = F \begin{bmatrix} \frac{1}{M} & \frac{1}{M} \\ \frac{L}{I} & -\frac{L}{I} \end{bmatrix} \begin{bmatrix} I_1 \\ I_2 \end{bmatrix} - B \begin{bmatrix} \frac{1}{M} & 0 \\ 0 & \frac{L^2}{I} \end{bmatrix} \begin{bmatrix} V_{ya} \\ \Omega_{za} \end{bmatrix} \tag{3.27}$$

$$\begin{bmatrix} \dot{V}_y \\ \dot{\Omega}_z \end{bmatrix} = F \; [\, J1] \begin{bmatrix} I_1 \\ I_2 \end{bmatrix} - B \; [\, J2] \begin{bmatrix} V_{ya} \\ \Omega_{za} \end{bmatrix} \tag{3.28}$$

where $[\, J1] = \begin{bmatrix} \frac{1}{M} & \frac{1}{M} \\ \frac{L}{I} & -\frac{L}{I} \end{bmatrix}$ and $[\, J2] = \begin{bmatrix} \frac{1}{M} & 0 \\ 0 & \frac{L^2}{I} \end{bmatrix}$

It can be seen from equation (3.28) that the matrix J1 is invertible for all non-zero positive values of L, I and M. The determinant of J1 is as follows :

$$\det\,(J1) = -2\frac{L}{MI} \neq 0 \tag{3.29}$$

It is independent of the operating parameters of the vehicle (V, Ω) and is a function of the geometrical or physical parameters of the vehicle (I, M, L). This characteristic allows the calculation of the inverse dynamic model for [I_1 and I_2] for any given (linear and angular) velocity and acceleration of the vehicle.

For the prototype differentially driven CONCIC-II AGV [1, 2] considered for simulation studies, the values of parameters in equation (3.27) are given by :

$F = n K_t / r_d$	= 15.0480	Newton/Amp.
$M = m + 2 n^2 J / r_d^2$	= 211.52	Kg
$B = (2 n^2 D / r_d^2) + 2 K_1 K_2 N_d$	= 3.528	Ns / m
$I = I_Z + 2 L^2 n^2 / r_d^2$	= 2370.3	Kgm^2

3.4.6 Inverse Dynamic Model

The inverse dynamic model has been developed based on the forward dynamic model presented above by equations (3.17) and (3.18). For the inverse dynamic model, the desired acceleration and velocity of the vehicular system are the inputs to the model while the actuators torques are obtained as the outputs. Referring to the forward dynamic model represented by equations (3.17) and (3.18), and the fact that these two equations are coupled and are functions of the two driving motors current, they are solved simultaneously to obtain equations providing expressions for the torque required by each motor to run the vehicle at the desired speed. From equations (3.27), (3.28) and (3.29), important features of the CONCIC II AGV dynamics can be found. The ease of invertibility of the Jacobian matrix [J1] in equation (3.29) and the existence of solution for all positive values of L, I and M are the two main features of this model. This makes an inverse of the dynamic model of this AGV feasible and easy to obtain. The generic form of the inverse dynamic equations for a differentially driven vehicle are given by equations (3.30) and (3.31). Neglecting the effect of side forces and considering only the payload and inertia changes, equations (3.30) and (3.31) can be simplified to equations (3.32) and (3.33) respectively, where I_1 and I_2 are the currents of the driving motors. Further simplification leads to equation (3.34)

$$I_1=\frac{1}{2}\frac{r_d}{nK_t}((m+2\frac{n^2}{r_d^2}J)\dot{V}_y+(2n^2\frac{D}{r_d^2}+2K_1K_2N_d)V_y+2K_1N_d+2\frac{nT_f}{r_d}+F_{ff}\cos(\delta_f)-F_{fn}\cos(\beta_f$$
$$+F_{rf}\cos(\delta_r)-F_{rn}\cos(\beta_r))-\frac{r_d}{2nLKt}((I_z+\frac{2n^2L^2}{r_d^2})\dot{\Omega}_Z+2(\frac{Dn^2}{r_d^2}+K_1K_2N_d)L^2\Omega_Z$$
$$-L_{ae}(F_{rn}\sin(\beta_r)-F_{rf}\sin(\delta_r)-F_{fn}\sin(\beta_f)+F_{ff}\sin(\delta_f)) \qquad (3.30)$$

$$I_2=\frac{1}{2}\frac{r_d}{nK_t}((m+2\frac{n^2}{r_d^2}J)\dot{V}_y+(2n^2\frac{D}{r_d^2}+2K_1K_2N_d)V_y+2K_1N_d+2\frac{nT_f}{r_d}+F_{ff}\cos(\delta_f)-F_{fn}\cos(\beta_f$$
$$+F_{rf}\cos(\delta_r)-F_{rn}\cos(\beta_r))+\frac{r_d}{2nLKt}((I_z+\frac{2n^2L^2}{r_d^2})\dot{\Omega}_Z+2(\frac{Dn^2}{r_d^2}+K_1K_2N_d)L^2\Omega_Z$$
$$-L_{ae}(F_{rn}\sin(\beta_r)-F_{rf}\sin(\delta_r)-F_{fn}\sin(\beta_f)+F_{ff}\sin(\delta_f)) \qquad (3.31)$$

$$I_1 = \frac{1}{2}\frac{r_d}{nK_t}((m+2\frac{n^2}{r_d^2}J)\dot{V}_y+(2n^2\frac{D}{r_d^2}+2K_1K_2N_d)V_y$$
$$-\frac{r_d}{2nLKt}((I_z+\frac{2n^2L^2}{r_d^2})\dot{\Omega}_Z+2(\frac{Dn^2}{r_d^2}+K_1K_2N_d)L^2\Omega_Z \qquad (3.32)$$

$$I_2 = \frac{1}{2}\frac{r_d}{nK_t}((m+2\frac{n^2}{r_d^2}J)\dot{V}_y+(2n^2\frac{D}{r_d^2}+2K_1K_2N_d)V_y$$
$$+\frac{r_d}{2nLKt}((I_z+\frac{2n^2L^2}{r_d^2})\dot{\Omega}_Z+2(\frac{Dn^2}{r_d^2}+K_1K_2N_d)L^2\Omega_Z \qquad (3.33)$$

$$I_1 = I_2 = A\,(M\,\dot{V}_y + B\,V_y) \tag{3.34}$$

where I_1 and I_2 are the current values supplied to the left and right side motors and

$A = r_d / (2\,n\,K_t)$ $= 0.0332$ Amp./Newton

$B = 2\,n^2\,D / r_d^2 + 2\,K_1\,K_2\,N_d$ $= 3.528$ N s / m

Referring to equations (3.32) and (3.33), the matrix form of the inverse dynamic model is obtained as

$$\begin{bmatrix} I_1 \\ I_2 \end{bmatrix} = \frac{-MI}{2LF} \begin{bmatrix} \frac{L}{I} & -\frac{1}{M} \\ \frac{L}{I} & \frac{1}{M} \end{bmatrix} \begin{bmatrix} \dot{V}_y \\ \dot{\Omega}_z \end{bmatrix} + \frac{B}{2F} \begin{bmatrix} -1 & -L \\ 1 & L \end{bmatrix} \begin{bmatrix} V_{ya} \\ \Omega_{za} \end{bmatrix} \tag{3.35}$$

From equation (3.35), a unique set of values for the actuators current [I1 and I2] can be calculated for all values of angular and linear acceleration and velocity of the AGV [$\dot{V}_y$, $\dot{\Omega}_y$]. It should be noticed here that the simulation studies presented in Chapter 5 are carried out using the full forms of the equations of the dynamic models. Forward dynamic model used is as presented in equations (3.17) and (3.18). Inverse dynamic model used is as presented in equations (3.30) and (3.31).

3.5 Other Simulation Models

To obtain a consistent performance of the electro-mechanical system, a control strategy must be designed and implemented to this system. This is to assure smooth operation of the vehicle. For the simulation of the vehicle operating under the effect of

different control schemes, the individual components of the vehicle controller have to be modelled. This includes the motors sets, the amplifier, the Digital to Analog Converter (DAC) used, the PID filter used and the guidance system. In the present study the guidance system is not modeled. The simulation study includes only the vehicle and the servo system. This is because the focus of the present study is on the control part of the vehicle and not the guidance scheme.

3.5.1 Digital to Analog Converter (DAC) Model

Digital to Analog Converters (DAC) are necessary to control an analog system by means of a digital computer. The role of the DAC is to convert the digital signals from a computer or an electronic circuit source to an analog signal.

An 8 bit DAC is used in the servo controller of the CONCIC II AGV [1, 14]. This DAC works in a range between -9.2 and 9.2 volts. This corresponds to the 8 bit digital value starting at zero and ending at 256. The resolution of this DAC can be calculated as follows

DAC resolution = full scale voltage output / 2^n = 18.4/256 = 0.071875 Volt

The 8 bit DAC accuracy = 1/(2x256) = 0.19%

A simple calculation can show that an input of 128 as a digital value would correspond to zero voltage as output. The mathematical model of the DAC and the relationship between inputs and outputs is as in [14] and is given below :

Digital input to the DAC (x) = Output from the Amplifier (C_n)+ 128

Voltage output of the DAC (y) = 0.0725 x - 9.2

To find the relation between the amplifier output (C_n) and the DAC output (y), both the

previous equations are solved together. The model finally is given as :

$$y = 0.0725\ C_n - 0.08 \qquad (3.36)$$

Or in other words : Analog Output = 0.0725 Digital Input - 0.08

It is to be mentioned here that this DAC model has been used in the simulation studies since it represents the real system available in the AGV.

3.5.2. Amplifier Model

The analog signal coming out of the DAC is sent to an amplifier as a control signal. The amplifier then outputs a proportional voltage to the actuators. In this case the DAC signal is treated as a reference signal while the amplifier sends a power output value to the motor proportional to this signal. The amplifier is chosen to deliver power in a range equivalent to the motors requirement, that is -24 and 24 volts. The characteristics of the power amplifier used can be found in [1, 14] and the model approximating these characteristics is given as :

Output Voltage (V_o) = 4.5 Input Voltage (V_i) $\quad V_i \leq 1.28$ V

= 6.74 (V_i - 0.93) $\quad 1.28 \leq V_i \leq 2.5$ V

= 9 (V_i - 1) $\quad V_i > 2.5$ V

This model was used in the simulation study of the vehicle.

3.5.3 Motor Model

The CONCIC II AGV has two driving motor units. Each of those includes a

permanent magnet (PM) motor of the brush type 24 volts dc. A motor can be approximated by a resistance, inductance and internal generated voltage as in [1, 14] and most literature found. A picture of the motor used is shown in Figure 3.5. The electrical equivalence of the motor can be written as :

$$V_m = L_m \frac{dI_1}{dt} + RI_1 + K_e\omega \qquad (3.37)$$

where L_m = the motor inductance, I = the current passing through the motor , R = the motor internal resistance, ω = the motor angular speed, K_e = the motor speed constant.

3.5.4 PID Filter Model

The PID filter is used in the control loop to achieve a fast and smooth response. Mainly, these filters include one of the following : a proportional gain (P), an integral effect and gain (I) or a derivative effect and gain (D). The filter could also include combinations of those (i.e. P, PD, PID, etc). PID is the most popular controller in industrial control and finds a wide range of applications [1, 14]. Figure 3.9 presents a typical control system using a PID controller. This controller is presented by the following transfer function :

$$G(s) = K_p + \frac{K_i}{s} + K_d\, s \qquad (3.38)$$

Some motion controller chips available in the market provide a digital form of the PID filter. An example is the LM628 chip [1]. This is a low level motion controller

described in details in [46]. For the simulation provided in this study, different filters settings are used for different situations. As an example, in the simulation presenting the CTC scheme application to the CONCIC II AGV a PI filter is used. Different methods are suggested in the literature to tune PID filters [44, 45]. The Ziegler-Nichols method is used in this thesis to obtain values for the control filters. These are not the unique set that provides the optimum response. The method helps in providing values close to the true ones, which in turn makes the search range narrower. The Zeigler-Nichols method allows the tuning process to be carried out without any prior knowledge of the transfer function of the plant [44]. The method is followed in this thesis experimentally. The steps of this method are as follows :

1. The transfer function needs to be transferred to the form :

$$G(s) = K_p \left(1 + T_d s + \frac{1}{T_i s} \right) \tag{3.39}$$

2. T_d is first set to zero.

3. T_i is brought up as large as possible.

4. K_p is adjusted upwards from near zero to find the system stability boundary.

5. At the onset of stability visibly observed, gain found would be the critical gain and observed frequency is the critical frequency.

6. Empirical results are : $K_p = 0.5\, K_c$

$T_i = 0.5\, T_c$

$T_d = 0.125\, T_c$

and for a PI controller $K_p = 0.45\ K_c$

$T_i = 0.85\ T_c$

Where K_c and T_c are the plant critical parameters.

Other methods can be found in the literature to tune up these filters as Hangs refined Zeigler-Nichols and Astrom-Hagglund gain phase method [45]. It is to be mentioned here that these methods are empirical and do not result in an exact solution.

3.6 Summary

In this chapter kinematic and dynamic models for a differentially driven automated vehicle and dynamic models of a motor used in the study has been presented and discussed. Further, components models of a typical servo loop are presented.

Differentially driven vehicles prove to be the simplest in modelling and the highest in maneuverability among other vehicles configurations provided by the literature. The features that differentially driven vehicles possess and make them superior to other vehicles configuration are summarized in the following points:

1. Kinematic invertibility. The inverse kinematic model can be obtained for all angualr and linear velocity values.
2. Dynamic invertibility. The inverse dynamic model is easy to obtain.
3. Ease in obtaining the dynamic models.
4. Maneuverability and motion flexibility. The AGV can " turn on a dime ".

Moreover, differentially driven vehicles have no singularities when it comes to the invertibility of their dynamic models.

Forward dynamic models are important in simulations to study the system performance. Inverse dynamic models are essential to design the system dynamic controller.

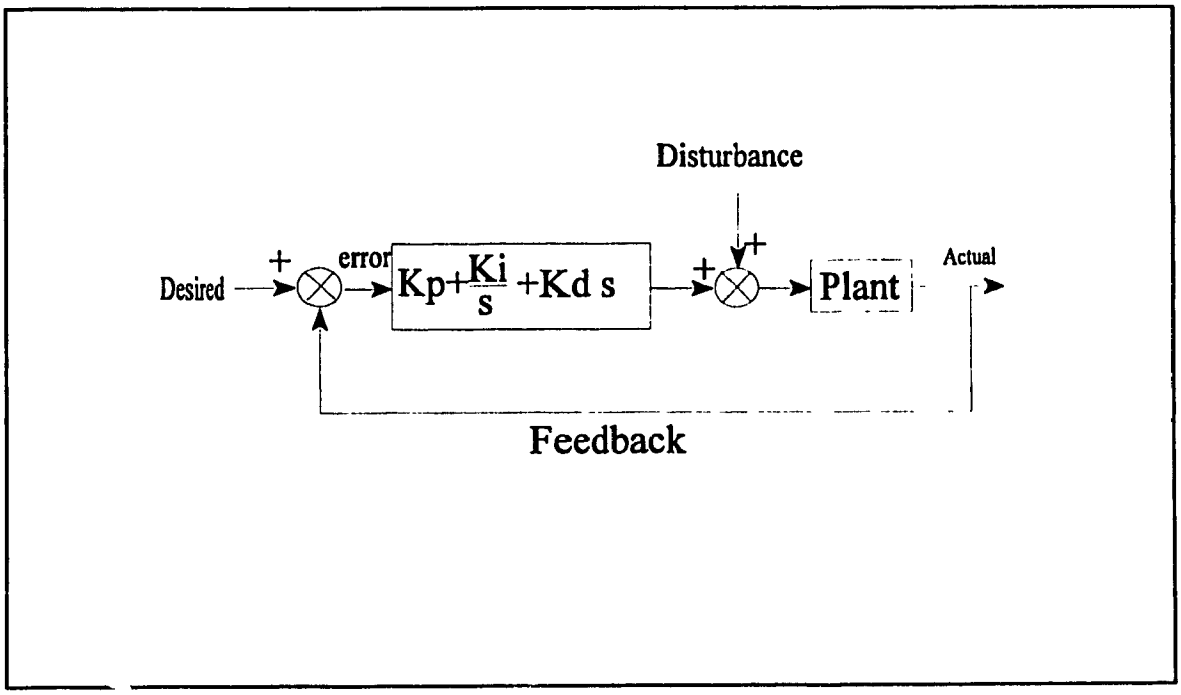

Figure 3.9 Typical control loop with a PID filter

CHAPTER 4 CONTROL STRATEGY

4.1 Introduction

Based on the literature review that is presented in Chapter 2 on the CTC scheme and the dynamic analysis that is discussed in Chapter 3 for CONCIC II AGV, it can be inferred that a dynamic-model based control scheme is expected to improve the performance of the AGV. Therefore, in this chapter, the CTC scheme is devised and implemented for CONCIC II AGV.

This chapter presents the control strategies used in the simulation studies and experimental validations. Control block diagrams or control loop schematics are also provided. Experimental validations are carried out using two electro-mechanical systems. The first system is the motor-test-rig and the second system is CONCIC II AGV. Both systems have been designed and developed in the Centre for Industrial Control (CIC) at Concordia University.

4.2 Principle of the Computed Torque Control (CTC) Scheme

The proposed CTC scheme of control finds applications in the field of electro-mechanical systems. In this study the suitability of the CTC scheme for the CONCIC II AGV operating in a dynamically changing environment is investigated. The dynamic parameters that change in real-time depend on the type of vehicle, its operating speed and the task carried out. For an AGV these parameters are the net change in payload, load shift while climbing slopes, changes in the load distribution, and changes in the coefficient of

friction between the wheels and the ground. The vehicle acceleration and controller gains have to be adjusted based on these changes. The vehicle acceleration can be modified by controlling the current delivered by the amplifiers. The control of which can be accomplished by (i) a computed torque control scheme which makes use of the known dynamic parameters of the vehicle and (ii) using sensors to provide data regarding these changes in real-time. This set up requires an inverse dynamic model of the vehicular system to compute the current requirement in order to account for changes in vehicle dynamics. As mentioned in the previous chapters, it has been reported in the literature for stationary robot arms that there is a significant reduction in the trajectory tracking errors as the dynamics are included in the control loop.

A general CTC scheme block diagram is presented in Figure 4.1. The inverse dynamics model of the system to be controlled works as a feed forward controller and the linear and angular velocities of the vehicle which are the parameter under consideration is being fed back. A PID filter or controller is included to achieve a fast and smooth response of the system to different changes.

4.3 Simulation Control Strategy

4.3.1 CTC Formulation and Control Loop

The simulation of the CONCIC II AGV is carried out while operating under the effect of a CTC scheme. The vehicle behaviour is presented by using its forward dynamic model as in equations (3.7) and (3.8). No terms are omitted from the model in the simulations for the sake of completeness. The loop includes the inverse dynamic model of

the vehicle as the feed forward controller. The velocity of the vehicle is chosen as the parameter to be monitored. Feed back is used to compare the real velocity to the desired velocity A PID controller consisting of a PI filter is used to achieve a fast and smooth response. The amplifiers of the motors are modeled and included as gains in the loop. Figure 4.2 presents the control block used in the simulation. Simulation of the vehicle is carried out while the vehicle experiences changes in the dynamic parameters during its operation. The current study investigates the effect of changes in payload and the contact friction between the tire and the ground.

4.3.2 Conventional Velocity Control Loop

The simulation of the CONCIC II AGV is also carried out while operating under the effect of the conventional Velocity Control scheme. In this thesis, the objective of the simulation is to monitor the vehicular system response when a dynamic parameter changes significantly during operation.

The control loop used for this simulation is presented in Figure 4.3. The controller makes use of the error in wheel velocities in conjunction with an inverse kinematic model to adjust the velocity commands for the actuators of the vehicle. This can be expressed as the low level servo control. The velocities of the actuators are altered by adjusting the voltage output of the amplifiers. Results are obtained and presented in the following chapter. A set of different cases of changing payload of the vehicle are simulated and tabulated in Table 5.1.

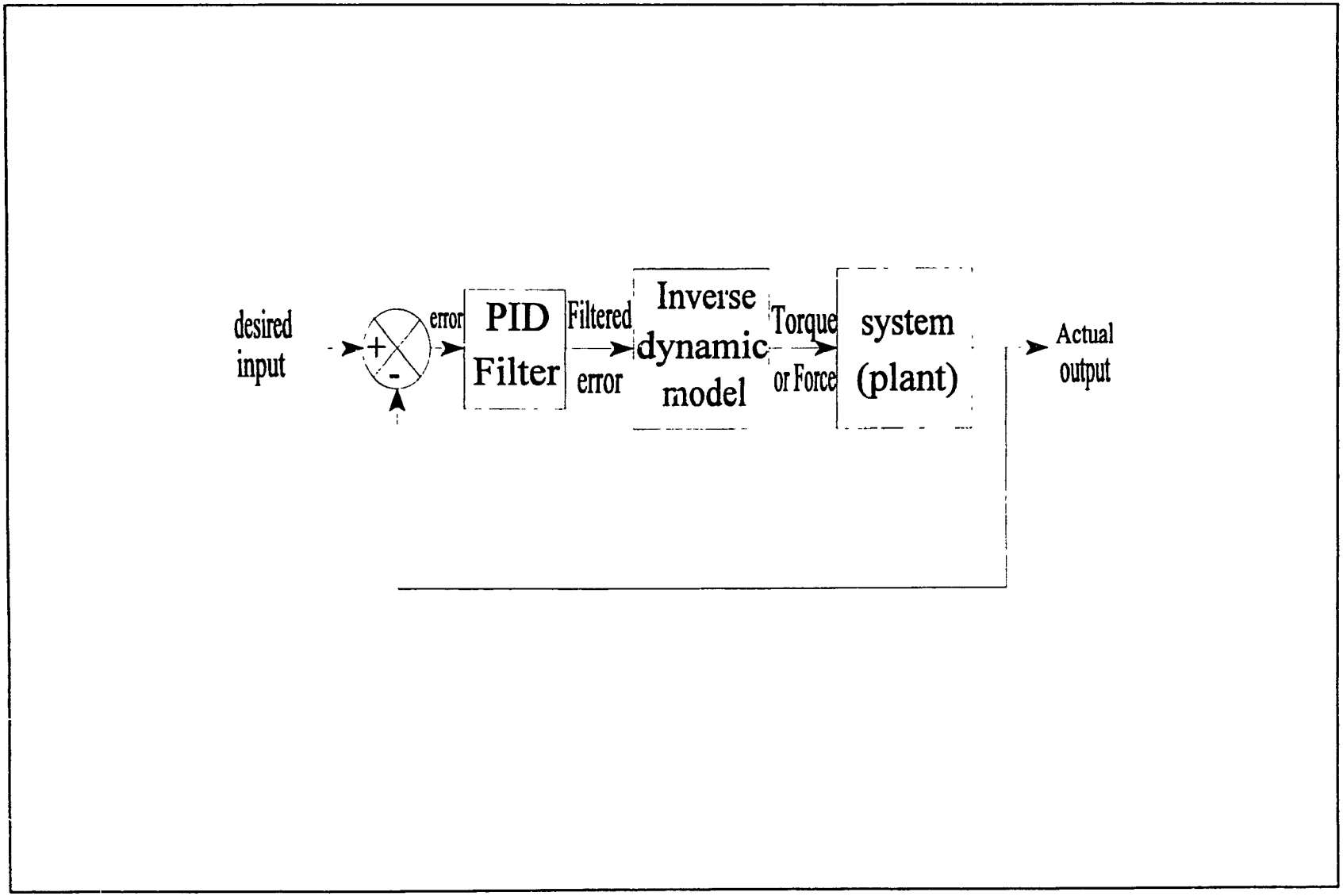

Figure 4.1 Schematics of a Computed Torque Control (CTC) Loop

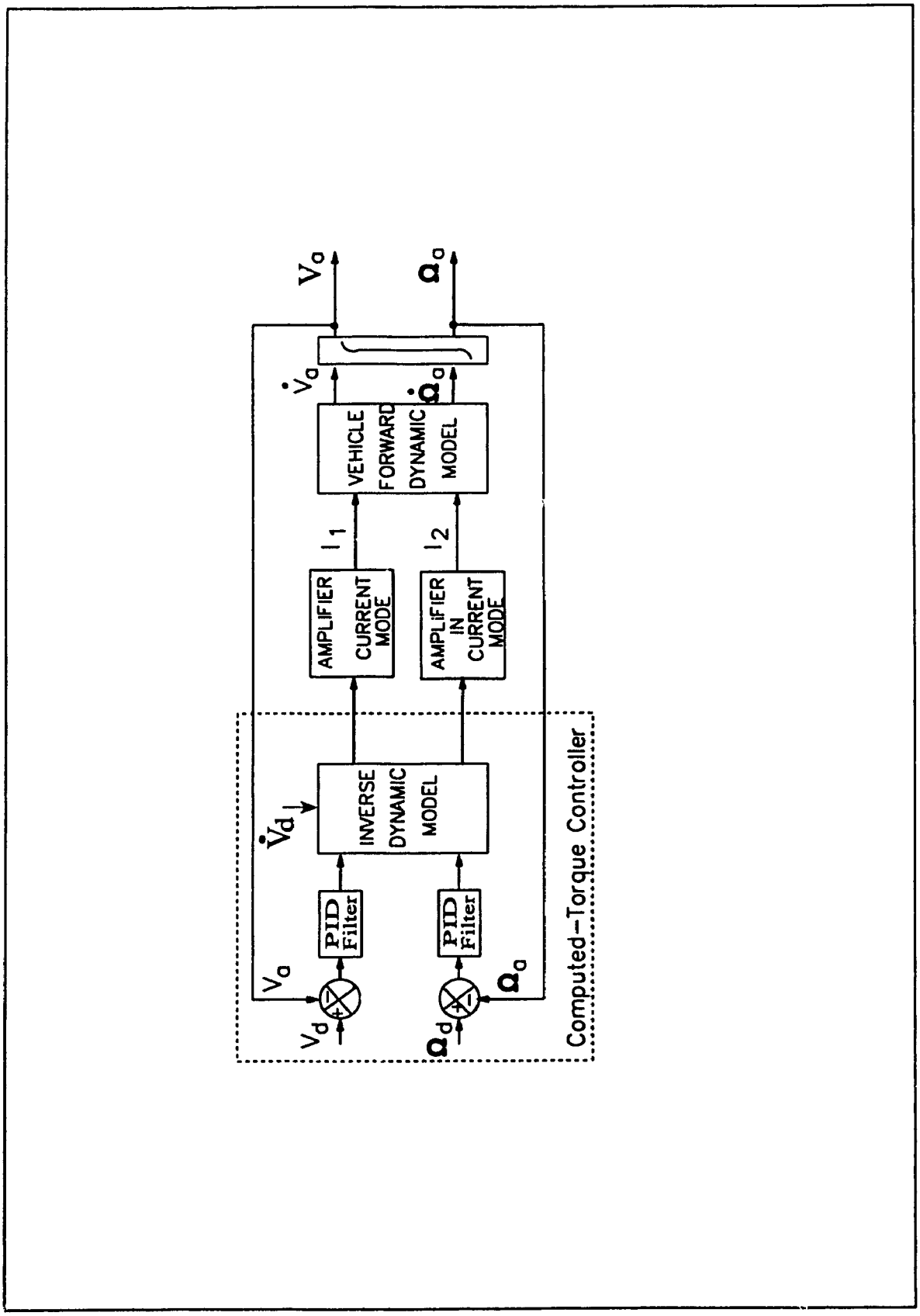

Figure 4.2 Schematic of the Computed Torque Control Scheme Loop of the AGV

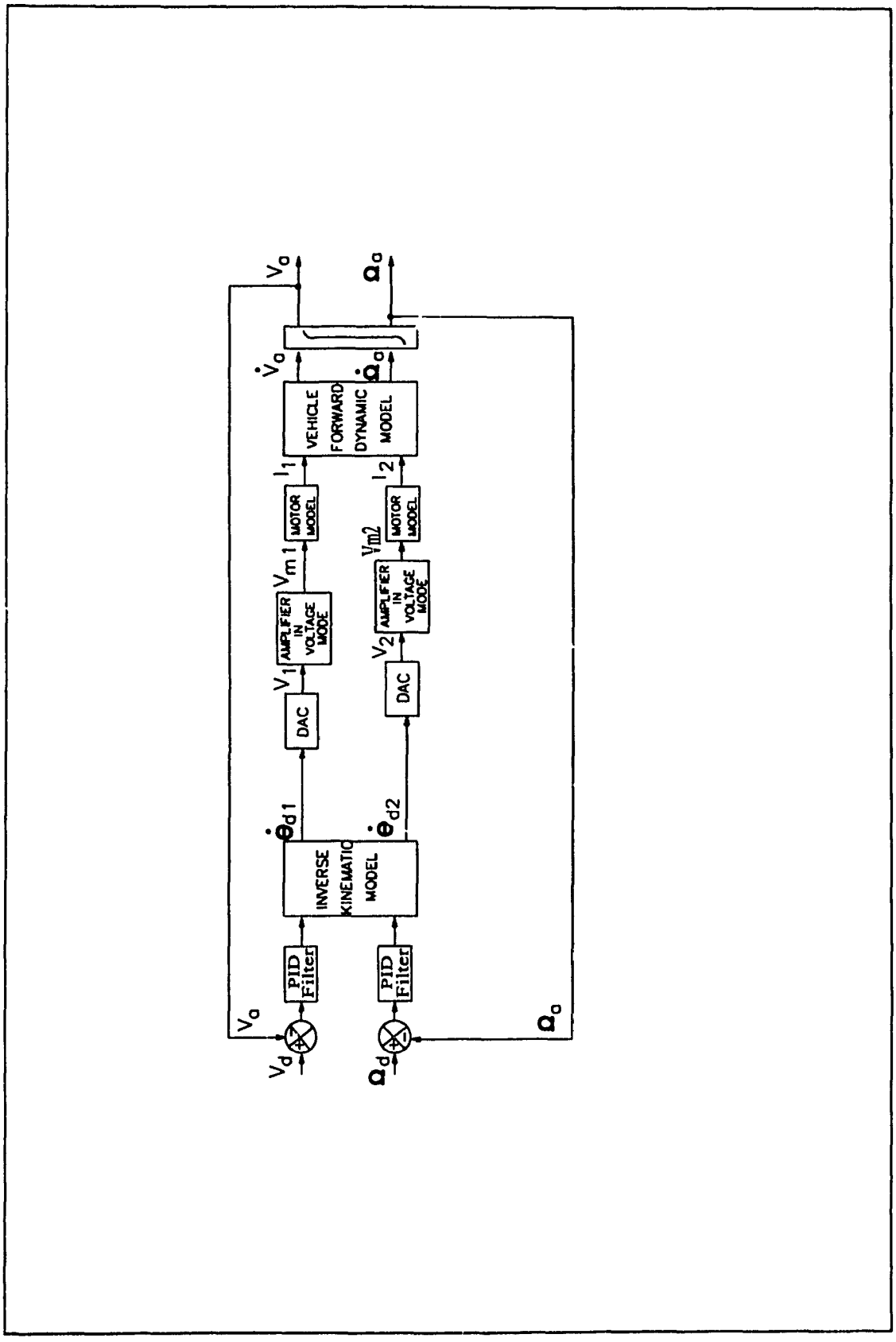

Figure 4.3 Schematic of the Conventional Velocity Control Loop of the AGV

4.4. Experimentation Control Strategy

4.4.1 Experimental motor-test-rig setup

An experimental setup has been designed and built in the Centre for Industrial Control (CIC) at Concordia University to monitor the motor response using different control schemes. In this case the CTC scheme and the conventional velocity control scheme are used to control the motor and monitor its response. Motor-test-rig detailed schematics and dimensions are presented in Appendix -B. The motor used is the same permanent magnet (PM) motor used as an actuator for the CONCIC II AGV. The control of the motor is accomplished from a PC through an interface card. The feed-back of the motor speed is read from an encoder through an LM628 chip [46] on the interface card designed for this purpose. Control loops that have been used for testing are presented below.

4.4.1.1 Computed Torque Control (CTC) Loop

To apply the CTC scheme to the motor rig, the control loop in Figure 4.4 has been designed and implemented. The objective of the control strategy is to maintain the motor speed constant in the presence of changes in its dynamics. This is achieved by controlling the current output to the motor. The current required by the motor is proportional to the amount of torque required to overcome the changes in its dynamics. In the CTC scheme the current required is pre-calculated using the inverse dynamic model of the system and a command signal is sent to the amplifier, which in turn will allow the motor to draw current in proportion to the command signal while operating in the current mode.

4.4.1.2 Conventional Velocity Control Loop

In the conventional control scheme the velocity error is used to form a velocity command to the motor and adjust its speed without considering the amount of current being consumed by the motor. Moreover, adjusting the motor speed is achieved through adjusting the motor terminals voltage. This kind of control scheme is sometimes named a PID controller in the literature. The main part that forms the forward controller is only the PID filter. Figure 4.5 shows the control loop of the conventional velocity control scheme used for the motor-test-rig.

4.4.2 The Automated Guided Vehicle AGV

4.4.2.1 Computed Torque Control CTC Loop

CONCIC II AGV is chosen as a platform to test the proposed CTC scheme. Figure 4.6 presents the control block diagram of the CTC scheme implementation on the AGV. Dynamic parameters that change while operating the AGV are previously incorporated in the inverse dynamic model of the AGV. The velocity of the AGV is the computed by monitoring the wheel speeds and fed back. The inverse dynamic model works as a feed forward controller for the AGV. The current required to run the AGV actuators at all cases is calculated using this model. The error in velocity is calculated and filtered using the PI filter. The calculation of velocity of the vehicle in relation to the actuator velocities is performed using a forward kinematic model of the AGV. The current command is then sent to the amplifiers through the DAC.

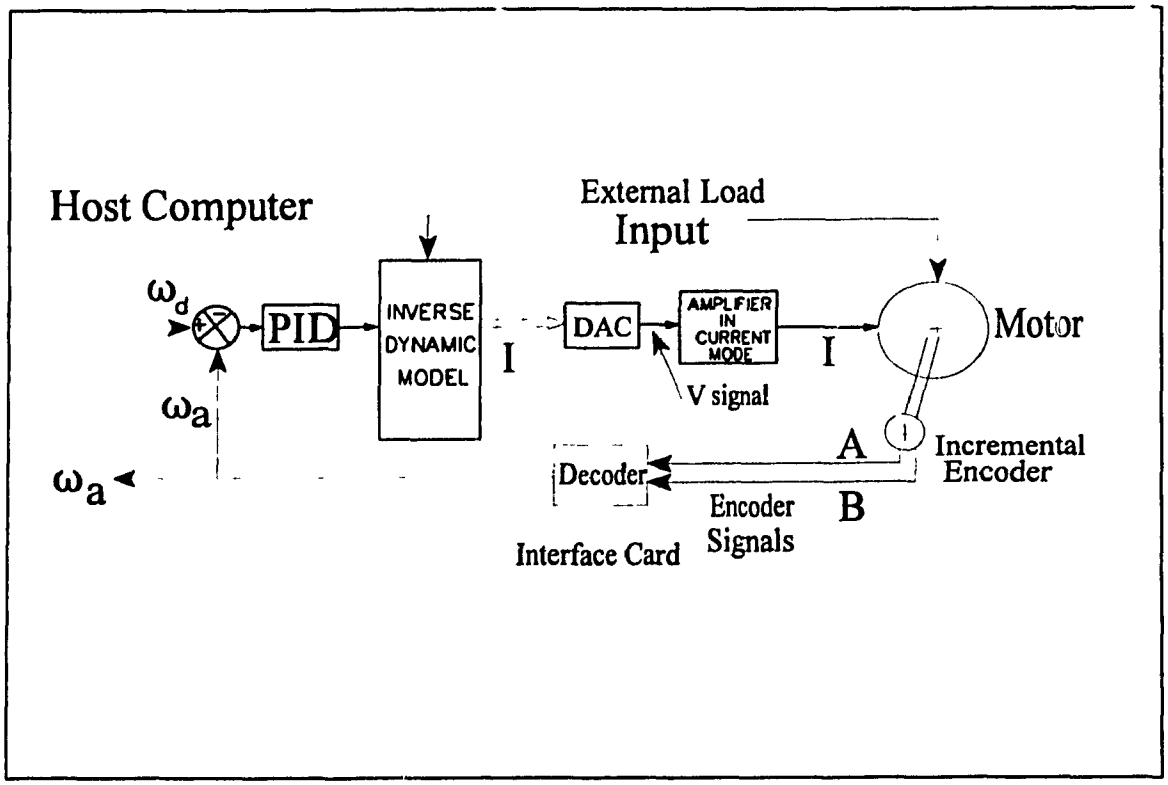

Figure 4.4 CTC Scheme Schematic for the Motor Test Rig

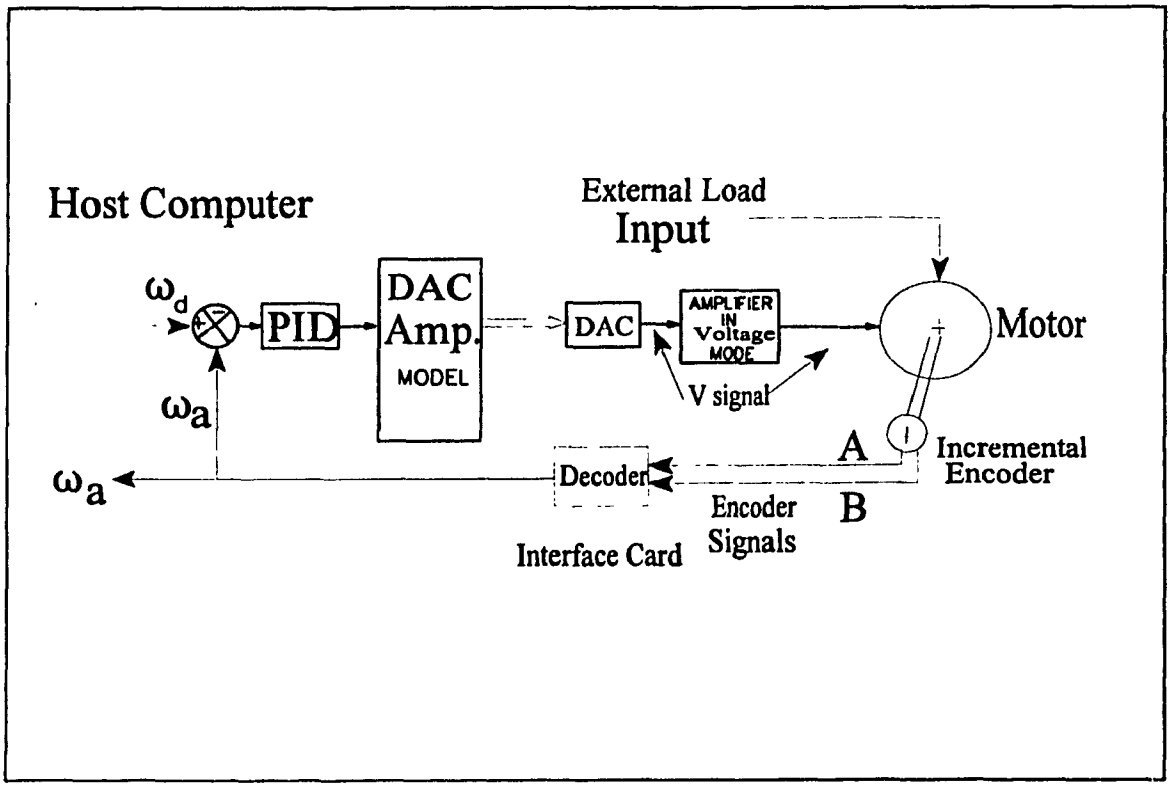

Figure 4.5 Conventional Velocity Control Scheme for the Motor Test Rig

4.4.2.2 The Velocity Control Loop

CONCIC II AGV is also operated under the effect of a conventional Velocity Control scheme. The scheme makes use of a PI filter and the kinematic models of the CONCIC II AGV to accomplish the cartesian level control of the vehicular system. The AGV velocity error is calculated from the speed of the actuators which are read by using the encoders in conjunction with the LM628 chips on the interface card in the pc. Figure 4.7 represents the block diagram of the conventional Velocity Control scheme applied to the AGV. The AGV velocity is monitored while in operation and dynamic parameters are changed similar to the changes that happen using the CTC scheme.

4.5 Summary

In this chapter the schematic diagrams presenting the control strategy implemented for the simulation studies and experimental validations are presented. A control strategy to simulate the CONCIC II AGV behaviour under the effect of the CTC scheme is designed and its schematic diagram is presented. In a similar fashion, a control loop is presented to explain the conventional velocity control scheme used to control the vehicle.

On the experimentation side, a motor-test-rig is used to validate the CTC scheme. This setup is used to start the experimentation before testing the CONCIC II AGV. The CTC loop is designed and presented for the motor-test-rig. The conventional velocity control loop schematics diagram is presented.

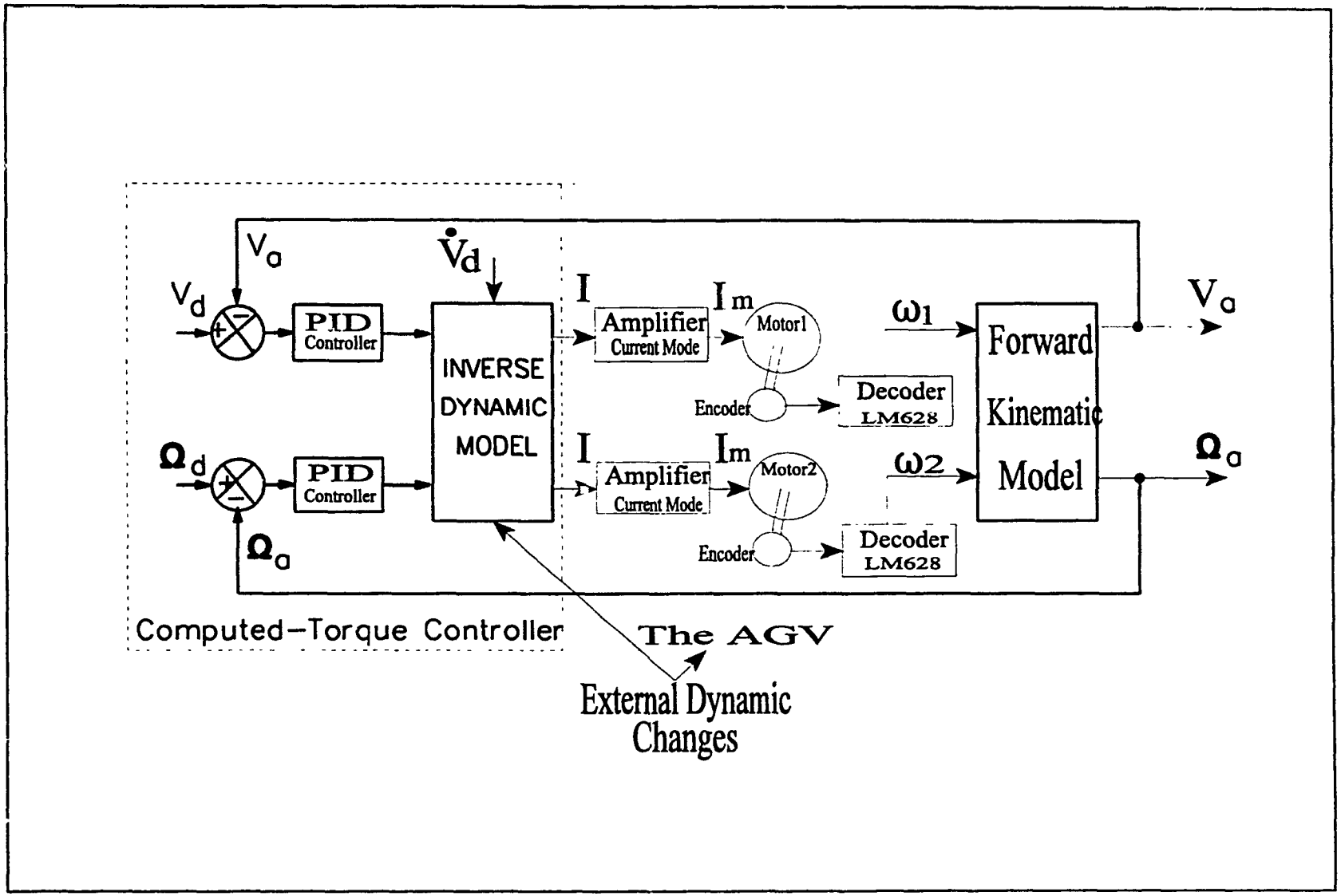

Figure 4.6 Schematics of the Computed Torque Control Scheme of the AGV

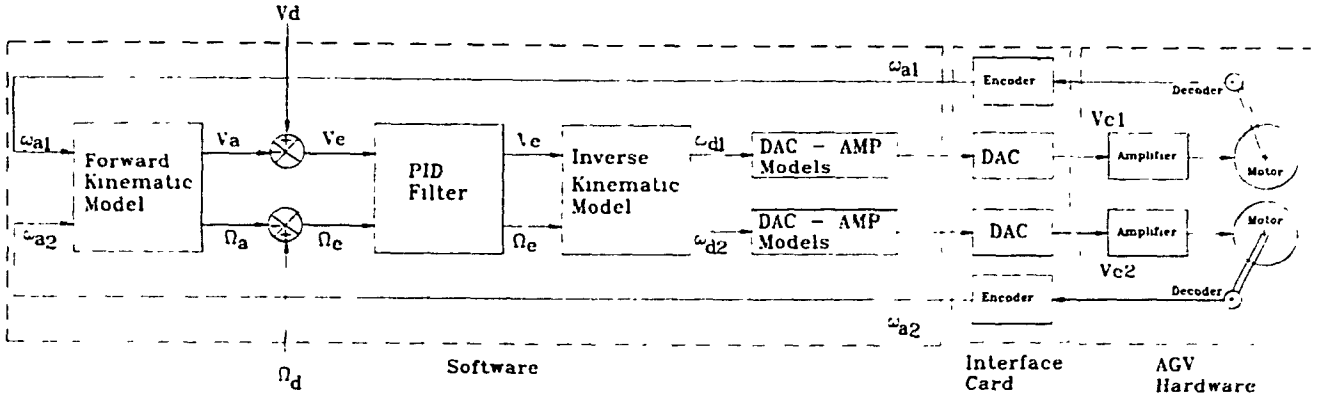

Figure 4.7 Schematics of the Velocity Control Sc[illegible]e of the AGV

Finally the CTC scheme loop of control is designed and presented for the CONCIC II AGV. In addition, a conventional velocity control loop is also presented to control the vehicle. The implementation of these control loops is accomplished and presented in the following chapters.

CHAPTER 5 SIMULATIONS

5.1 Introduction

Simulation study of dynamic systems is used as an efficient tool to study the performance of the system under various operating conditions. Further, simulation allows the design and development of various control schemes without having to build the actual system. Indeed, it is necessary to validate the findings of the simulation studies with an experimental system. In this thesis, simulations of the CONCIC II AGV have been carried out extensively under the influence of the proposed CTC scheme. The results are compared with those obtained using a velocity control scheme. Simulations are carried out for the following changes in the dynamic parameters of the vehicle and the environment.

(i) Payload changes on the vehicle by 5 times its gross mass (200 kg) while operating at different desired velocities (1, 2 and 5 m/s).

(ii) Different coefficient of friction for rolling (3 and 10 times the nominal value) between the wheels and the ground with payload change.

(iii) Vehicle on a curved path and undergoing payload changes as mentioned above.

In all these simulations, the maximum peak current delivered by the amplifiers have been restricted to 20 amps. This value is chosen as the motors used in the experimental vehicle have a peak current of 39 Amps and the amplifier can allow this current to be available only for a short time (1 to 2 seconds at the most).

5.2 CTC Simulation Software

The proposed simulation schematic of the CTC scheme for CONCIC II AGV is presented in Figure 5.1. This schematic diagram illustrates the interaction between the commands and outputs of different modules of the vehicular system. A software program in modular form has been developed to carry out the simulation study. A flow chart of the program is shown in Figure 5.2. The significant modules of this program are explained in the following sections.

5.2.1 Main Module

This module acts as the coordinator for the simulation process and calls other modules in addition to providing the final output. The desired parameters for operating the AGV, namely, the desired linear and angular velocities and accelerations of the vehicle, the load changes, changes in rolling friction coefficient, and their specific instant of change and the desired outputs to be monitored, are provided.

In this module the variables of the program are initialized and all the counters of the program are included and checked for different specified moments. The flow chart of this module is shown in Figure 5.2.

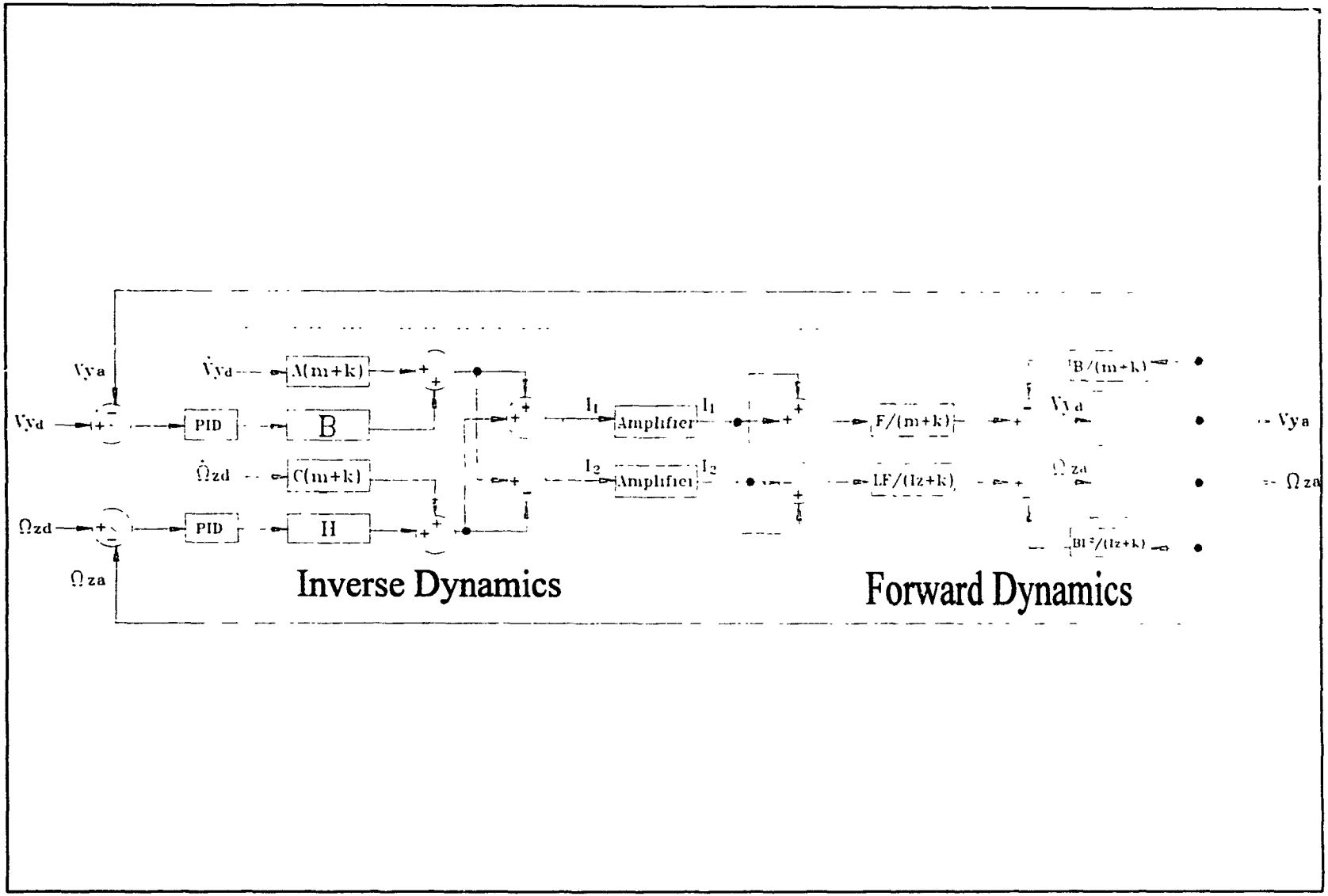

Figure 5.1 Schematic of the CTC Scheme Implementation for Simulation Studies

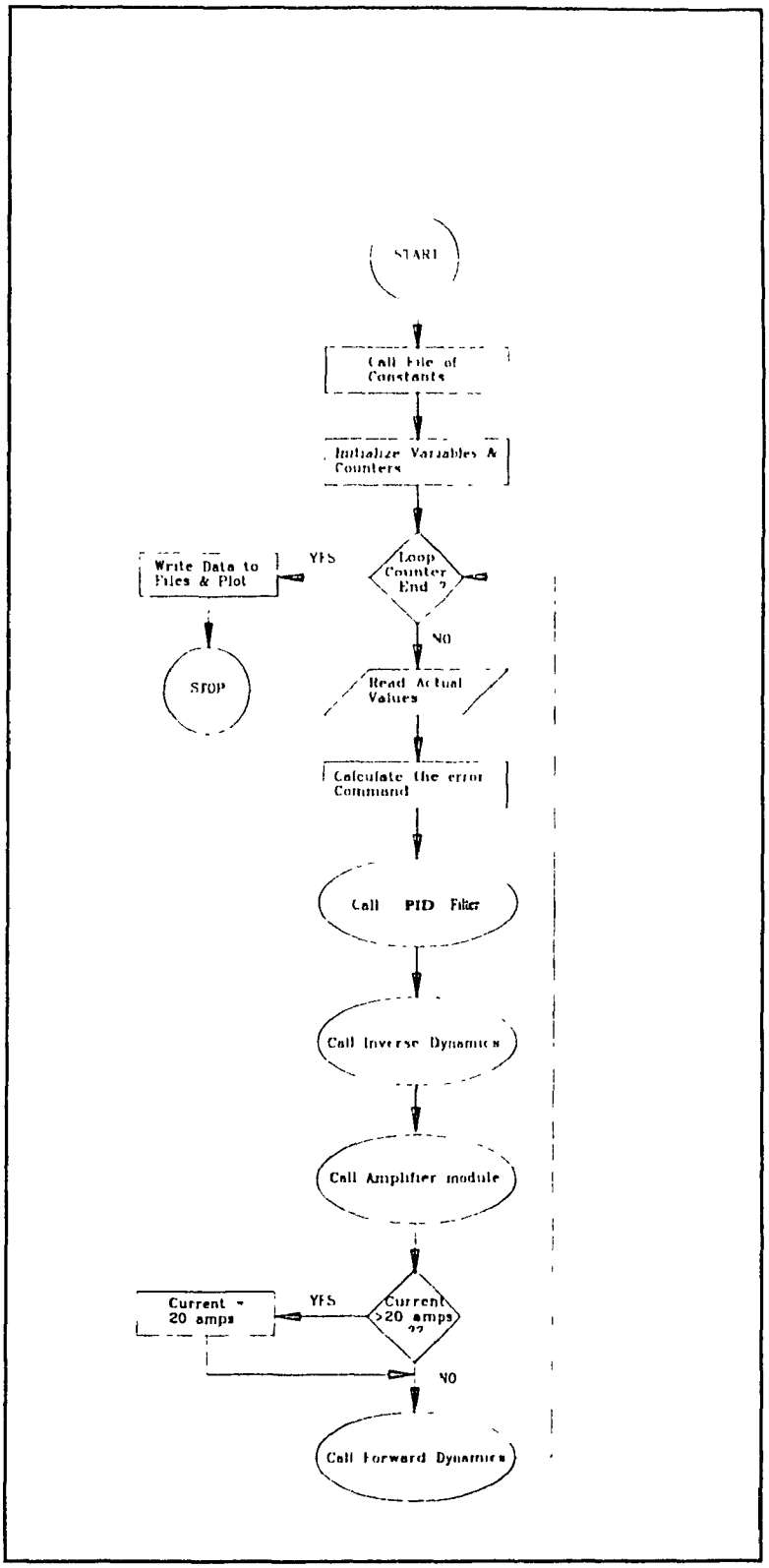

Figure 5.2 Flow chart of the MAIN Simulation Program of the CTC Scheme Implementation

5.2.2 Inverse Dynamic Module

This module contains the inverse dynamics model of the AGV. It receives the error command in linear and angular velocity as an input and calculates the current command required by the actuators as an output. Figure 5.3 shows a flow chart of the function performed by this module.

5.2.3 Forward Dynamic Module

This module simulates the movement of the vehicle. The inputs to this module are the current values for the vehicle actuator models provided by the amplifiers models. The outputs are the angular and linear acceleration of the vehicle. This module calls a numerical integration module to calculate the velocities from the computed accelerations. This module is updated at a faster rate than the external simulation loop. This is because at a constant control command the parameters of the vehicle (position, velocity) are not constant. Further, by the time the control command is calculated and sent to the system, the system parameters would have changed already. Figure 5.4 presents the flow chart of this module.

5.2.4 PID Filter Module

This module contains a PI filter alone and is used in the control loop. A proportional gain is used to achieve a fast response of the system. An integral gain is used to eliminate steady state errors. The gain values where initially tuned using the Zeigler-Nichols method mentioned in Chapter 3 and then fine tuned experimentally for the case of the AGV operating

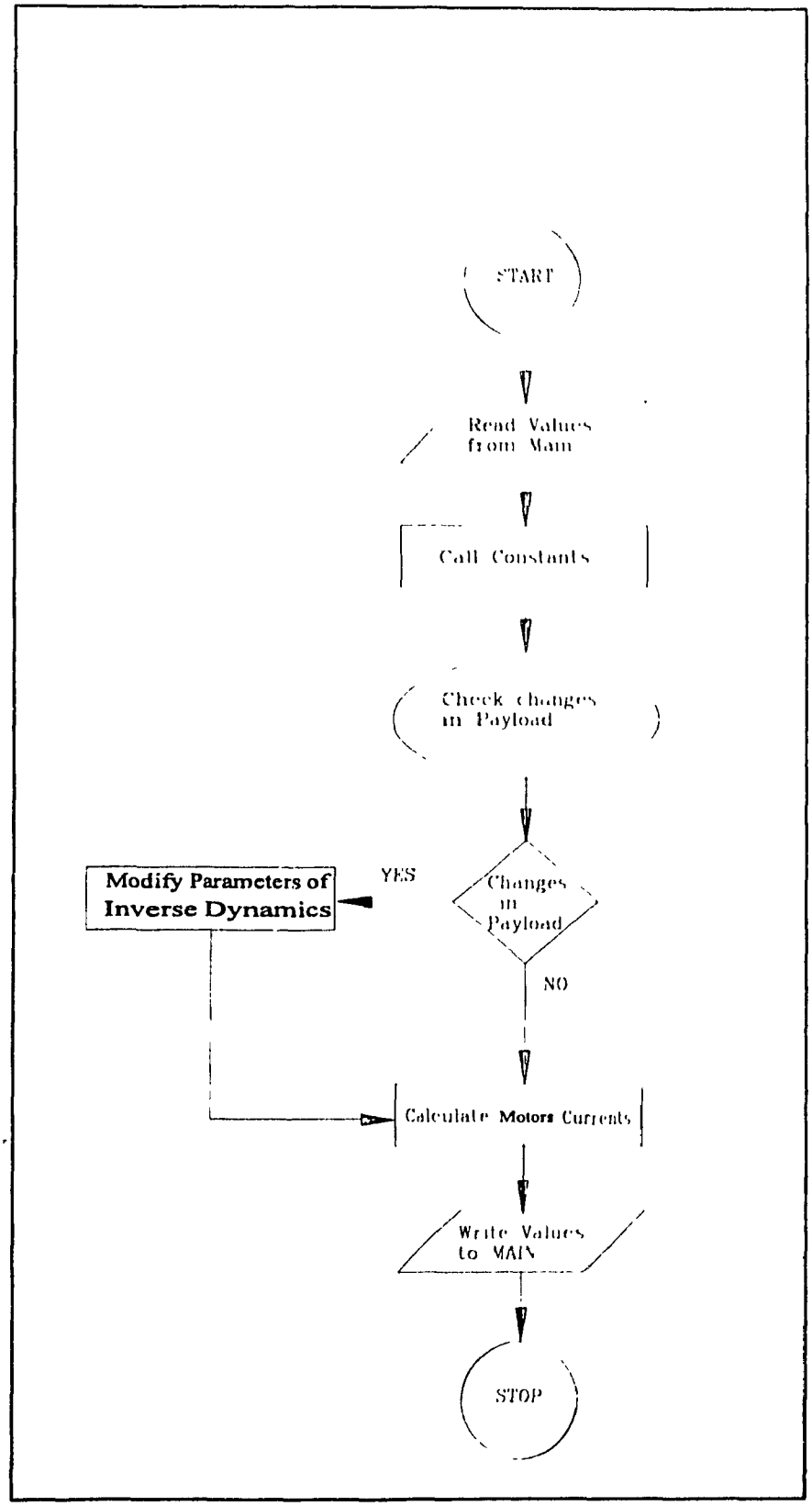

Figure 5.3 Flow Chart of the Inverse Dynamics Module

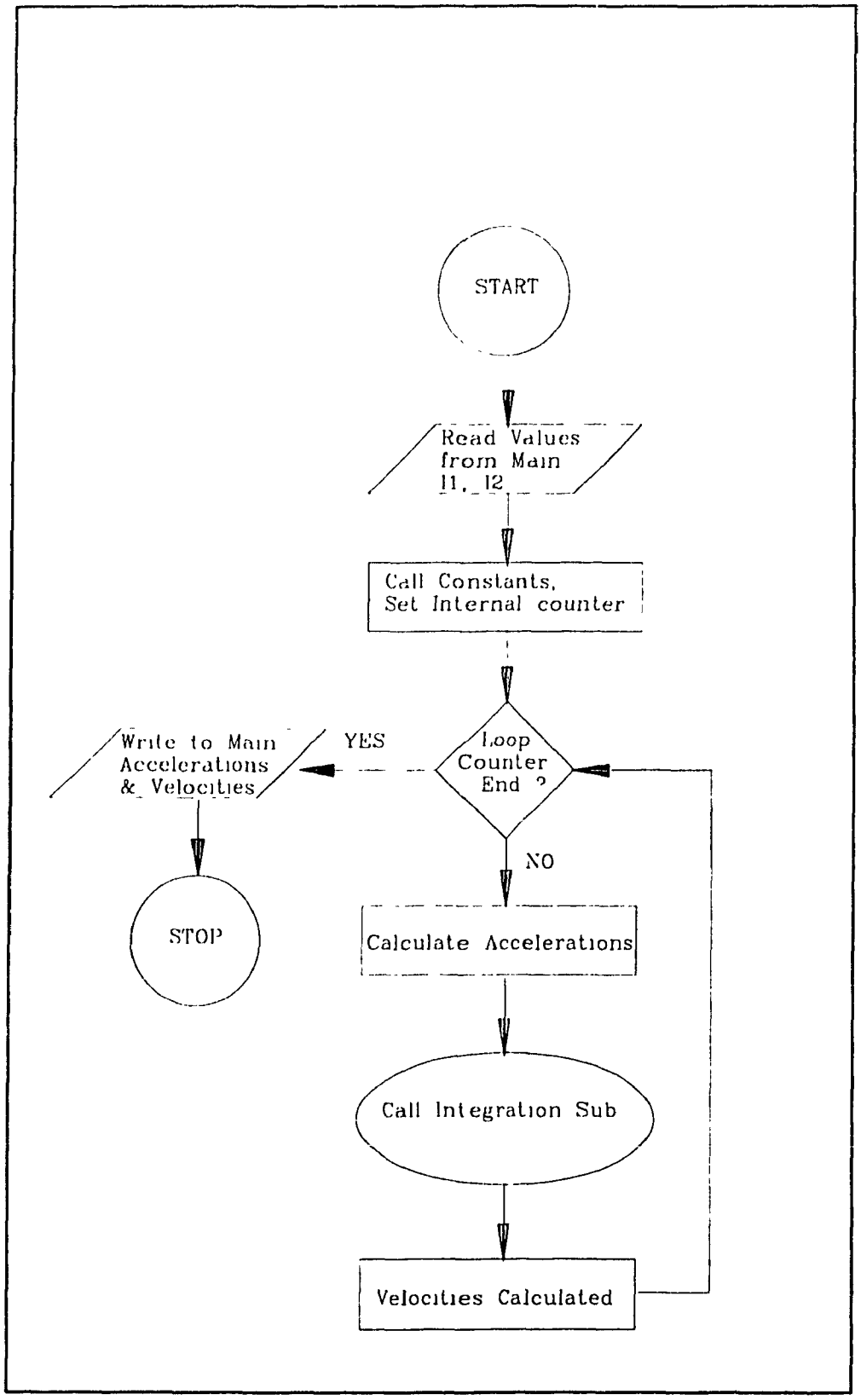

Figure 5.4 Flow Chart of the Forward Dynamics Subroutine

at a linear velocity of 1 m/s and no loads added while moving along a straight line. It is to be mentioned here that the same set of gains used has provided excellent response for all operating conditions.

5.3 Conventional Velocity Control Scheme Simulation Software

The simulation of the CONCIC II AGV is also carried out while operating under the influence of a velocity control scheme shown in Fig. 5.5.

A program has been written to carry out this simulation study. Figure 5.5 presents a schematic of this simulation. The interaction between commands and different modules of the software are illustrated in this schematic. The program is in a modular form as shown in the flow chart of Figure 5.6 where the main module is presented. The module containing the CONCIC II AGV dynamic model is the same as the one used in the simulation program for the CTC scheme.

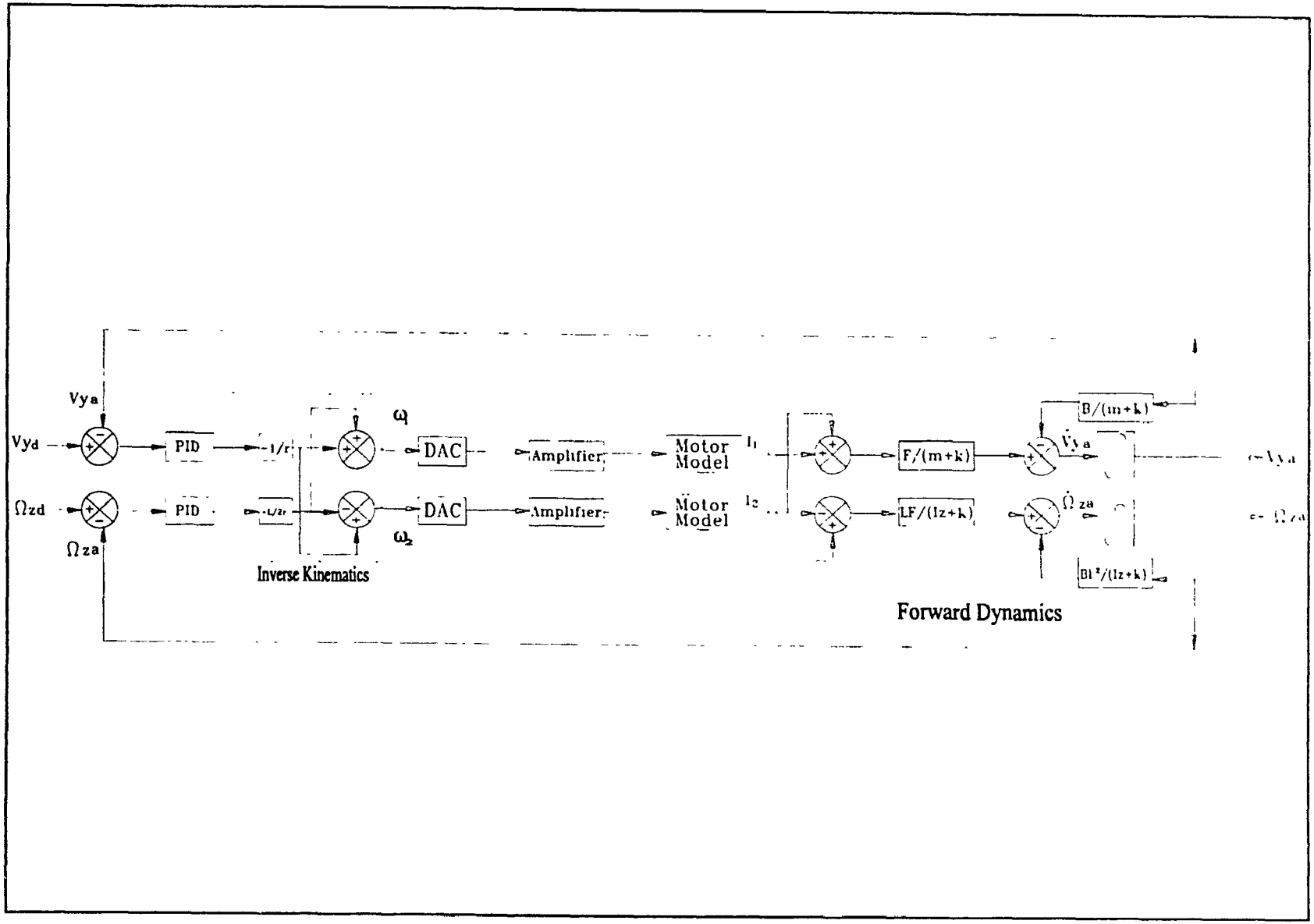

Figure 5.5 Schematic of the Conventional Velocity Control Scheme Simulation

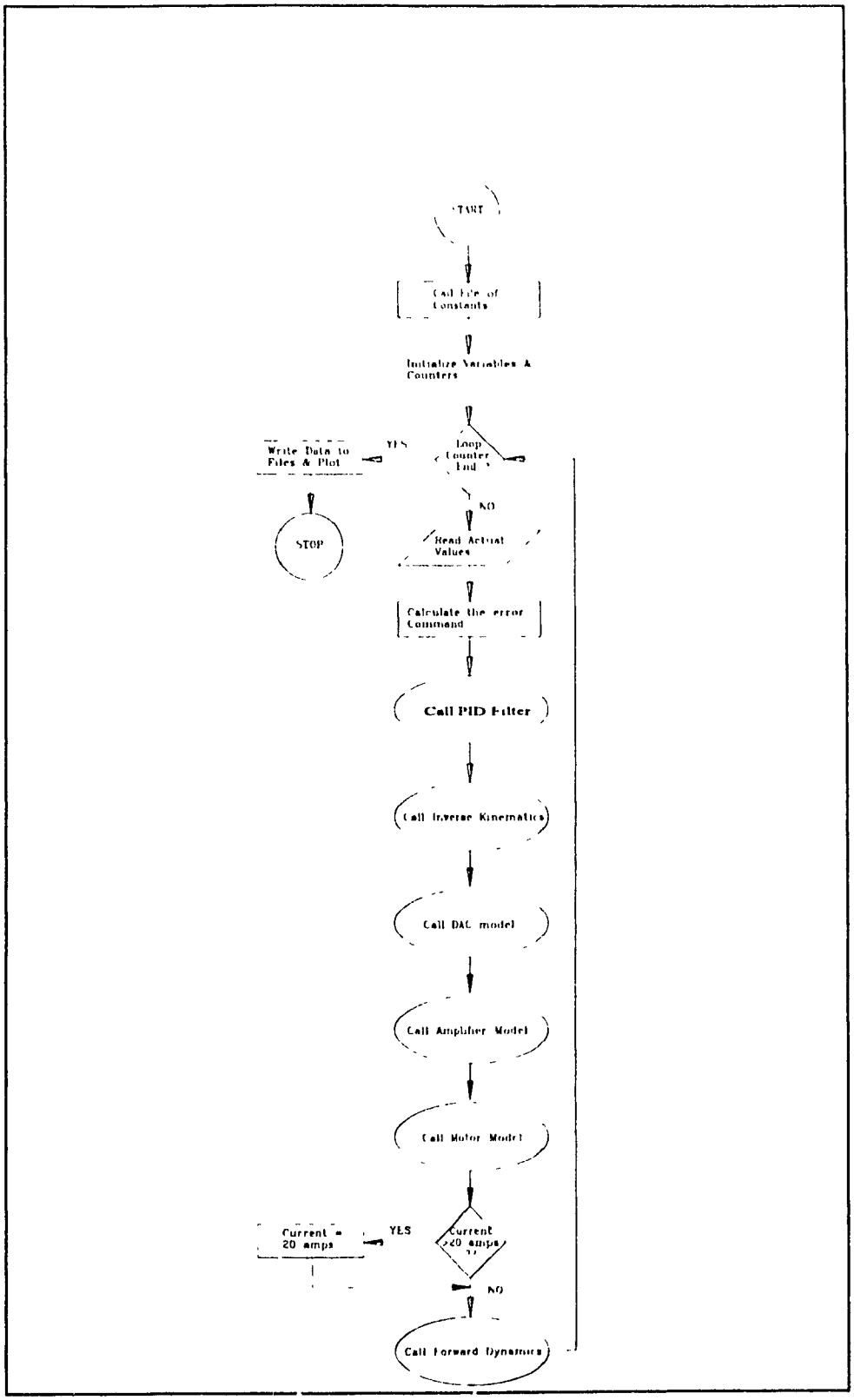

Figure 5.6 Flow Chart of the MAIN Simulation Program of the Velocity Control Scheme Implementation

5.3.1 Main Module

This module is similar to the main module used for CTC simulation. This module is the coordinating module that calls all the other modules. The flow chart for this module is shown in Figure 5.6. The following modules are the ones different from the modules comprising the CTC scheme simulation.

5.3.2 Inverse Kinematic Module

This module includes the equation for inverse kinematics of the CONCIC II AGV as presented in Chapter 3. The input to this module are the linear and angular velocities of the vehicle and the outputs are the wheels speeds.

5.3.3 Motor Module

This module includes a mathematical formulation representing the motors used on-board the CONCIC II AGV. This module receives the voltage as an input and calculates the corresponding current as an output. The output of this module is checked by the main module for maximum power availability and then fed as an input to the forward dynamics model module, which is explained in Section 5.2.3.

5.3.4 Amplifiers and DAC Modules

These modules include the equations presented for both the DAC and the amplifier in Chapter 3. The mathematical relations included in those modules are for the physical components currently available to control the CONCIC II AGV.

5.4 Results and Discussion

Simulation has been carried out using the above mentioned MATLAB programs. Operating conditions considered for study are summarized in Table 5.1. The results are presented for the CONCIC II AGV operating under the influence of both the CTC scheme and the conventional velocity control scheme. For straight paths, the linear velocity and acceleration are presented. For curved paths the angular velocity and acceleration in addition to the above, are also included.

5.4.1 AGV Response without any Change in Dynamic Parameters

Figures 5.7 to 5.12 show the AGV response for both schemes of control with no changes in vehicle dynamics. The tests are performed for the vehicle moving along a straight line with different desired linear velocities. Figure 5.7 presents the velocity of the vehicle when the desired velocity input is 1 m/s. Figure 5.8 presents the acceleration of the vehicle for the same desired velocity input. For a desired velocity of 2 m/s the performance of the vehicle is presented by Figure 5.9 for velocity and Figure 5.10 for acceleration. In the case of the desired velocity being 5 m/s, Figure 5.11 presents the vehicle velocity response and Figure 5.12 presents the vehicle acceleration . From these figures it can be seen that the CTC scheme exhibits faster response to attain the desired velocities compared to the conventional velocity control scheme. Since the maximum available power limit is implemented by setting an upper limit to the current at 20 amps, for both schemes, the effects can be seen in the acceleration response plots. For example, it can be seen from the simulation results presented in Figure 5.7 that the velocity control scheme takes 1.6 seconds

to reach the desired speed of 1 m/s, while the CTC scheme requires only 0.8 seconds. This time can be reduced further by (i) increasing the vehicle acceleration, (ii) changing the gain settings for the PI filter used, and (iii) having a higher current limit. At higher speeds (> 1 m/s) the conventional control scheme requires a larger period of time to provide the required response compared to the CTC scheme. The chosen filter gains for the CTC scheme still provide a satisfactory response at all speed ranges considered in this simulation study (0 to 5 m/s).

5.4.2 Response for Payload Change

Results of payload changes are shown in Figures. 5.13 to 5.20. Figure 5.13 is the vehicle velocity response and Figure 5.14 is the vehicle acceleration response to payload increase by 5 times the vehicle mass, with a desired velocity input of 1 m/s. The jump in the vehicle velocity once the payload is increased is a result of an increase in the vehicle acceleration. The later increases because of the increase in the current calculated and allowed to the motors to compensate for the payload increase. This same effect can be seen through the Figures 5.13 to 5.16. In the case of payload decrease, Figures 5.17 to 5.20, the current calculated and allowed for the motors is reduced and accordingly a deceleration occurs causing a cancellation of the vehicle velocity jump that is produced by payload reduction. Figure 5.15 and 5.16 are the vehicle velocity and acceleration response respectively for payload increase by 5 times the vehicle mass and a desired velocity of 2 m/s. Figure 5.17 and 5.18 are the vehicle velocity and acceleration response respectively for a payload decrease from 5 times the vehicle mass to no payload at a desired velocity of 1 m/s.

Figure 5.19 and 5.20 are the vehicle response in terms of velocity and acceleration respectively for load decrease off the vehicle from 5 times the vehicle mass to no payload with a desired velocity of 2 m/s. It can be seen from these figures that the CTC scheme exhibits faster response and provides good control to maintain the linear velocity after load change at the desired level compared to the velocity control scheme. Vehicle acceleration response plots presented in Figures (5.14, 5.16, 5.18, 5.20) illustrate the reason for higher speed of response of CTC compared to the velocity control scheme. For example, at a velocity of 1 m/s and after increasing the payload, the steady state speed is 0.96 m/s for the conventional velocity control scheme, while it attains the desired value of 1.0 m/s in a short interval under the influence of the CTC scheme. The same can be seen when the vehicle speed is 2 m/s. The velocity control scheme does not alter the vehicle acceleration after load change and hence the drop in linear velocity. In the case of payload decrease, the AGV is assumed to start the motion with the payload. At t = 5 seconds the payload is removed from the vehicle. CTC scheme still maintains faster and more accurate response than the conventional control scheme. At that instant of time the conventional control scheme would still be in a transient period of response. This means that the AGV is still accelerating to reach the desired velocity. The payload decrease helps the controller to reach its limit faster, although the acceleration response is not as smooth or as fast (almost half the value under CTC scheme) as the one obtained using the CTC scheme.

5.4.3. Response to Payload Change on One Wheel or One Castor

This test simulates the practical situation of unequal load distribution on the AGV,

load shift while moving along a curved path or accelerating from rest, going up a hill or down a hill. Figures 5.21 and 5.22 present the vehicle response when one of the driving wheels is loaded. In the case of having velocity control scheme, velocity drops by 4%, while under the influence of the CTC scheme the velocity is maintained as desired. Figures 5.23 and 5.24 show the response for payload change on one of the castors. For the case of velocity control scheme, the velocity drops by 3%, while the CTC scheme maitains the desired velocity value. Figure 5.24 shows the drop in acceleration of the vehicle when loaded and then the response of the controller by acceleration increase to assure maintaining the velocity of the vehicle at the desired level. In both cases, the CTC scheme exhibits a faster response with less oscillations while maintaining the overshoots minimum. A jump in the velocity caused by a jump in acceleration for both cases is caused by the increase in current calculated and allowed to the driving motors by the forward model-based controller.

5.4.4 Response for Change in Rolling Friction Coefficient

The set of simulations represented in Figures (5.25 to 5.28) illustrates the AGV response to payload change while having a different rolling friction coefficient between the wheels and the ground. The coefficient is increased 10 times the original value (0.007). The CTC scheme exhibits excellent control compared to the velocity control scheme in the presence of changes in tire friction coefficient. These characteristics are similar to the ones shown by the test in Section 5.4.2. In this test the velocity due to payload increase drops to 60 % of the desired value after 5 seconds of operation, since the dynamic change took place while the vehicle is under the velocity control scheme. The velocity of the vehicle is still

showing a decreasing response after that. The speed attained is 95 % of the desired value at a friction factor increase of 3 times the original and for the same scheme of control and payload increase. For the CTC scheme, the vehicle speed is maintained at the desired value for all changes in thye friction factor.

5.4.5 Response for Moving along a Curved Path

The AGV is tested in simulation for travelling along a curved path of 5 meters radius at a linear velocity of 1 m/s and an angular velocity of 0.1 rad/s. The linear and angular velocity response is presented in Figures (5.29 to 5.40). The CTC scheme exhibits faster response with and without change in payload and rolling friction coefficient. This can be seen particularly in the Figures 5.37 to 5.40 where the payload change is combined with a rolling friction coefficient increase. Velocity is maintained at all cases by the CTC scheme at the desired value 1 m/s. In the case of the velocity control scheme the attained velocity is 95 % of the desired value due to friction coefficient change and 85 % after payload increase. Figure 5.29 presents the vehicle linear velocity for both schemes of control. With no dynamic changes imposed on the vehicle, both schemes maintain the vehicle linear velocity at the desired value. Figure 5.30 presents the angular velocity of the vehicle performing under the effect of both schemes of control and with no dynamic changes. The CTC scheme maintains the desired angular velocity while under the effect of the velocity control scheme the vehicle is still building up the angular velocity response to reach the desired value. The desired value is not reached even after 25 seconds of running. Figures 5.31 and 5.32 represnt the acceleration of the vehicle related to the velocities in Figures 5.29

5.30 respectively. Figures 5.33 and 5.34 represent the vehicle linear and angular velocity response respectively. In this case a payload increase is applied to the vehicle at time = 10 seconds. Combining these Figures with the acceleration of the vehicle presented by Figures 5.35 for linear acceleration and 5. 36 for angular acceleration, the CTC scheme shows a superior performance compared to the velocity control scheme in maintaining the desired vehicle response. It is to be noticed that in all Figures a jump in velocity and acceleration of the vehicle shows upwards for payload increase and downwards for payload decrease as a result of increasing or reducing the current calculated and allowed for the motors by the model-based forward controller to compensate for the payload change.

5.5 Summary

In this chapter a simulation study of the CONCIC II AGV is presented. A comparison between the AGV response with a CTC scheme and a conventional velocity control scheme is provided. The CONCIC II AGV behaviour is investigated and monitored using a forward dynamic model of the vehicle in simulation. Different situations where dynamic changes can occur are identified and tested. The results indicate that the CTC scheme maintains the desired velocity in the presence of changes of dynamics of the vehicle where the velocity control schemes fails to achieve the same output. For a desired velocity of 1 m/s, the velocity control scheme maintains the velocity at 95 % of the desired value under a payload change of 5 times the vehicle mass. For changes in friction coefficient between the wheels and the floor by 10 times the original value (0.007) the velocity drops to 60 % of the desired value in a 5 seconds period, and it continues to decrease. Further, the CTC scheme always exhibits a faster response than the velocity control scheme.

Table (5.1) List of the tests of simulation of the AGV and the figures of results related.

No	Type of Test	V m/s	Ω rad/s	Figure No. & Type of response
1	No Dynamic Changes	1	0	(5.7) Linear Velocity (5.8) Linear Acceleration
2	No Dynamic Changes	2	0	(5.9) Linear Velocity (5.10) Linear Acceleration
3	No Dynamic Changes	5	0	(5.11) Linear Velocity (5.12) Linear Acceleration
4	Payload Increase	1	0	(5.13) Linear Velocity (5.14) Linear Acceleration
5	Payload Increase	2	0	(5.15) Linear Velocity (5.16) Linear Acceleration
6	Payload Decrease	1	0	(5.17) Linear Velocity (5.18) Linear Acceleration
7	Payload Decrease	2	0	(5.19) Linear Velocity (5.20) Linear Acceleration
8	Payload Increase on The Left Driving Wheel Only.	1	0	(5.21) Linear Velocity (5.22) Linear Acceleration
9	Payload Increase on The Rear Castor Only.	1	0	(5.23) Linear Velocity (5.24) Linear Acceleration
10	Payload Increase & Rolling Friction Coefficient Increase 3 times	1	0	(5.25) Linear Velocity (5.26) Linear Acceleration

No	Type of Test	V m/s	Ω rad/s	Figure No. & Type of response
11	Payload Increase & Rolling Friction Coefficient Increase 10 times	1	0	(5.27) Linear Velocity (5.28) Linear Acceleration
12	No Dynamic Changes Moving on a Curved Path	1	0.2	(5.29) Linear Velocity (5.30) Angular Velocity (5.31) Linear Acceleration (5.32) Angular Acceleration
13	Payload Increase	1	0.2	(5.33) Linear Velocity (5.34) Angular Velocity (5.35) Linear Acceleration (5.36) Angular Acceleration
14	Payload Increase and Rolling Friction Coefficient Increase 10 times.	1	0.2	(5.37) Linear Velocity (5.38) Angular Velocity (5.39) Linear Acceleration (5.40) Angular Acceleration

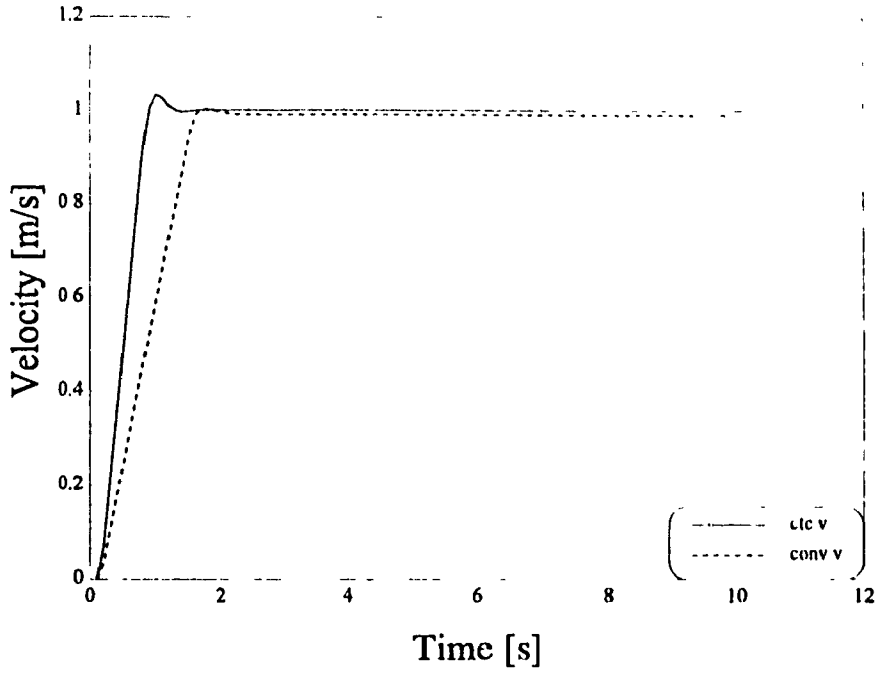

Figure 5.7 AGV Velocity Response for CTC and the Conventional Schemes

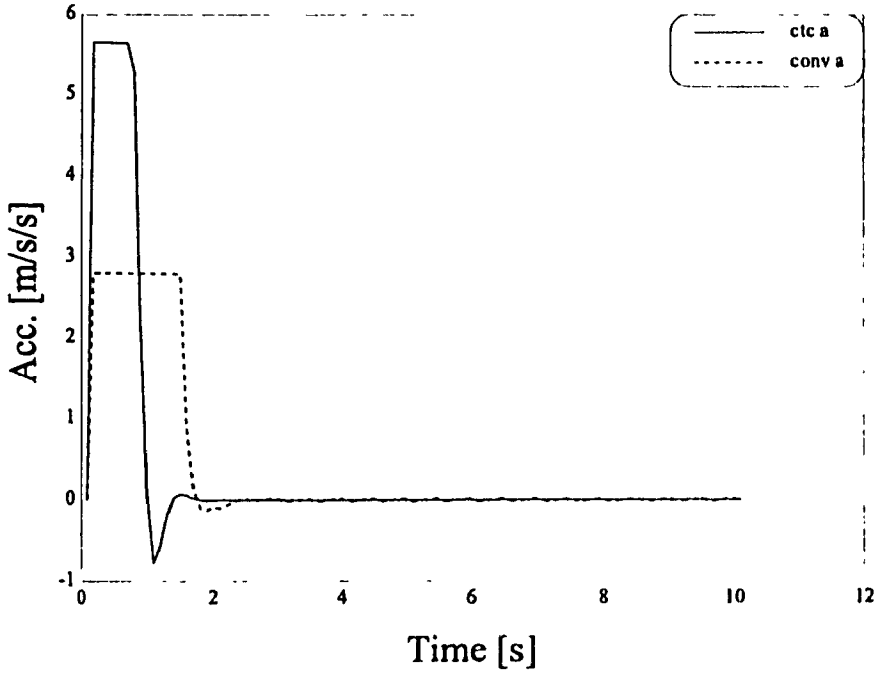

Figure 5.8 AGV Acceleration Response for CTC and the Conventional Schemes

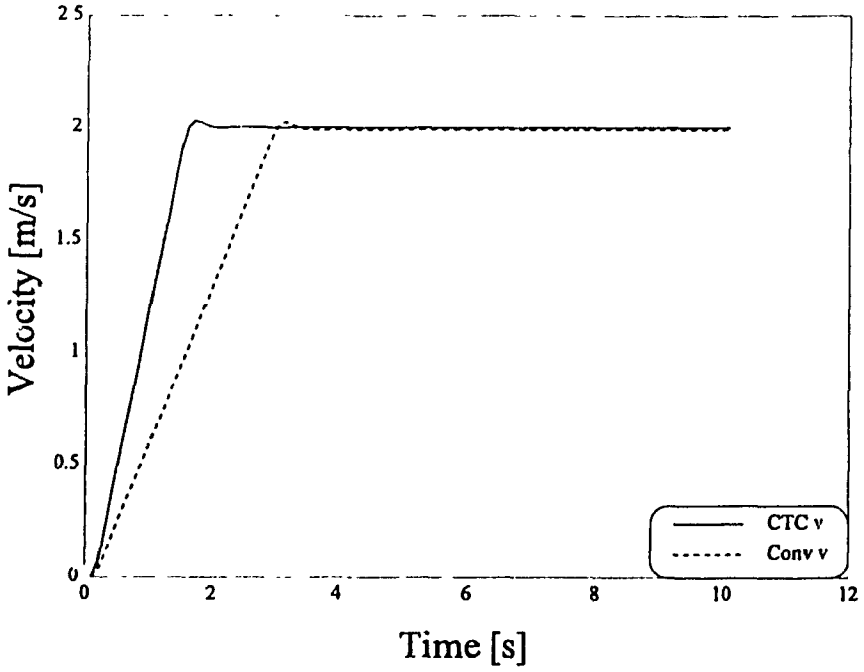

Figure 5.9 AGV Velocity Response for CTC and the Conventional Schemes, Velocity = 2 m/s

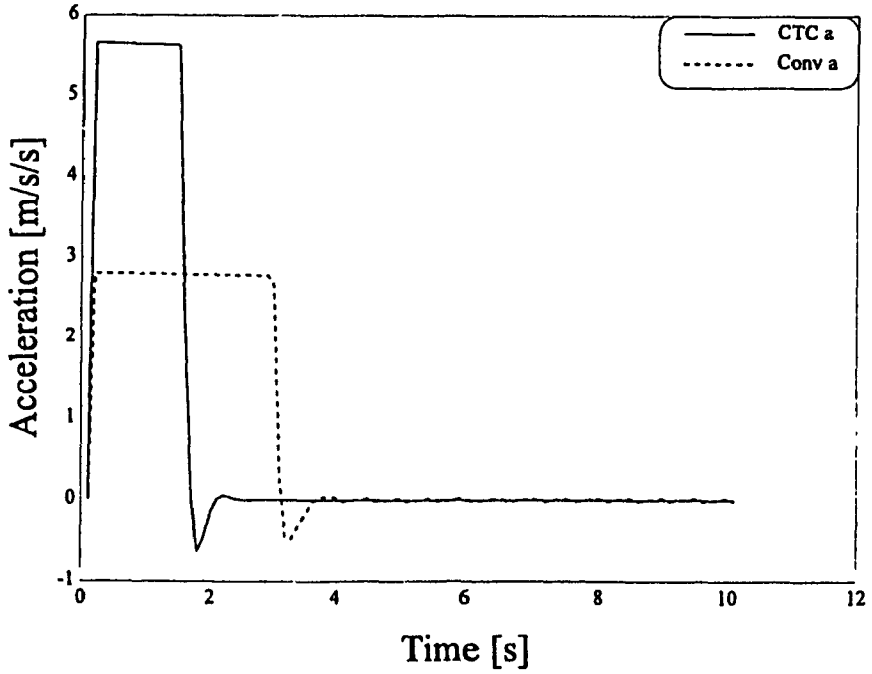

Figure 5.10 AGV Acceleration Response for CTC and the Conventional Schemes, Velocity = 2 m/s

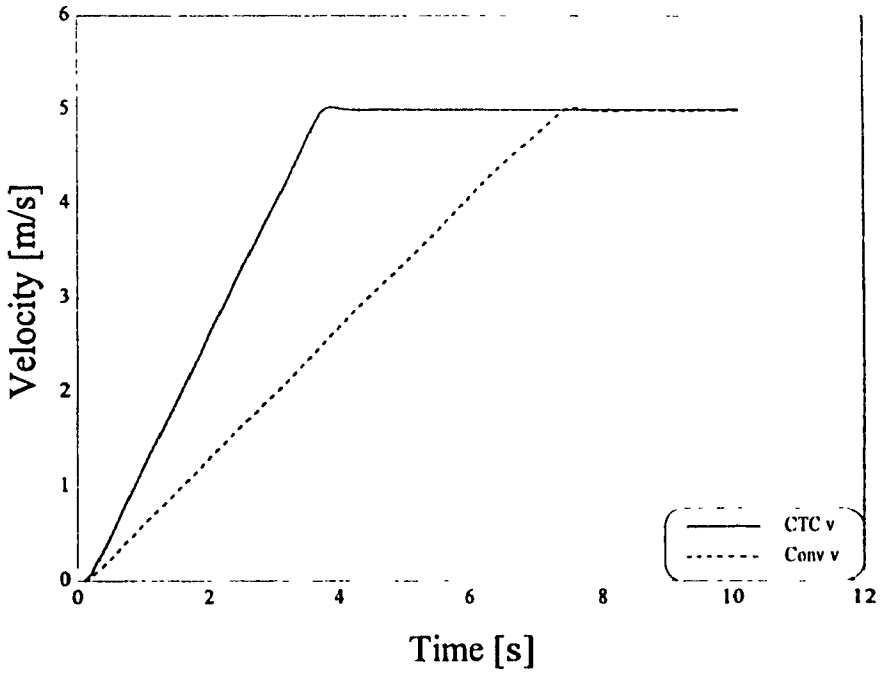

Figure 5.11 AGV Velocity Response for CTC and the Conventional Schemes, Velocity = 5 m/s

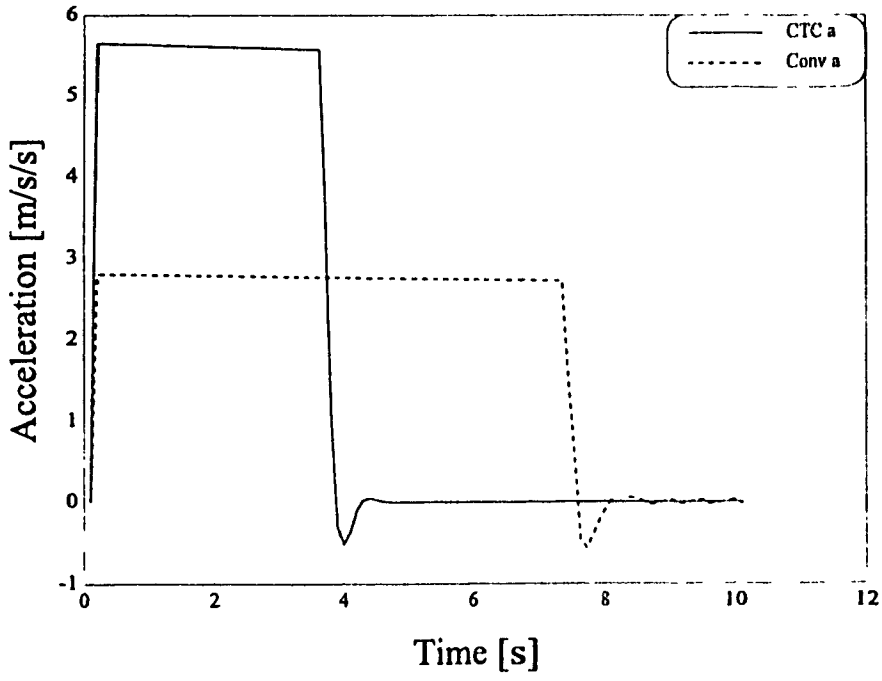

Figure 5.12 AGV Acceleration Response for CTC and the Conventional Schemes, Velocity = 5 m/s

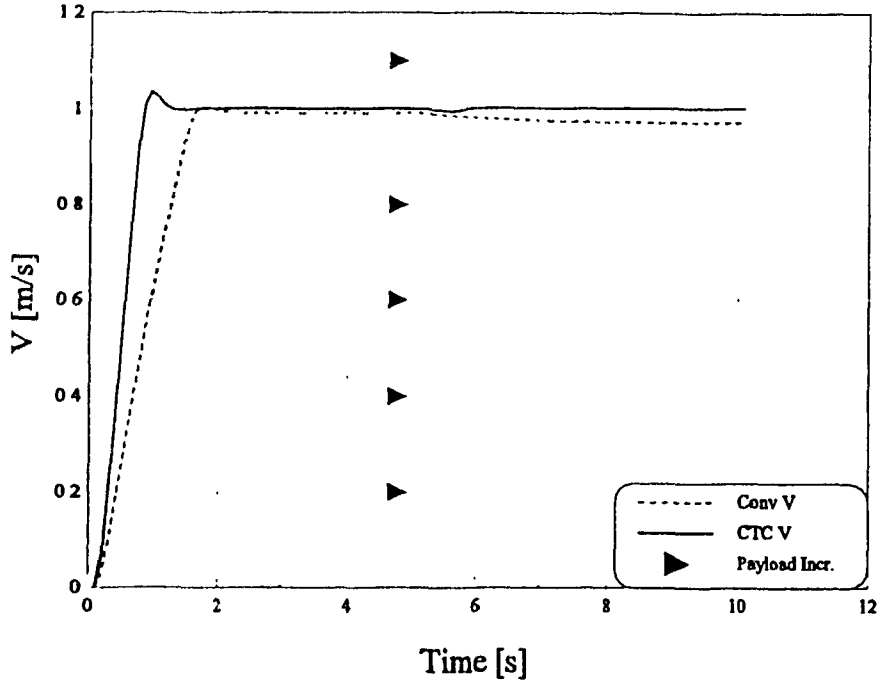

Figure 5.13 AGV Velocity Response for Payload Increase by 5 times the vehicle mass

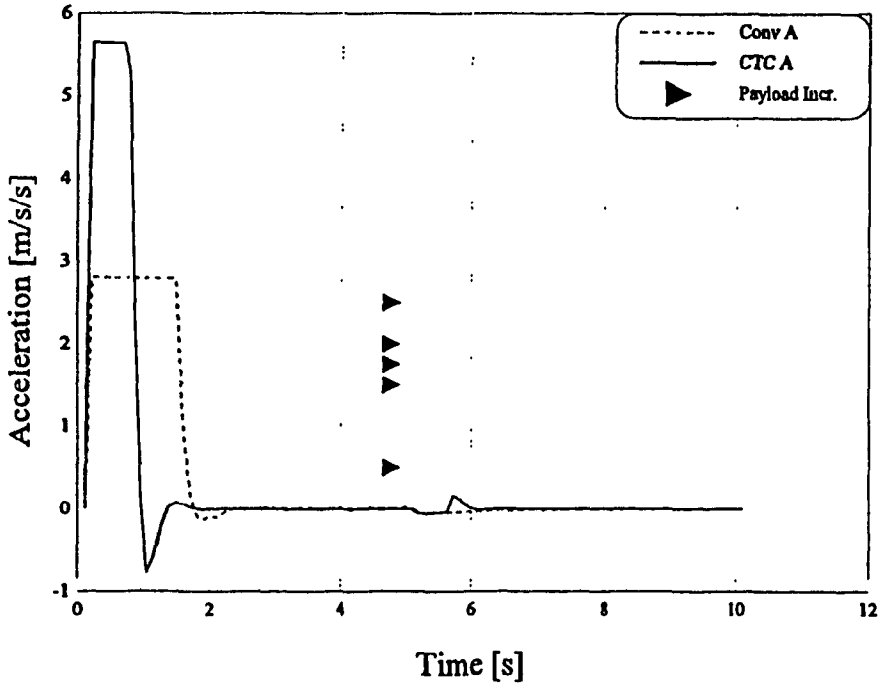

Figure 5.14 AGV Acceleration Response for Payload Increase by 5 times the vehicle mass.

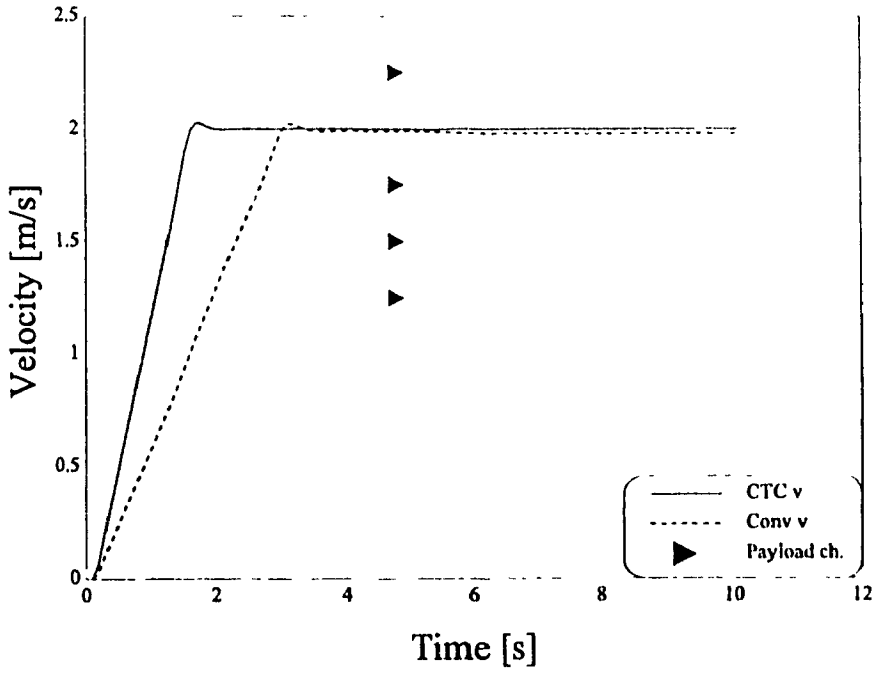

Figure 5.15 AGV Velocity Response for CTC and the Conventional Schemes, Desired Velocity = 2 m/s, Payload Increase by 5 times vehicle mass

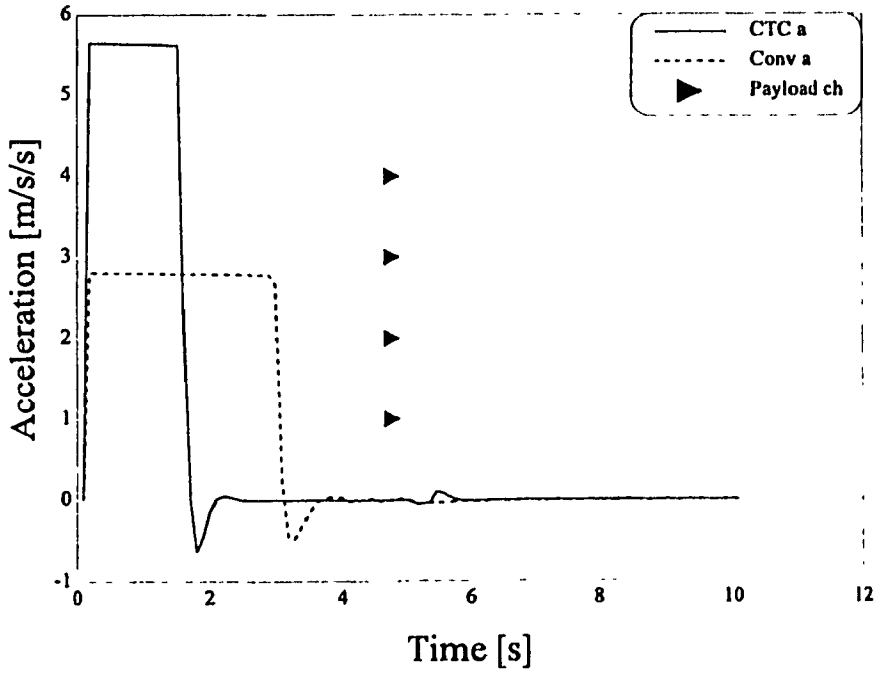

Figure 5.16 AGV Acceleration Response for CTC and the Conventional Schemes, Desired Velocity = 2 m/s, Payload Increase by 5 times vehicle mass

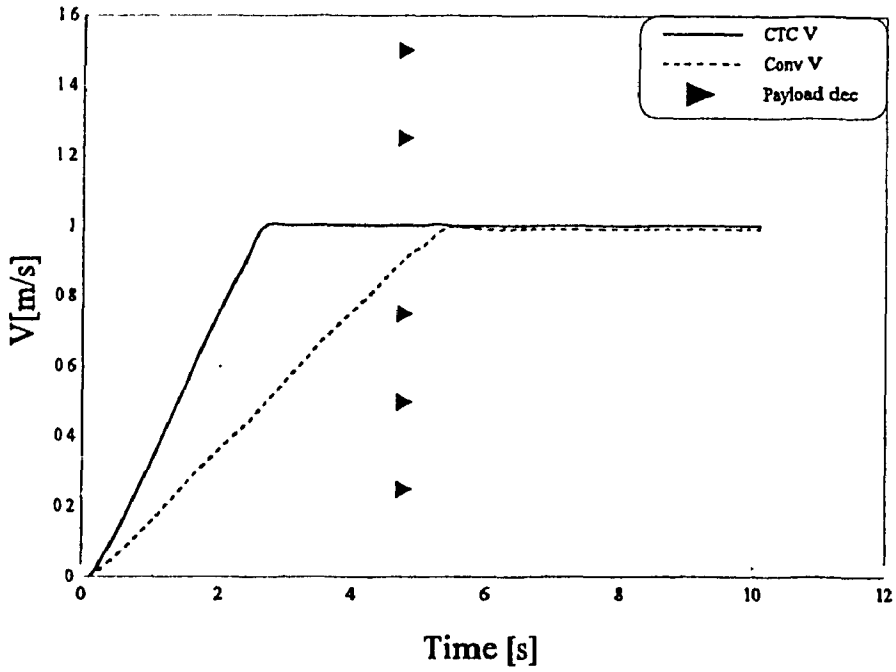

Figure 5.17 AGV Velocity Response for Payload Decrease From 5 Times Vehicle Mass to No Payload

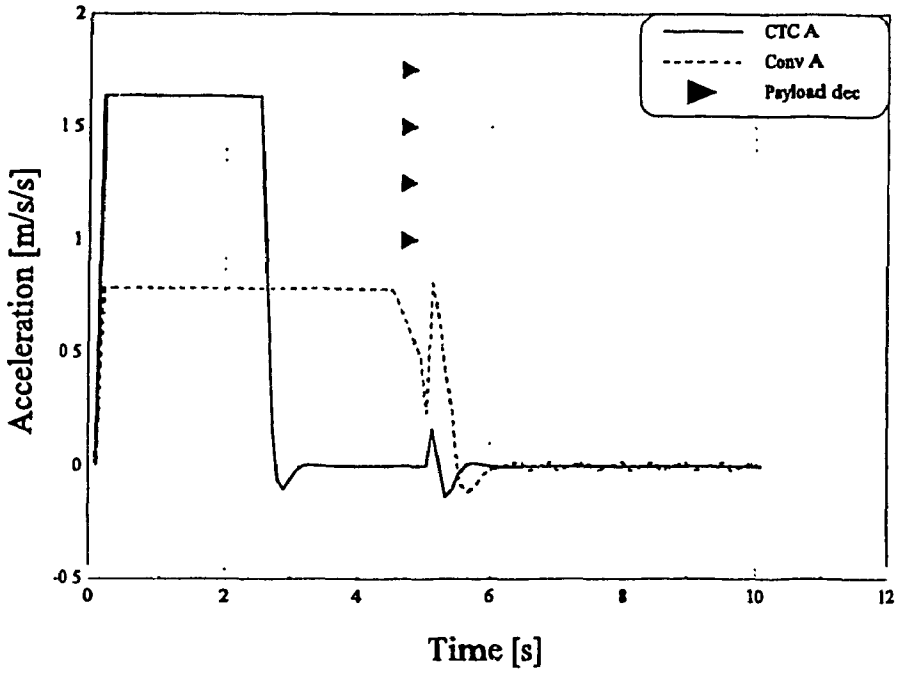

Figure 5.18 AGV Acceleration Response for Payload Decrease From 5 Times Vehicle Mass to No Payload.

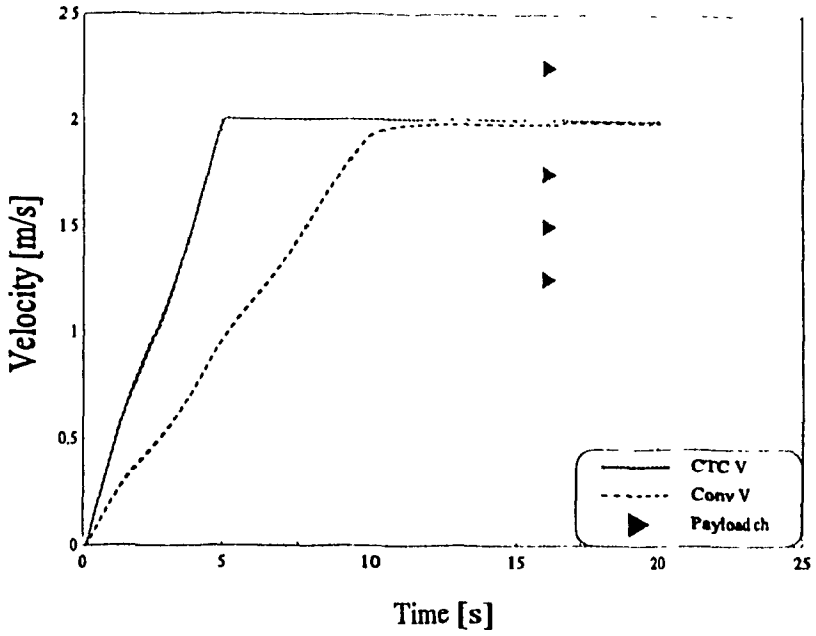

Figure 5.19 AGV Velocity Response for CTC and the Conventional Schemes, Payload Decrease From 5 Times Vehicle Mass to No Payload, at a Desired Velocity = 2 m/s

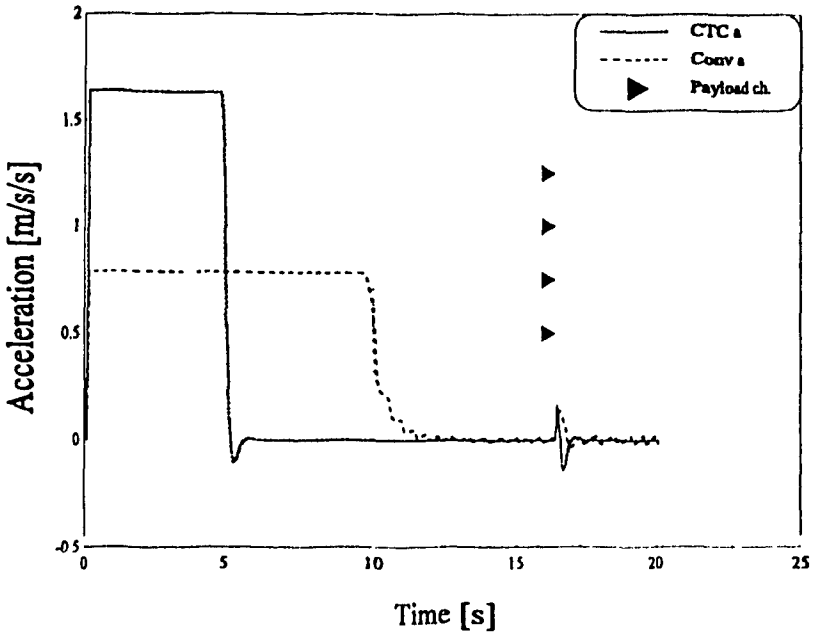

Figure 5.20 AGV Acceleration Response for CTC and the Conventional Schemes, Payload Decrease From 5 Times Vehicle Mass to No Payload, at a Desired Velocity = 2 m/s

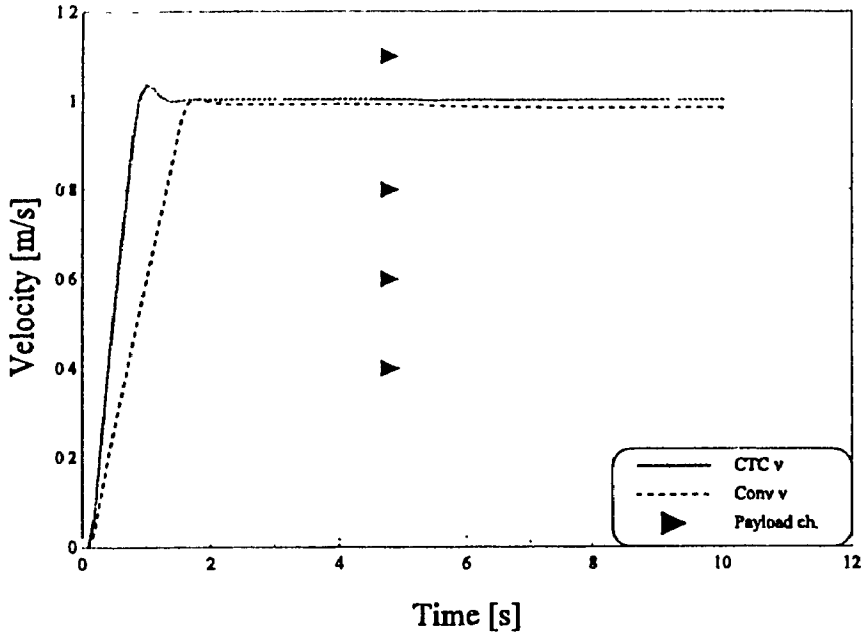

Figure 5.21 AGV Velocity Response for the CTC and the Conventional Schemes, Payload Increase on the Left Driving Wheel Only

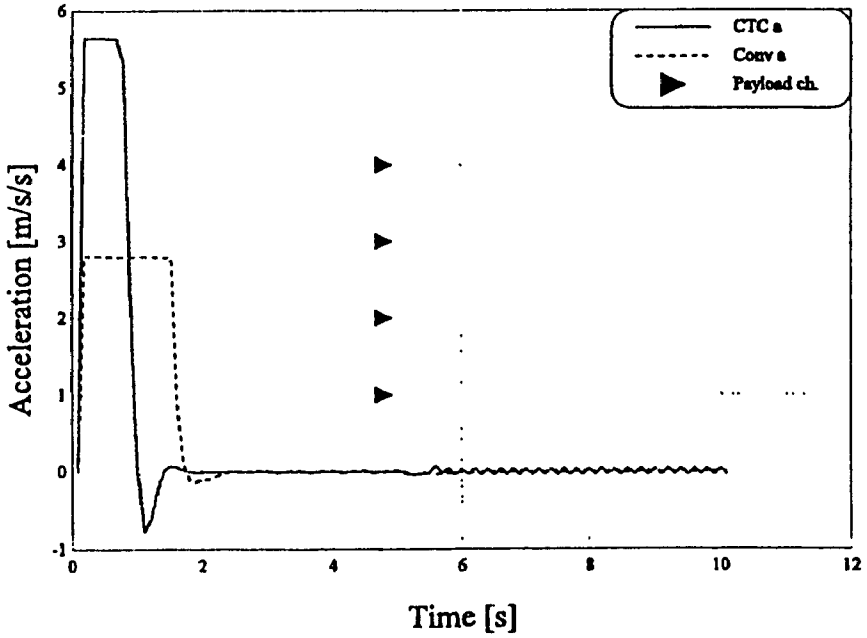

Figure 5.22 AGV Acceleration Response for CTC and the Conventional Schemes, Payload Increase on the Left Driving Wheel Only

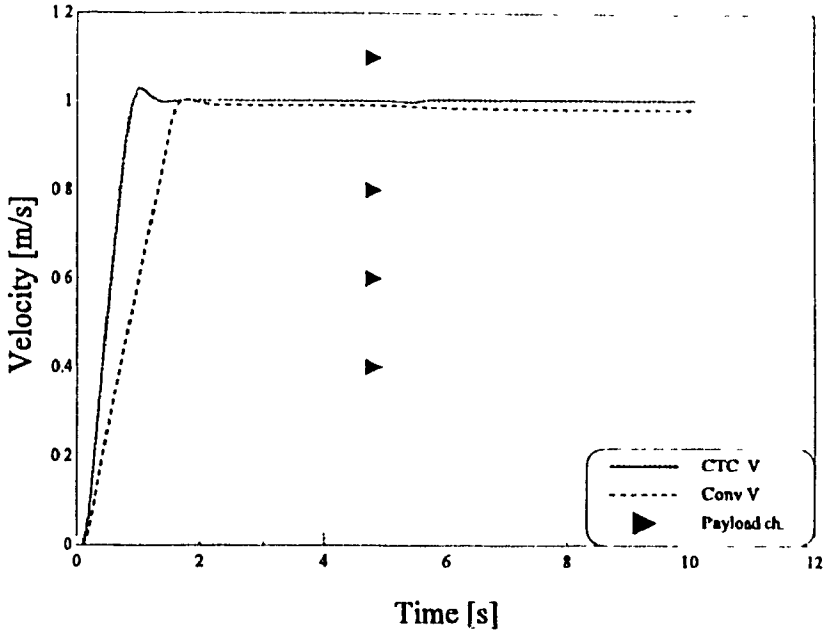

Figure 5.23 AGV Velocity Response for CTC and the Conventional Schemes, Payload Increase on the Rear Castor Only

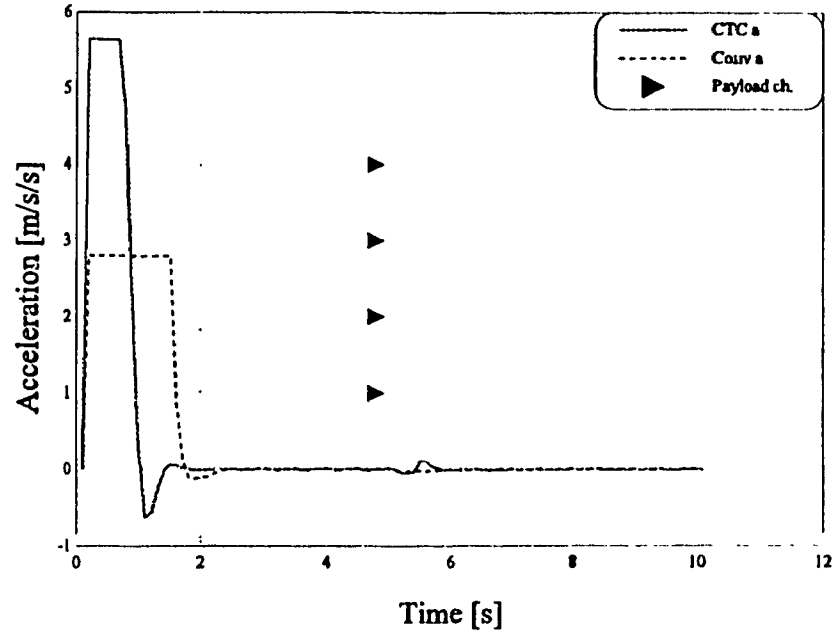

Figure 5.24 AGV Acceleration Response for CTC and the Conventional Schemes, Payload Increase on the Rear Castor Only

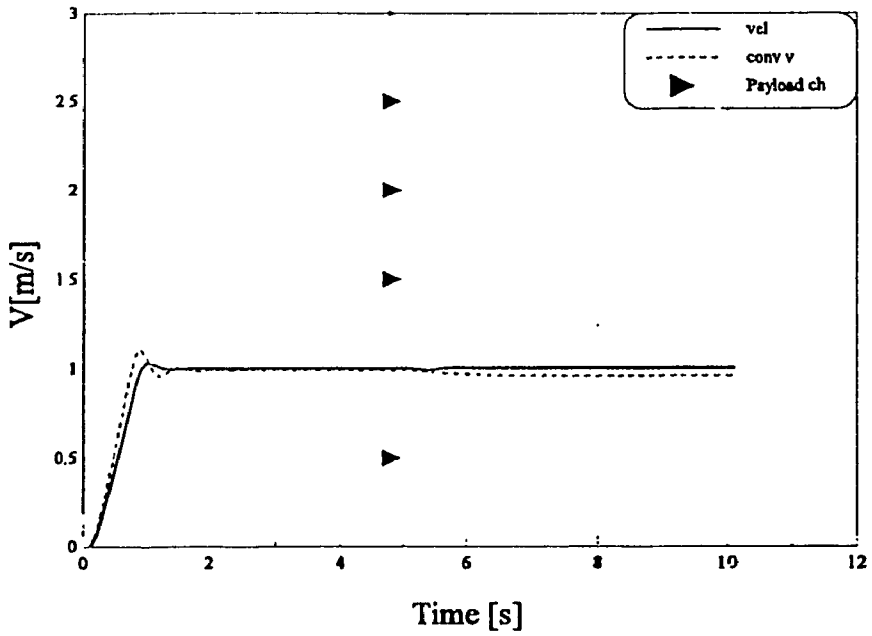

Figure 5.25 AGV Velocity Response for Payload Increase and a Friction Coefficient 3 Times the Original Value

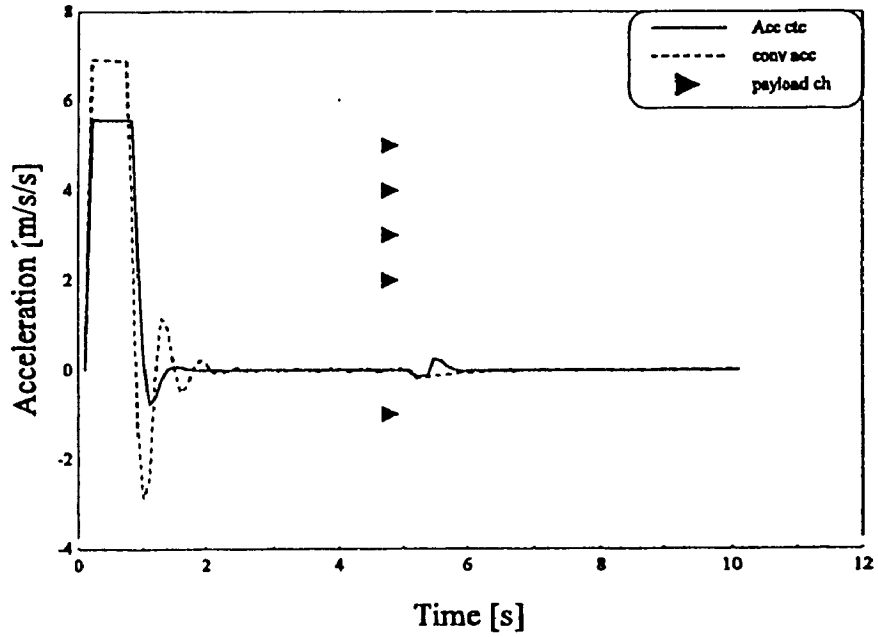

Figure 5.26 AGV Acceleration Response for Payload Increase and a Friction Coefficient 3 Times the Original Value

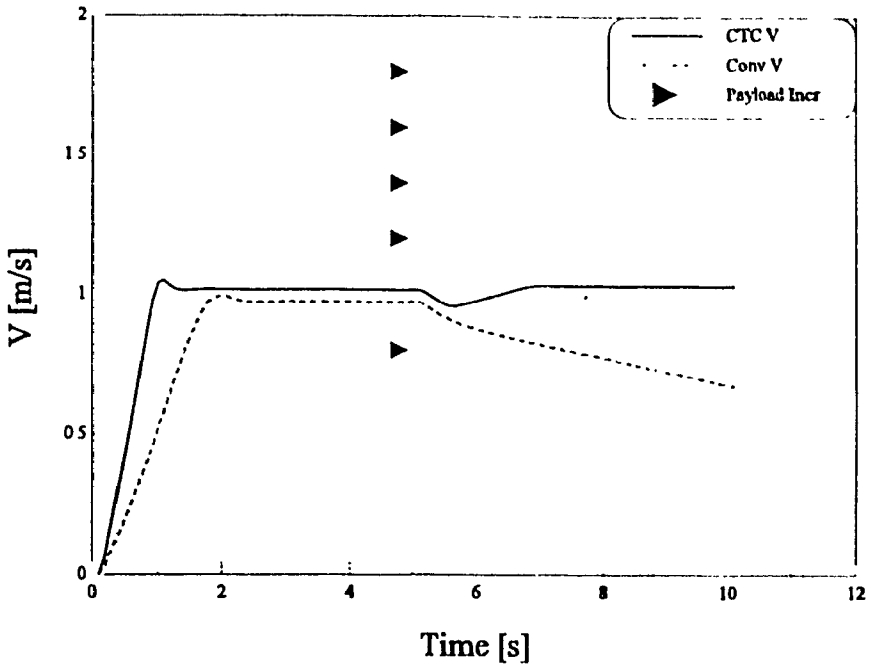

Figure 5.27 AGV Velocity Response for Payload Increase and an Increased Friction Coefficient 10 times the original value

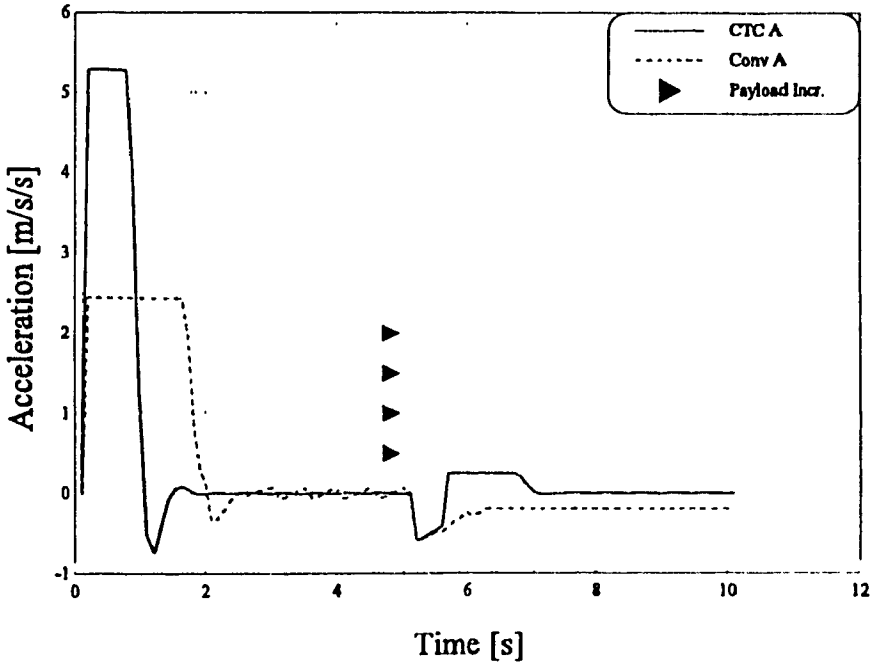

Figure 5.28 AGV Acceleration Response for Payload Increase and an Increased Friction Coeffiient 10 times original value

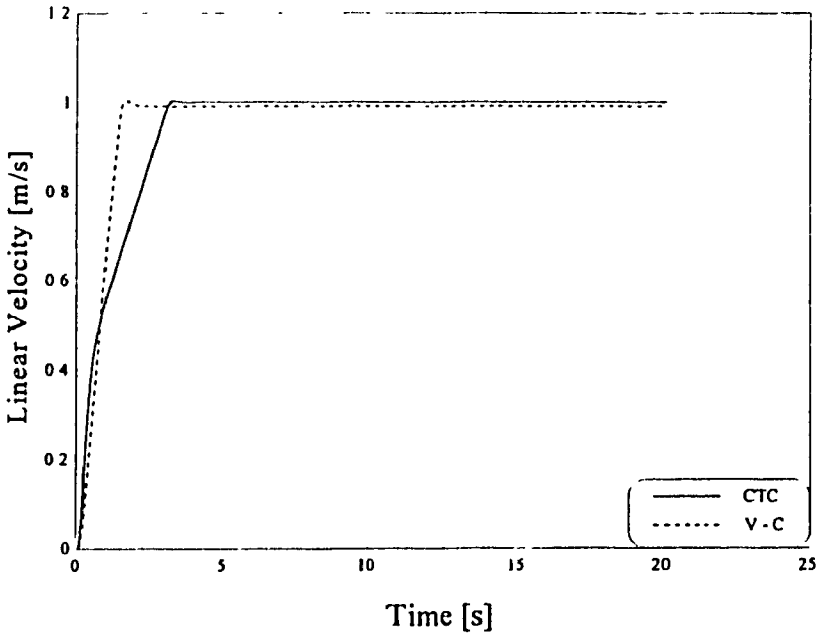

Figure 5.29 AGV Linear Velocity Response for CTC and the Velocity Control Schemes, With a Desired Angular Velocity of 0.1 rad/s

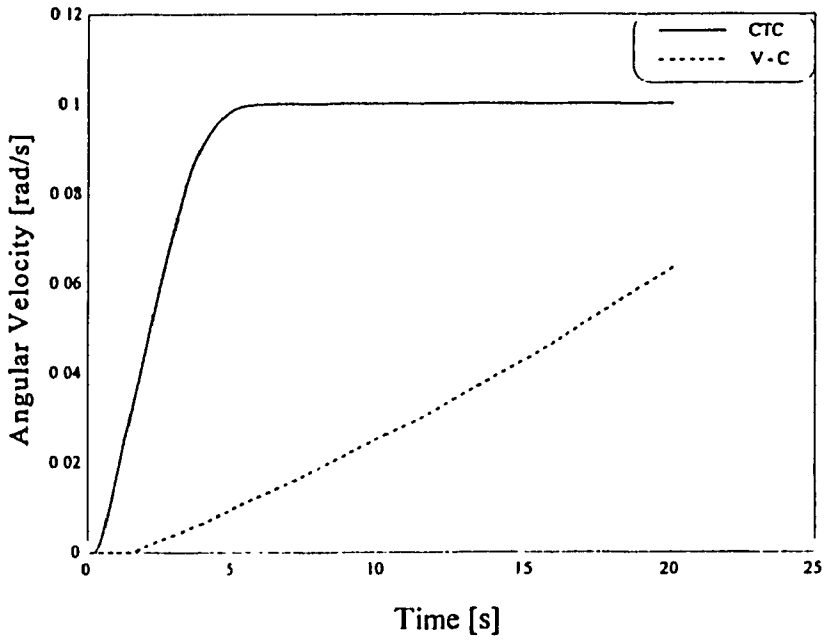

Figure 5.30 AGV Angular Velocity Response for CTC and the Velocity Control Schemes, Angular Velocity Desired = 0.1 rad/s.

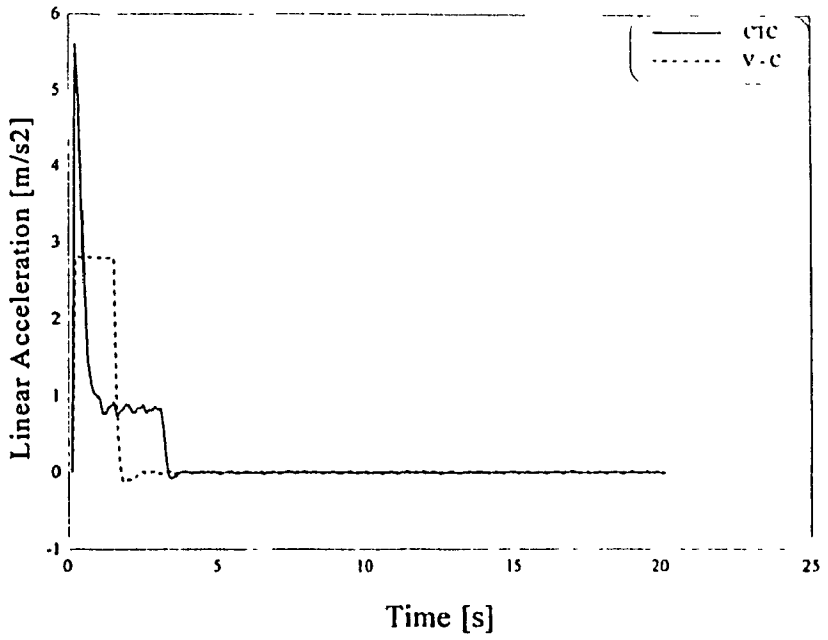

Figure 5.31 AGV Linear Acceleration Response for CTC and the Velocity Control Schemes, With a Desired Angular Velocity = 0.1 rad/s

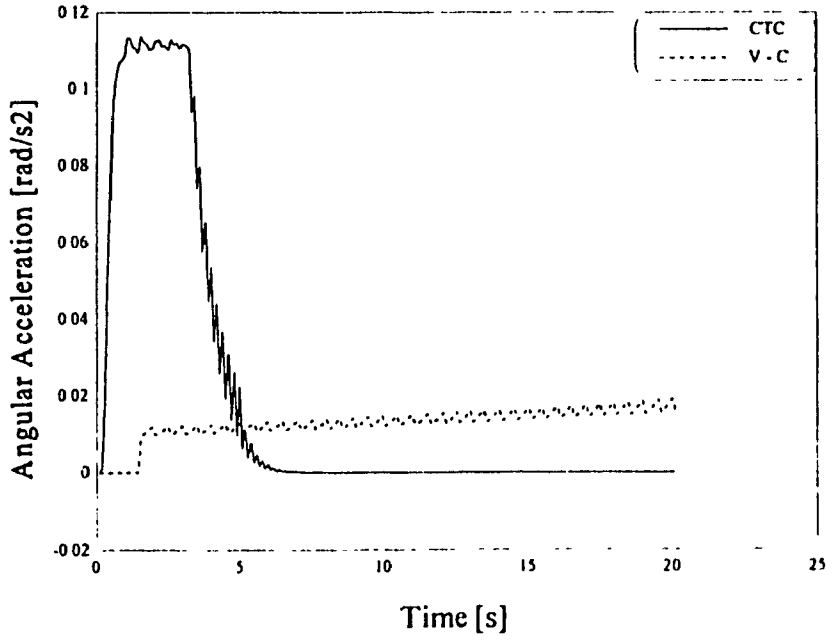

Figure 5.32 AGV Angular Acceleration Response for CTC and the Velocity Control Schemes, Desired Angular Velocity = 0.1 rad/s

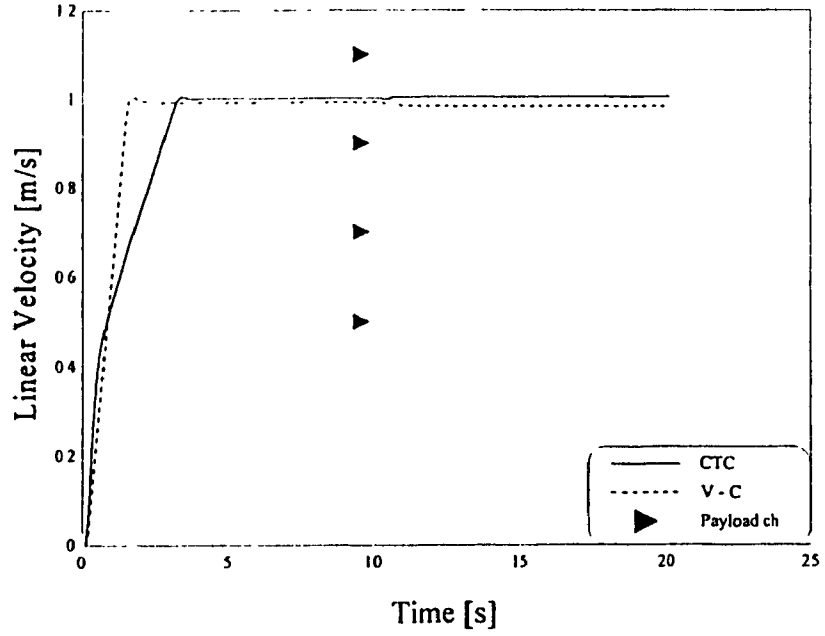

Figure 5.33 AGV Linear Velocity Response for CTC and the Velocity Control Schemes, Payload Increase at t = 10 s, by 5 times the vehicle mass

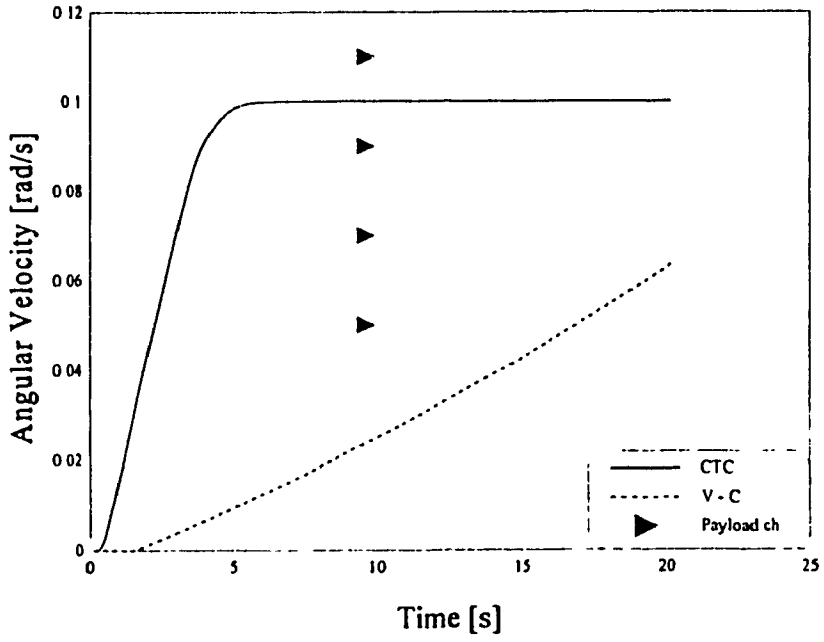

Figure 5.34 AGV Angular Velocity Response for CTC and the Velocity Control Schemes, Payload Increase at t = 10 s, by 5 times the vehicle mass

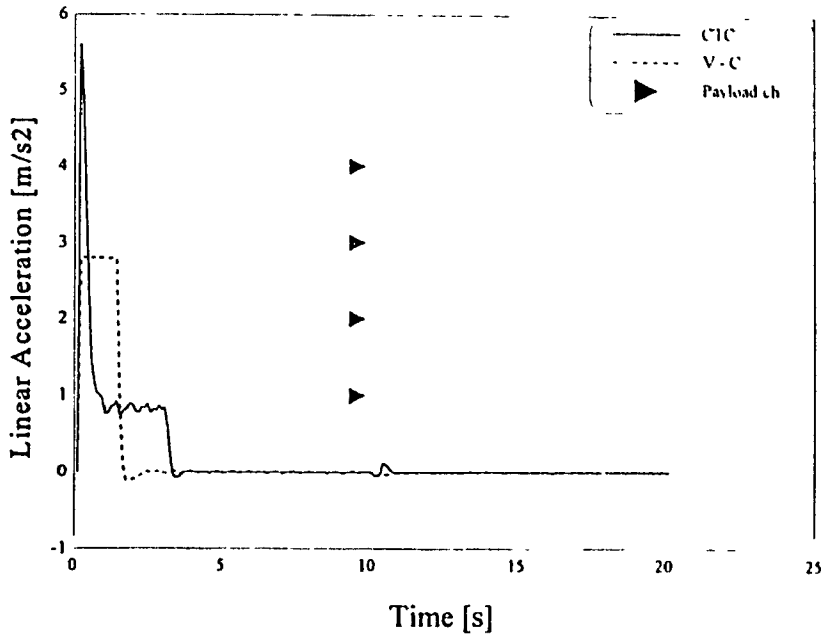

Figure 5.35 AGV Linear Acceleration Response for CTC and the Velocity Control Schemes, Payload Increase at t = 10s, by 5 times the vehicle mass

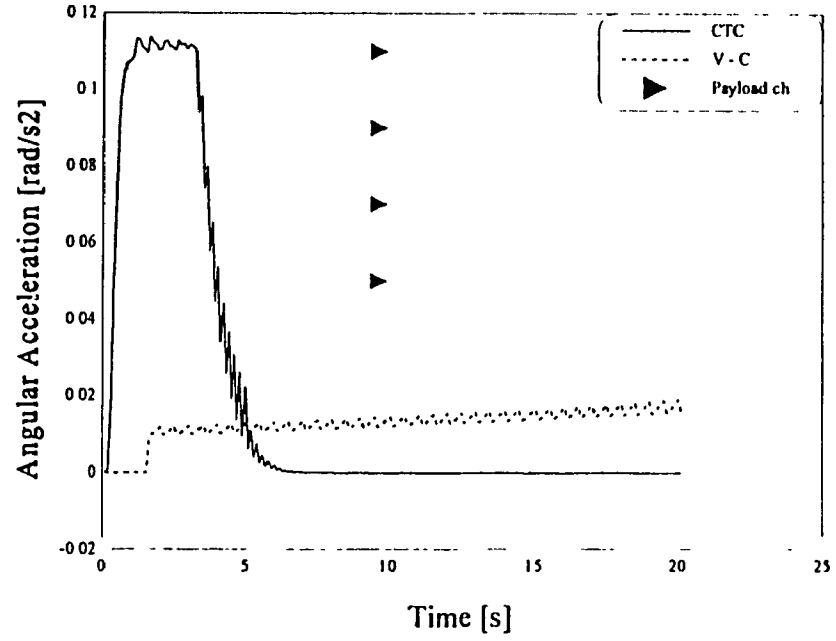

Figure 5.36 AGV Angular Acceleration Response for CTC and the Velocity Control Schemes, Payload Increase at t = 10 s, by 5 times the vehicle mass

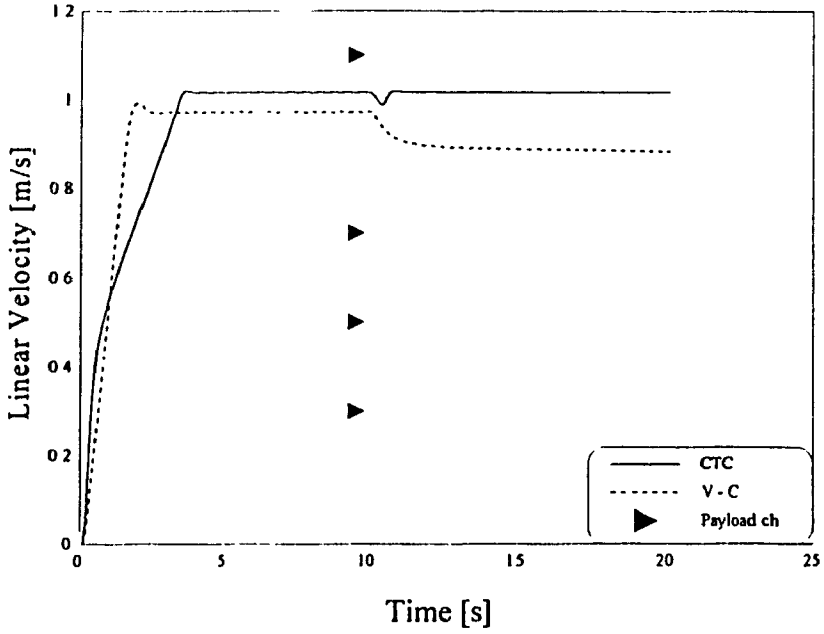

Figure 5.37 AGV Linear Velocity Response for CTC and the Velocity Control Schemes, Payload Increase by 5 Times The Vehicle Mass and Friction Coefficient 10 Times The Original Value

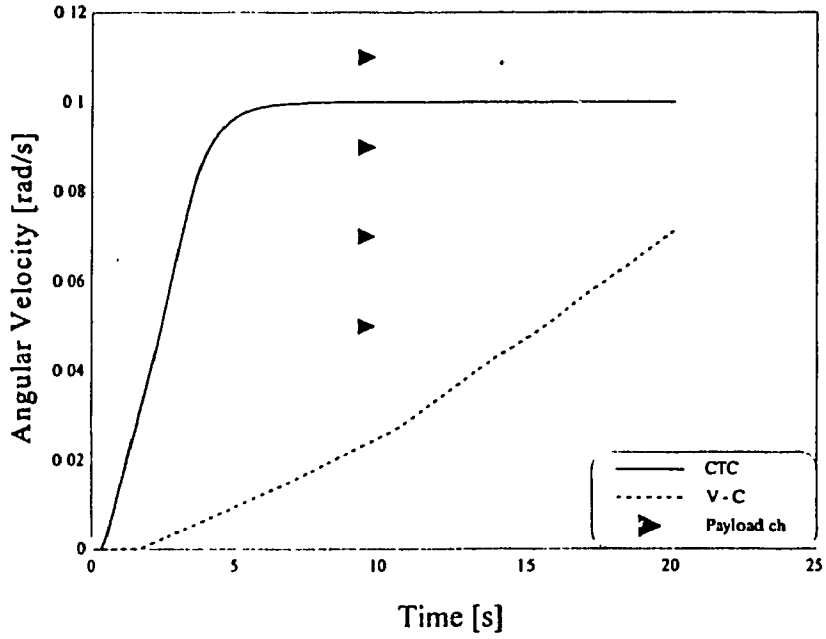

Figure 5.38 AGV Angular Velocity Response for CTC and the Velocity Control Schemes, Conditions of Figure 5.37

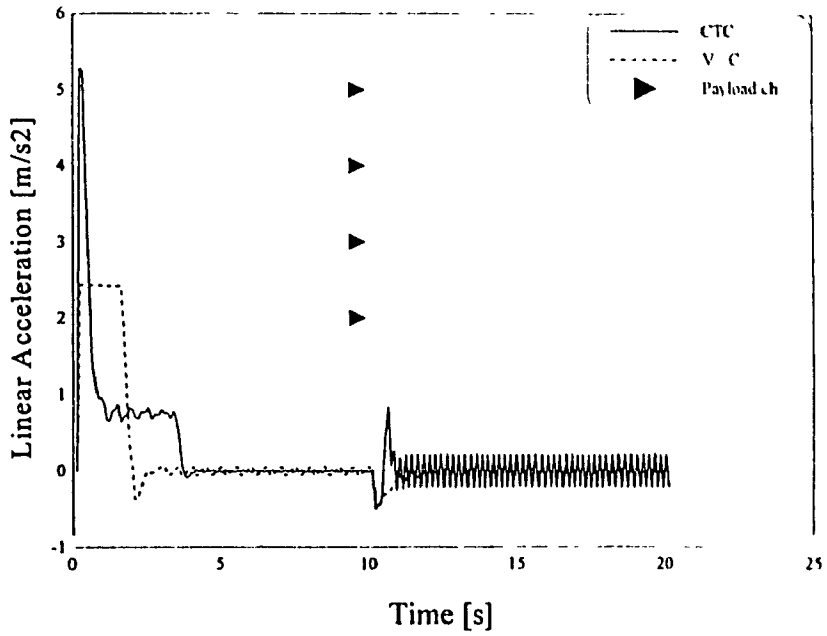

Figure 5.39 AGV Linear Acceleration Response for CTC and the Velocity Control Schemes, Conditions of Figure 5.37

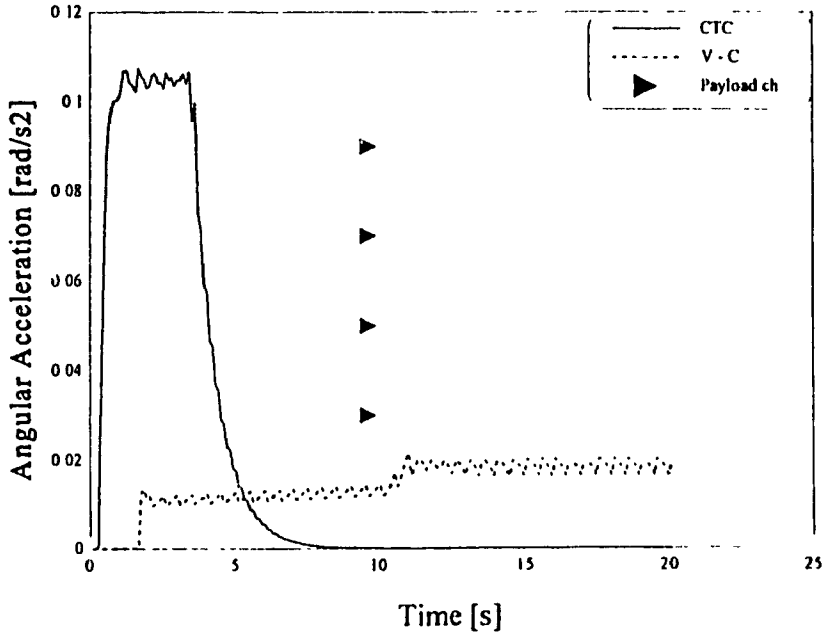

Figure 5.40 AGV Angular Acceleration Response for CTC and the Velocity Control Schemes, Conditions of Figure 5.37

CHAPTER 6 EXPERIMENTAL RESULTS

6.1 Introduction

The practical aspects of the Computed Torque Control (CTC) scheme for electro-mechanical systems are addressed in this chapter. This control scheme makes use of the inverse dynamic model of the electro-mechanical system to drive the system in a dynamically changing environment. Experimentation is performed on two electro-mechanical systems. The first is a setup using the motor-in-wheel drive unit of CONCIC II AGV and a loading arrangement as described in section 6.2. The second system is the prototype CONCIC II AGV. Both systems are designed and built in the Centre for Industrial Control (CIC) in the Department of Mechanical Engineering at Concordia University. The electronic interfaces and the control software developed to carry out experiments are described in Sections 6.2.2, 6.2.3 and 6.4.2. Section 6.3.3 presents the results of experiments using the motor-test-rig. The tests carried out using the prototype vehicle are elaborated in Section 6.4.3.

6.2 The Experimental Motor-Test-Rig

A motor-in-wheel drive unit that is currently used to drive industrial Automated Guided Vehicles (AGVs) is chosen for experimentation. The motor characteristics are presented in Appendix-A. A control strategy based on the CTC scheme and explained in Section 4.2 is implemented to control the motor. The real time control of the motor is carried out using a PC based on an 80486, 66 Mhz microprocessor. An interface card has

been designed for this purpose as explained in Section 6.2.2. The interface card allows control of the motor using the velocity control loop as well as the CTC scheme. Figure 6.1 shows a top and side view of the motor-test-rig. Detailed schematics of the motor-test-rig are presented in Appendix-B.

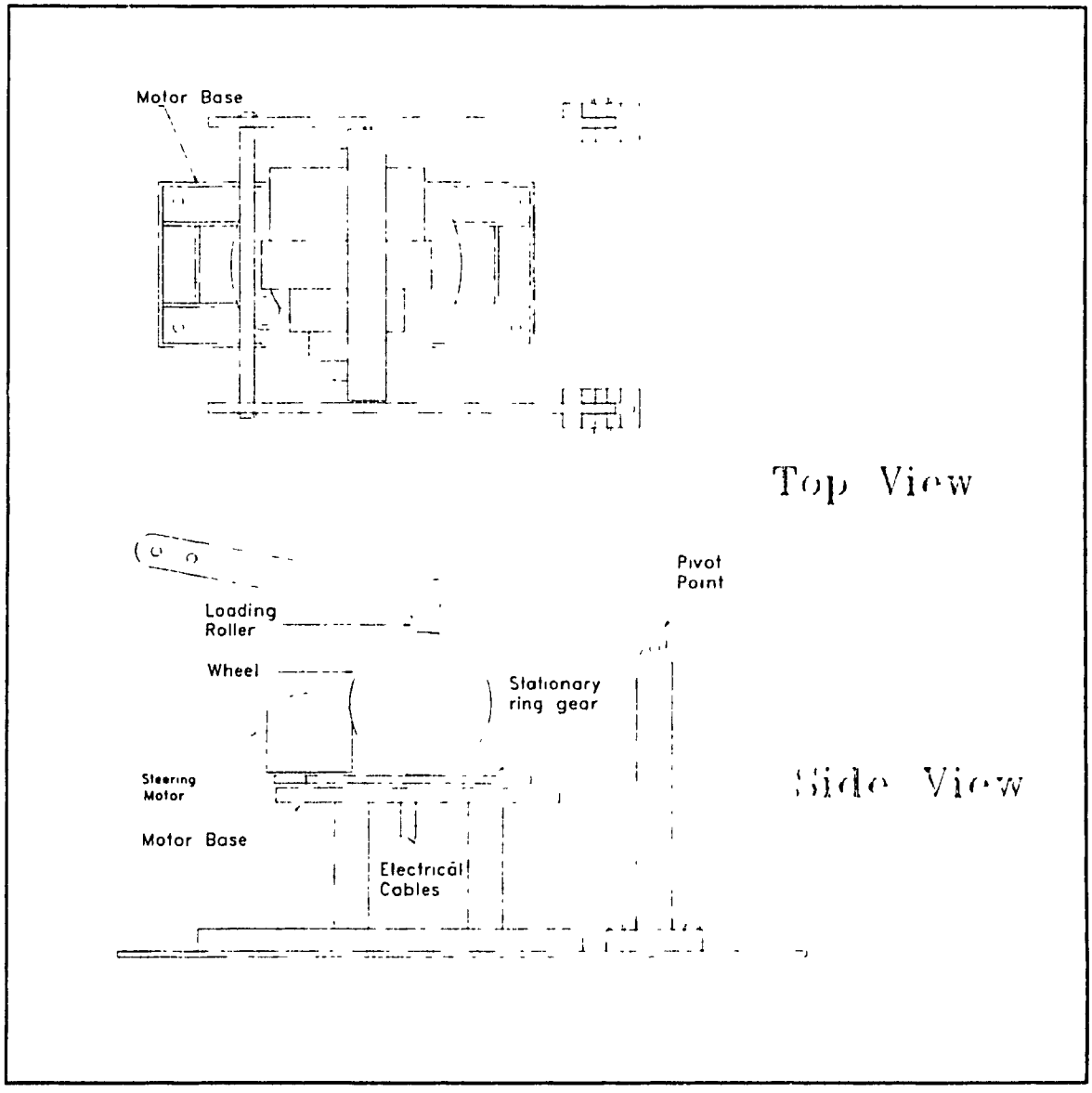

Figure 6.1 Top and Side Views of the Motor Test Rig

6.2.1 Components of the Motor-Test-Rig

The rig consists of a base and holding side panels. The panels support a loading arm which has the form of a "U" and contains a roller. The motor set is fitted to the base of the rig up side down. This is to allow a contact between the wheel of the motor set and the roller. The loading arm allows to change the vertical load on the motor while in motion. In addition, the motor is fitted with an encoder for feedback. The motor terminals are connected to the power amplifier. The amplifier is controlled through the interface card. The encoder lines are connected to a decoder (LM628 motion controller) to obtain the actual position of the motor and then calculate the velocity of the motor.

6.2.2 The Interface Card

To facilitate communication between the amplifier, the encoder and the host computer, an interface card has been designed and built. On-board the interface card a low level motion controller (LM628) performs the decoding of the encoder readings [47]. The LM628 specifications can be found in the LM628/629 manual by National Semiconductor Corporation [46].

Layout of the interface card is shown in Figure 6.2. On-board the interface card, Generic Array Logic (GAL) chips are used to perform address decoding, generate chip select signals and process data and control signals from the pc to the interface card components.

Also on-board the interface card is an 8254 Counter-Timer Circuit chip. This chip is used in real-time to obtain the cycle time of the control software [48].

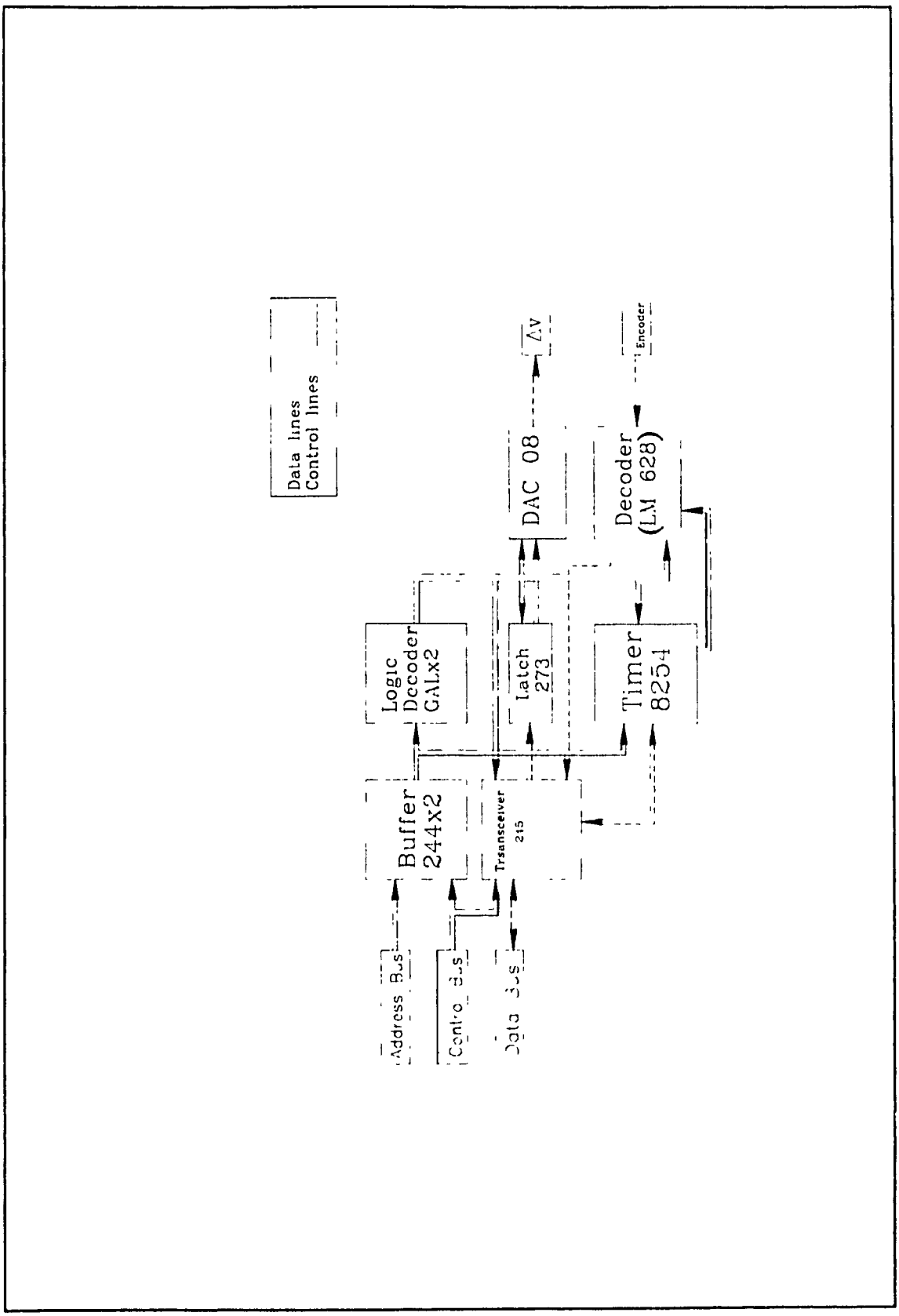

Figure 6.2 Layout of the Interface Card

6.2.3 Control Software

A program is written to control the motor on line through the PC to implement the CTC scheme. An inverse dynamic model is included in the program where current values are calculated and sent to the motor every 2 ms. Another program is written to carry out the Velocity Control (VC) scheme. These programs communicate with the motor and the amplifier through the interface card previously mentioned in Section 6.2.2. The motor speed and the cycle time of each loop are monitored by the program. Results of the run are being stored directly into data files for further use. The flow charts of the programs are presented in Figures 6.3 and 6.4 respectively. Further, a data acquisition system is used to collect current data by monitoring the amplifier current. This system is installed in a separate computer. This system consists of an interface card and a software to perform the task of on-line data acquisition. Details of this system are found in the reference manual by National Instruments corporation [49].

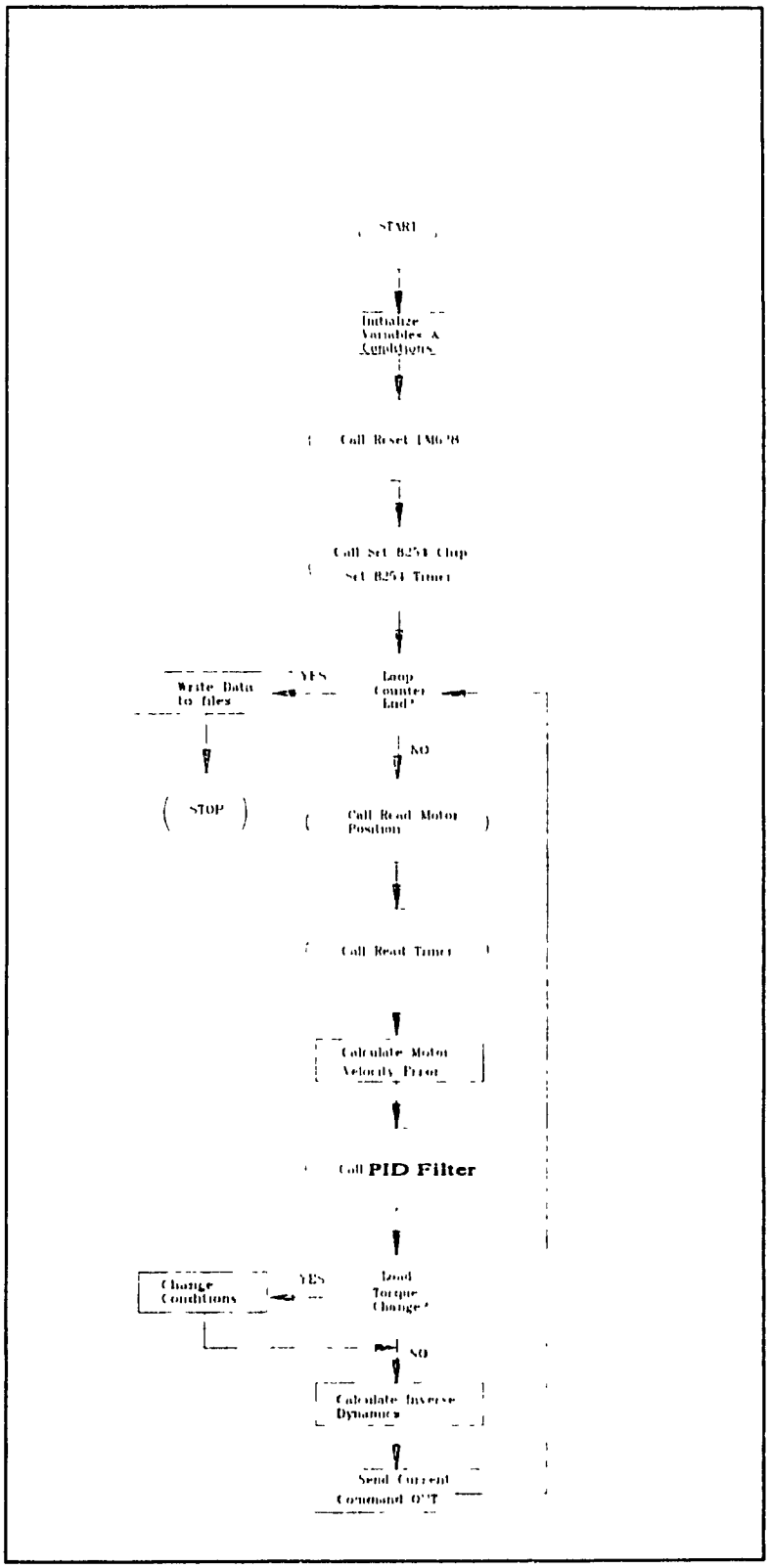

Figure 6.3 Flow Chart of the CTC Scheme Software for the Motor-Test-Rig

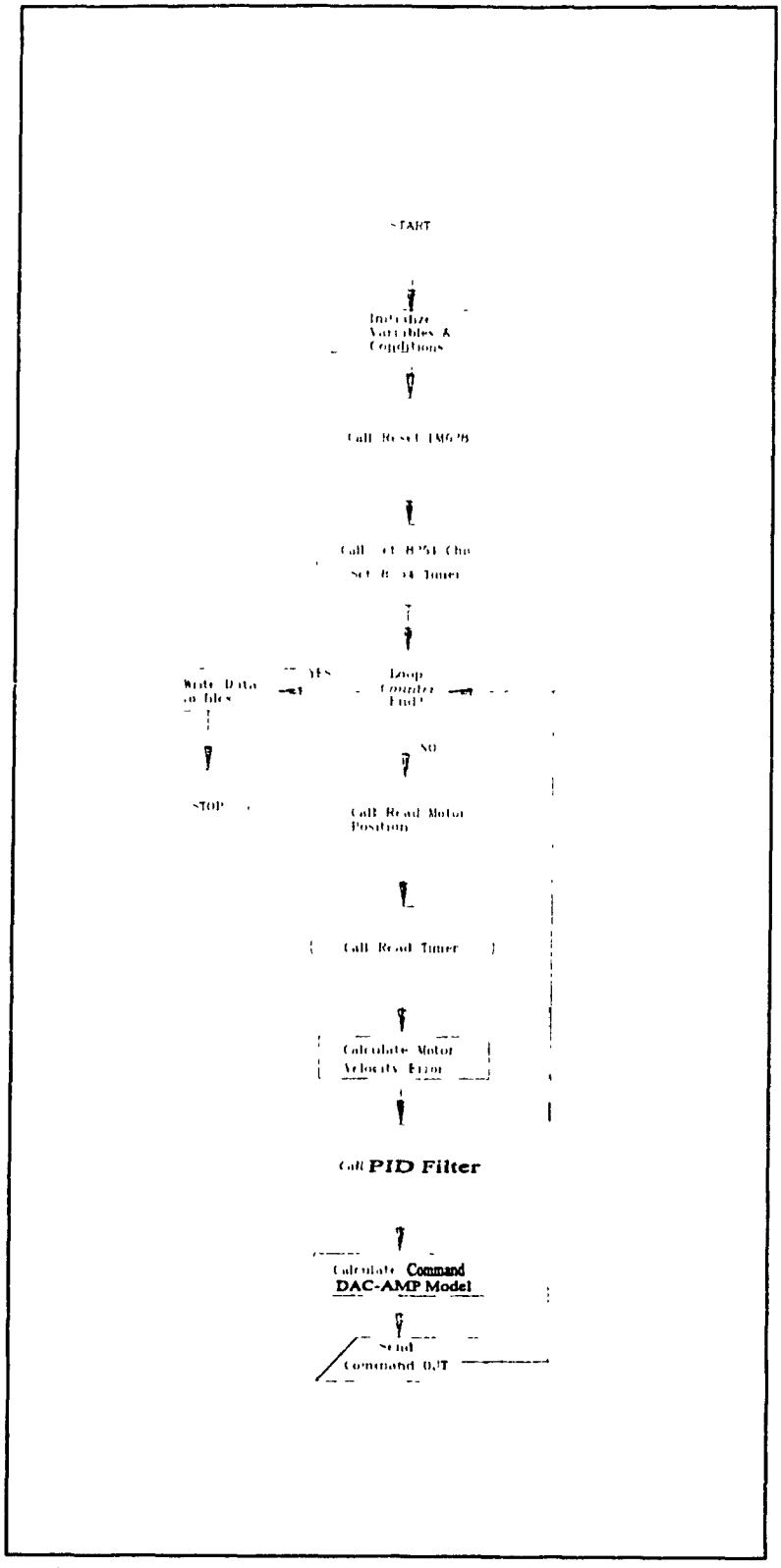

Figure 6.4 Flow Chart of the Velocity Control Scheme Software for the Motor-Test-Rig

6.3 Tests Using the Motor-Test-Rig

6.3.1 Calibrations

Calibration of the DAC - Amplifier combination as well as the Motor - Amplifier combination has been carried out. The results of such calibrations are shown in Figures 6.5 to 6.7. Figure 6.5 shows the relationship between the DAC input in digital values and its output in voltage. Figure 6.6 is obtained between the digital input to the DAC and the current output of the amplifier when in current mode. Figure 6.7 shows the relationship between the DAC digital input and the amplifier voltage output (motor terminal voltage) when in voltage mode.

The equations of these curves and the regression accuracy index are as follows:

Figure (6.5): $Y = 0.0383\ X - 4.884$, $R^2 = 0.9999$

Figure (6.6): $Y = 0.30222\ X - 38.635$, $R^2 = 0.9996$

Figure (6.7): For the non-zero slope part of the curve:

$$Y = 9.2957\ X - 1221.411, \quad R^2 = 0.9922$$

Figure (6.8): For the non-zero slope part of the curve:

$$Y = 1.09786\ X - 143.3189, \quad R^2 = 0.9945$$

where X is always the digital input value to the DAC and Y is the respective output as per the curve in the respective Figure. R^2 presents the accuracy of the fitted curve in relation to the data points used.

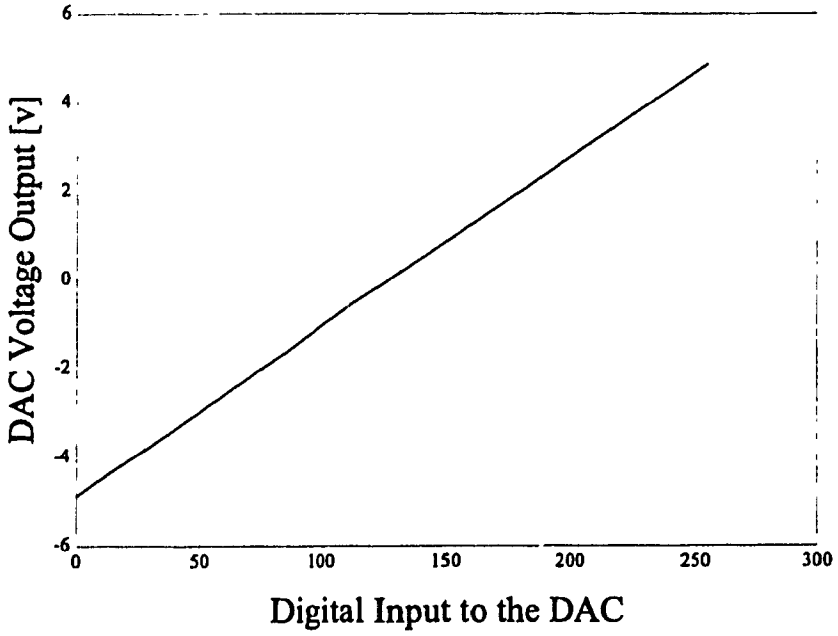

Figure 6.5 DAC 08 Calibration Curve

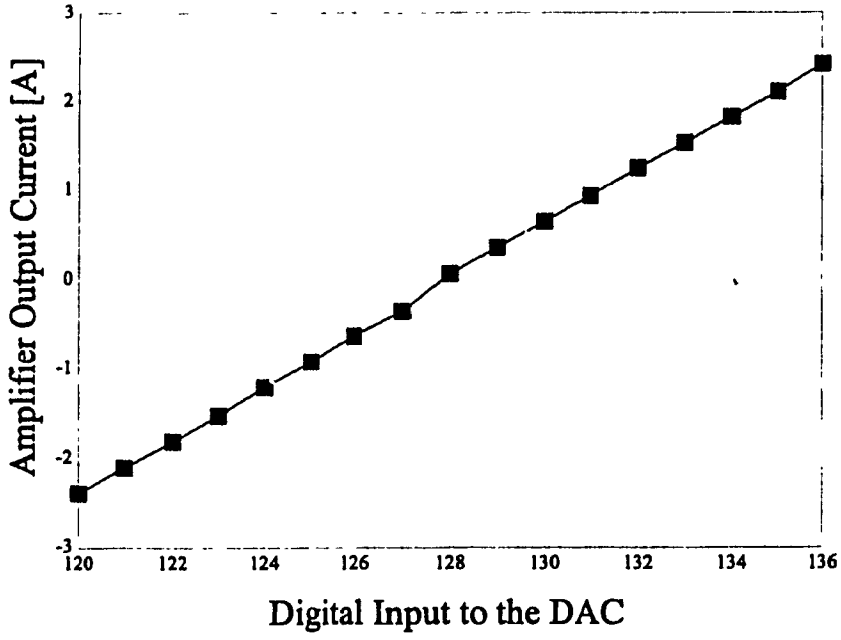

Figure 6.6 Calibration Curve of the DAC and Amplifier in Current Mode

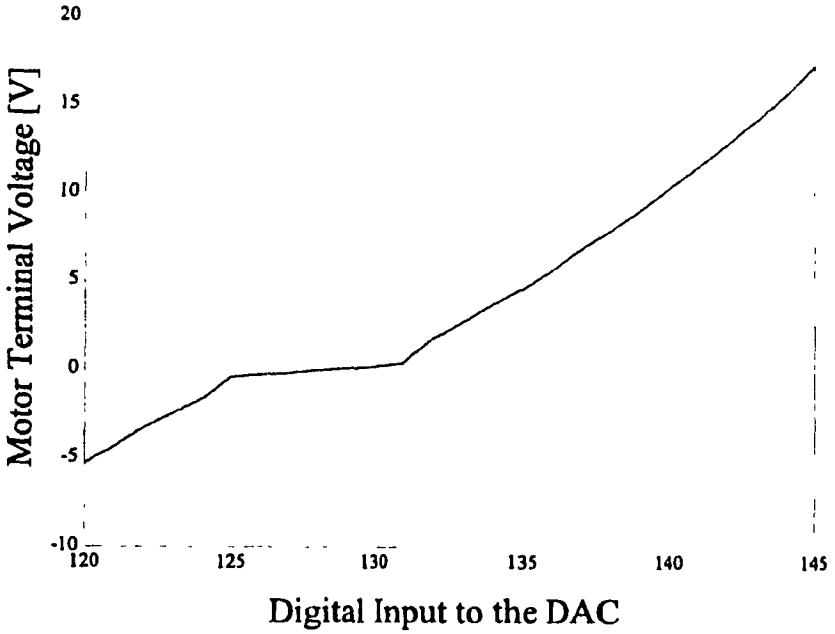

Figure 6.7 Calibration Curve of the DAC and Amplifier in Voltage Mode

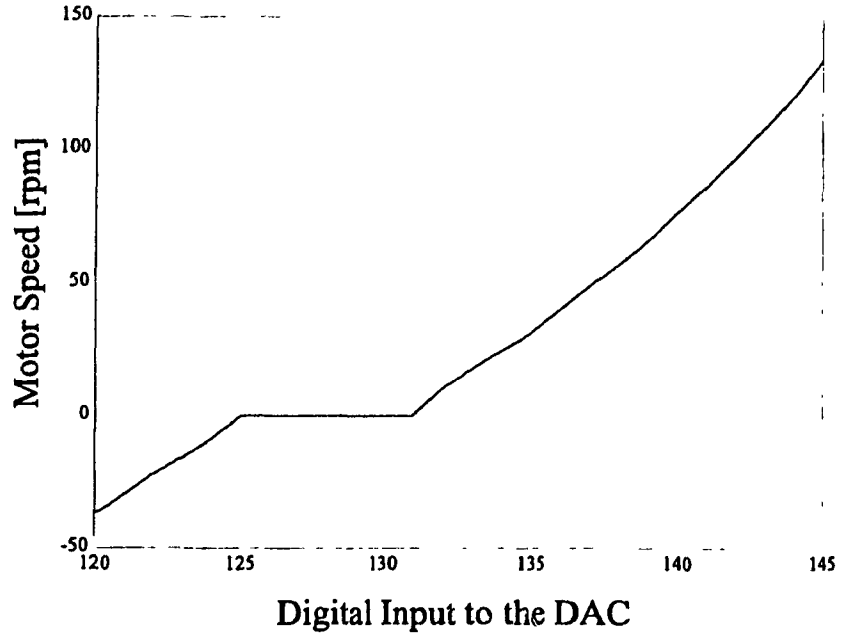

Figure 6.8 Calibration Curve of the DAC and Motor Speed

6.3.2 Tests Results

Different loads were applied to the motor by hanging them to the torque arm which - in turn - transfers the load to the motor through a roller held by bearings. The motor was controlled by two software modules mentioned in Section 6.2.3 for CTC and VC schemes. The experiments are conducted by commanding the motor to run at a desired speed of 60 rpm and 120 rpm. Figures 6.9 to 6.20 present the motor performance (actual speed and current) with the CTC and VC schemes for various loads. Figure 6.9 shows the velocity of the motor under the effect of both control schemes with a desired velocity of 60 rpm. Figure 6.10 shows the current drawn by the motor while running at this velocity. Higher value and range of change of current level appears when the velocity control scheme is in effect. No load change on the motor has been applied during this experiment. The same experiment was carried out for a desired operating velocity of the motor of 120 rpm and the results are shown by Figure 6.15 for velocity and Figure 6.16 for current. Similar behaviour to the experiment of 60 rpm velocity show also in the case of 120 rpm velocity. In the case of a higher operating velocity, the difference in performance of the motor under the effect of the different control schemes is magnified and a clear superiority in maintaining less current drawn by the motor shows with the use of the CTC scheme. Figure 6.11 and 6.13 show the motor velocity when having a payload change of 10 kg and 20 kg added to it respectively. The current drawn by the motor is monitored for both cases and plotted in Figure 6.12 and 6.14 respectively. The same experiments are carried out with an operating speed of 120 rpm and the velocity results are shown in Figures 6.17 and 6.19. Current drawn by the motor for both cases is plotted in Figures 6.8 and 6.20 respectively. These tests show that the Velocity

Control scheme does not compensate for the reduction in velocity when loaded. For example, at a speed of 60 rpm and when the motor is loaded with 10 kg (Figure 6.11), the speed is reduced by 25% in the case of the VC scheme. The speed reduction is almost 34% when the load is 20 kg (Figure 6.13). Operating at a speed of 120 rpm with the VC scheme and 10 kg added as in Figure 6.17 and 20 kg added as in Figure 6.19, the steady state speed reduction is by 12.5 % and 20 % respectively. On the other hand. it can be seen that the CTC scheme maintains the speed for the same desired speed and loading conditions. It compensates for the load addition to the motor and brings the speed to the desired value.

In summary, in all cases the CTC scheme attains the performance to the desired level while in the VC scheme case the performance deviates from the desired value.

From the current plots, it can be seen that the amount of current drawn by the motor is always less in the case of CTC scheme. With the CTC scheme in effect the value of current consumed by the motor fluctuates less than that used in the case of VC scheme in effect. At the higher speed (120 rpm) the current drawn by the motor in the case of the CTC scheme in effect is even more stable than in the case of the VC scheme in effect. Further, the motor current consumed values fluctuate similarly in the case of loads or no loads when having the CTC scheme in effect. On the other hand, when having the VC scheme in effect the motor shows more disturbance in the current consumed values and the fluctuation in these values in the case of loading the motor. The current fluctuations become higher as load is added to the motor.

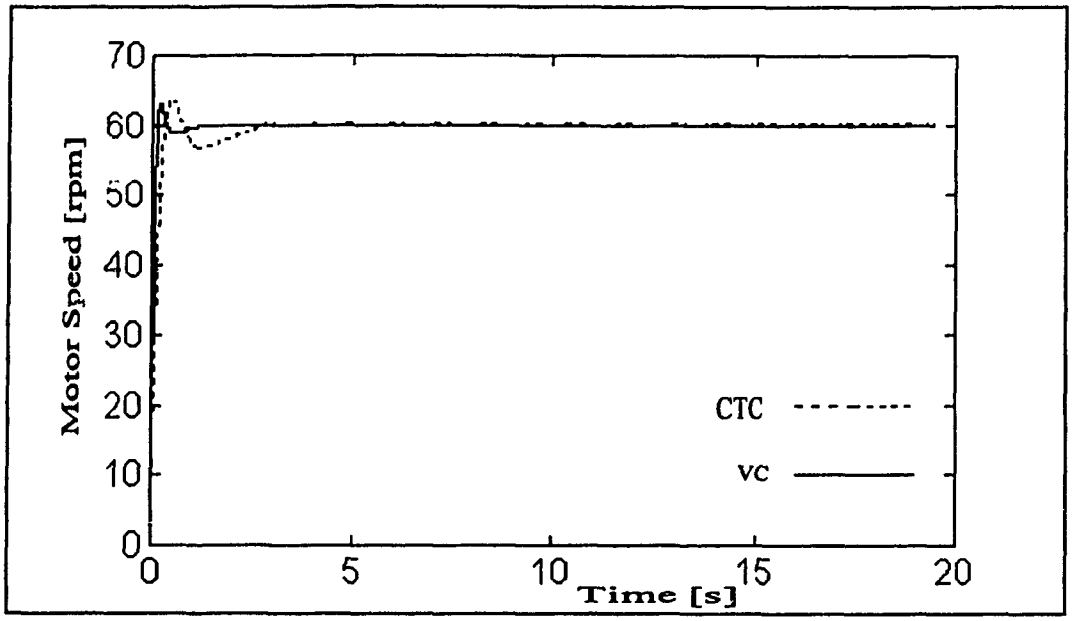

Figure 6.9 Velocity of the Motor in Motor Rig Test, Desired Speed 60 rpm, No Payload Change

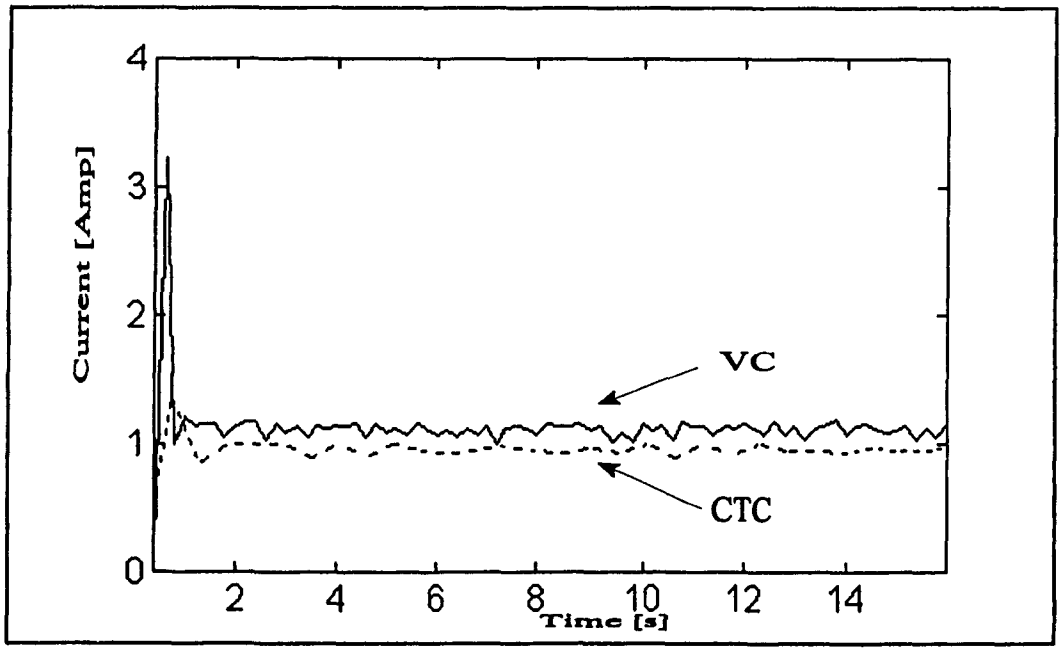

Figure 6.10 Current Drawn by the Motor in Motor Rig Test, Desired Velocity 60 rpm, No Payload Change

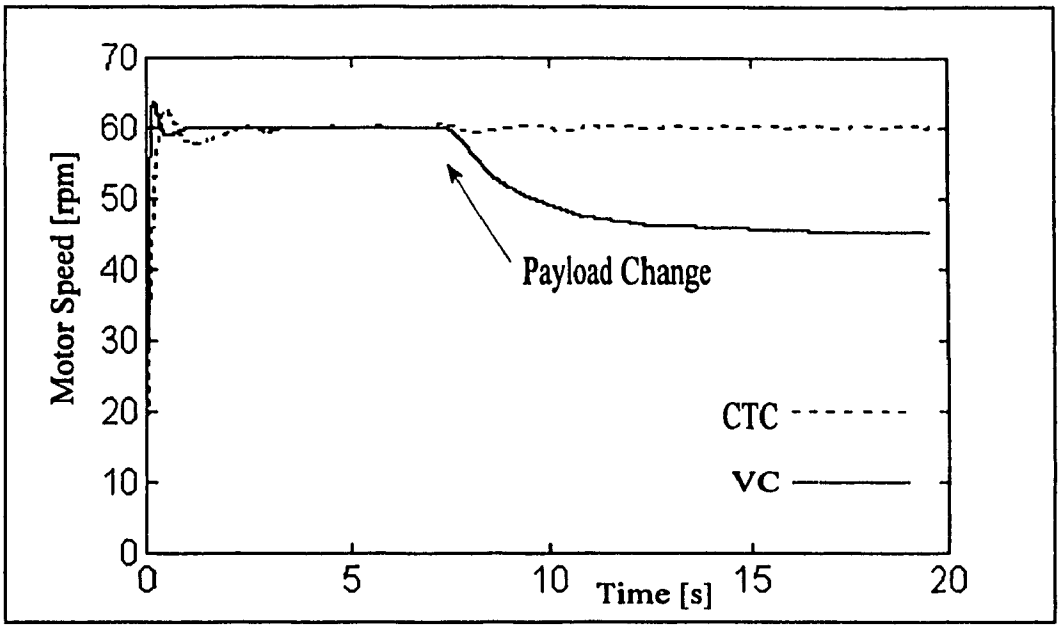

Figure 6.11 Velocity of the Motor in the Motor Rig Test, Desired Velocity 60 rpm, Load Increase 10 kg

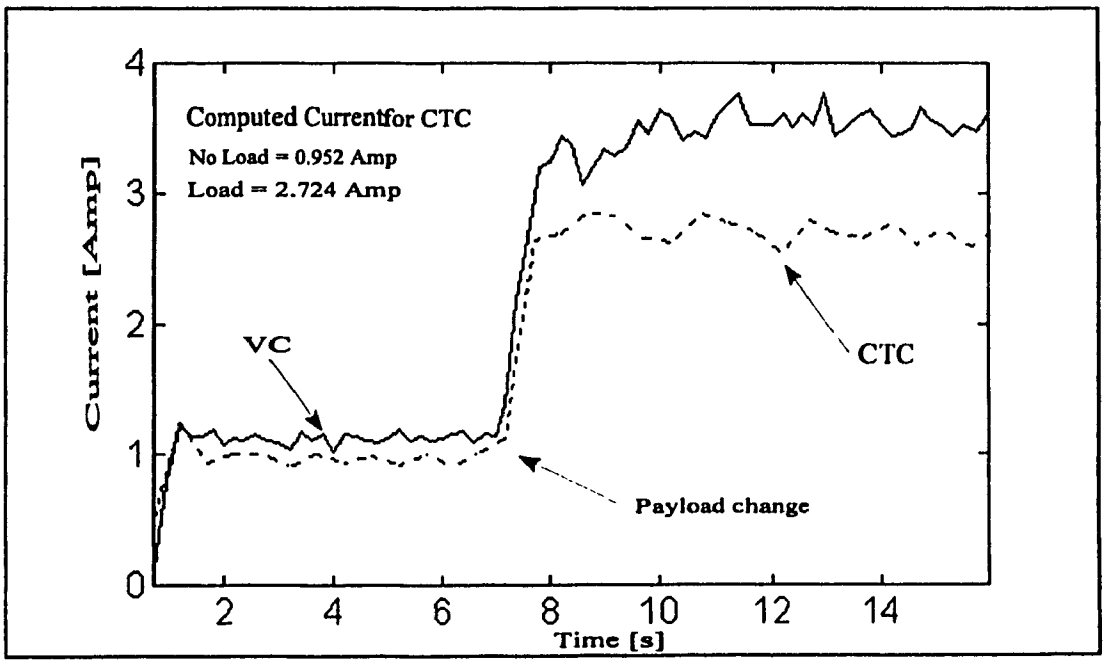

Figure 6.12 Current Drawn by the Motor in Motor Rig Test, Desired Velocity 60 rpm, Payload Increase 10 kg

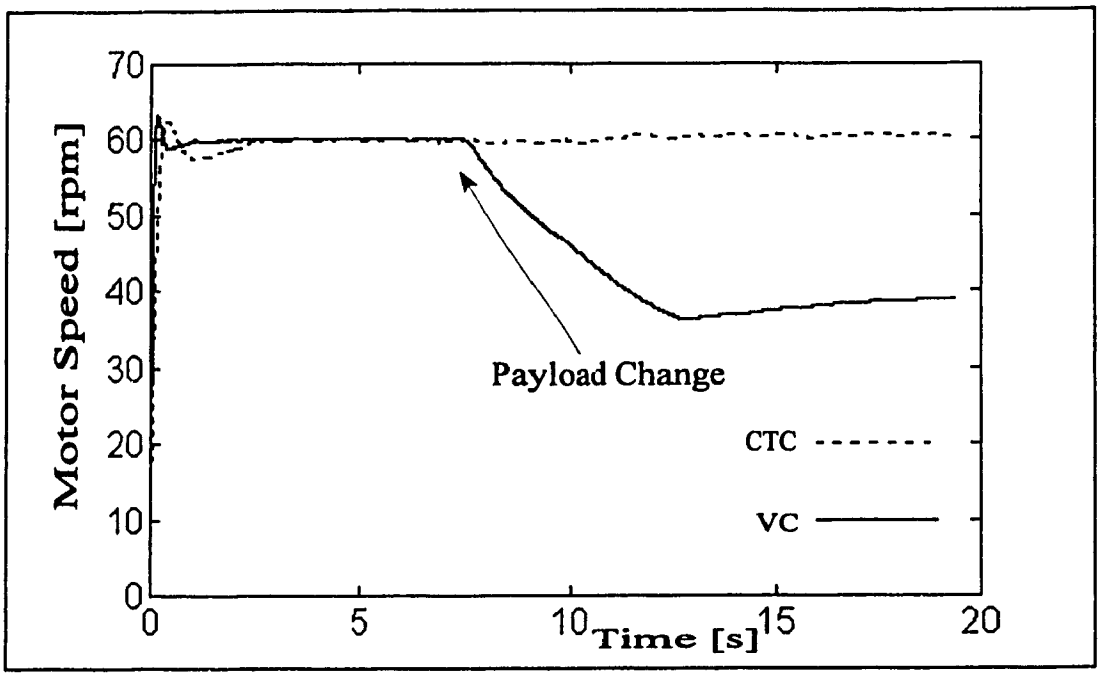

Figure 6.13 Velocity of the Motor in Motor Rig Test, Desired Velocity 60 rpm, Payload Increase 20 kg

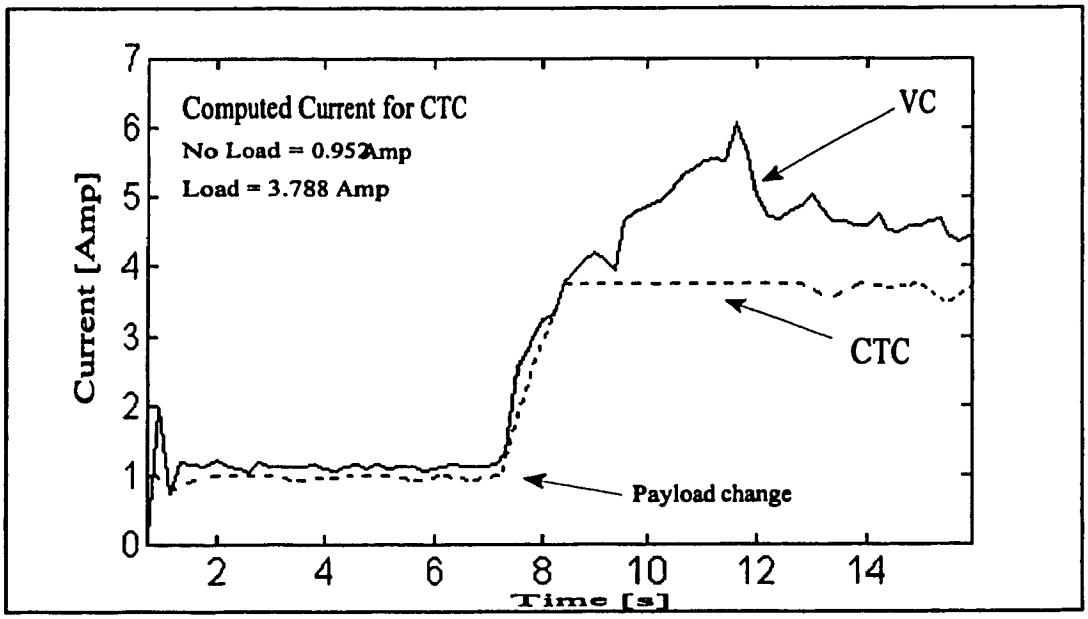

Figure 6.14 Current Drawn by the Motor in Motor Rig Test, Desired Velocity 60 rpm, Payload Increase 20 kg

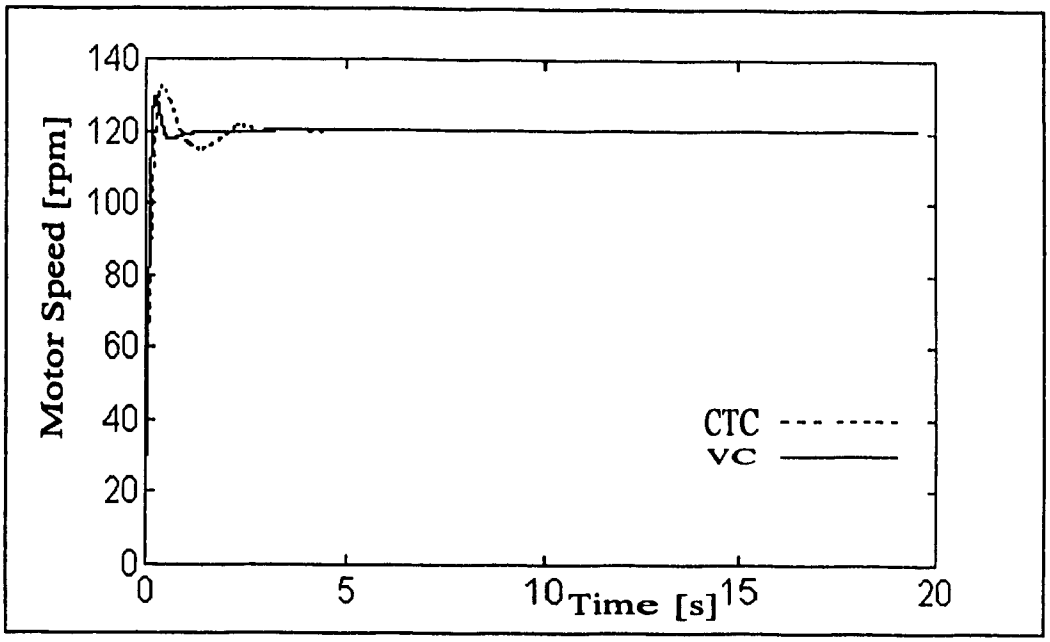

Figure 6.15 Velocity of the Motor in Motor Rig Test, Desired Velocity 120 rpm, No Payload Change

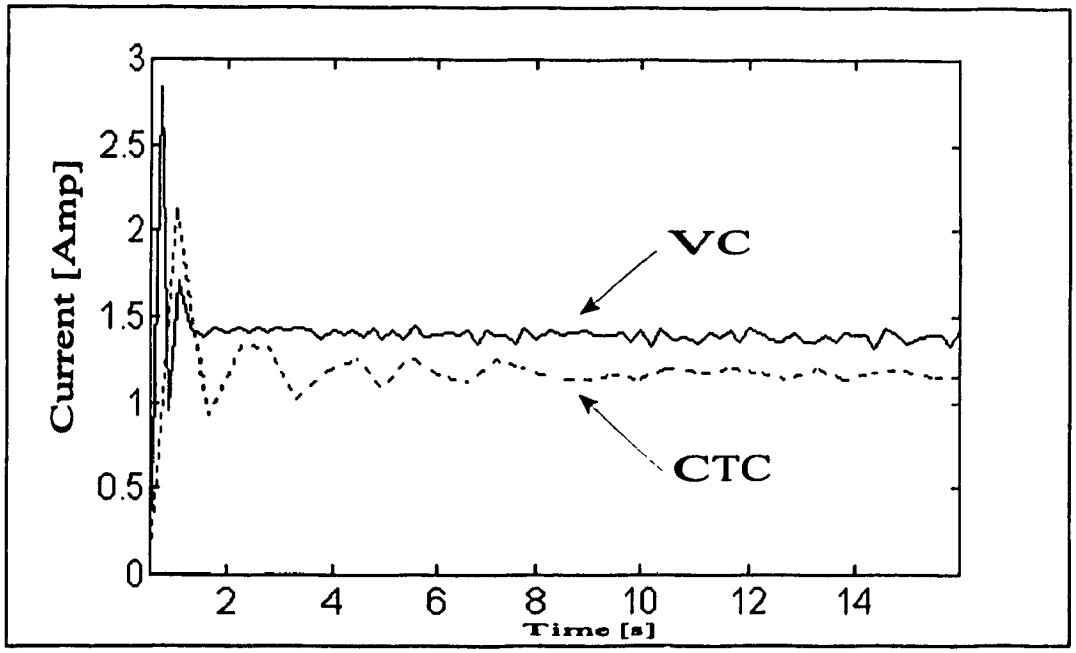

Figure 6.16 Current Drawn by the Motor in Motor Rig Test, Desired Velocity 120 rpm, No Payload Change

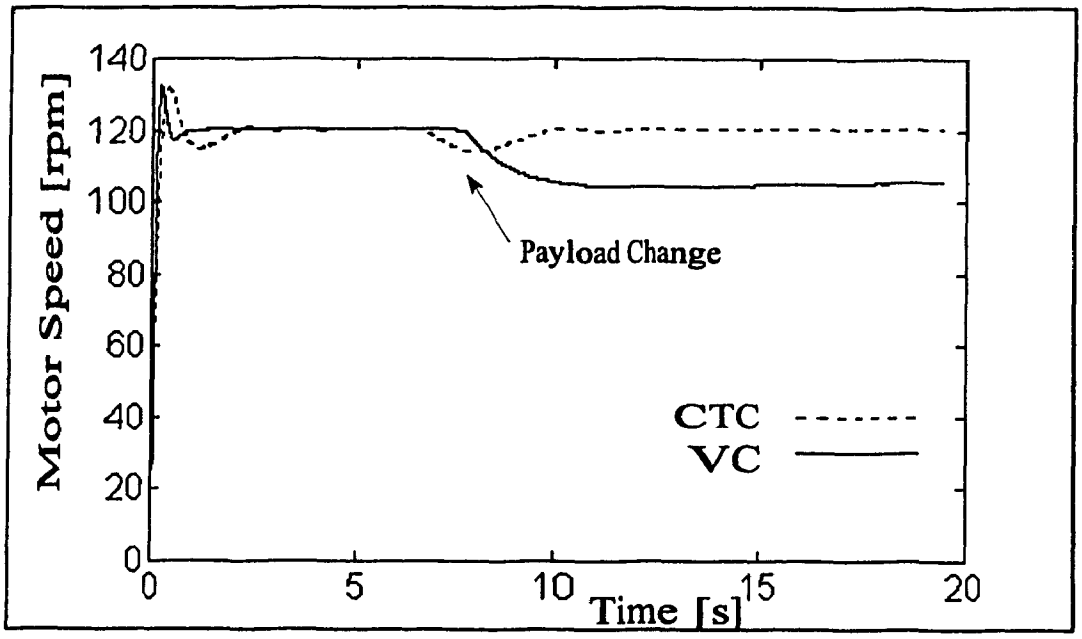

Figure 6.17 Velocity of the Motor in Motor Rig Test, Desired Velocity 120 rpm, Payload Increase 10 Kg

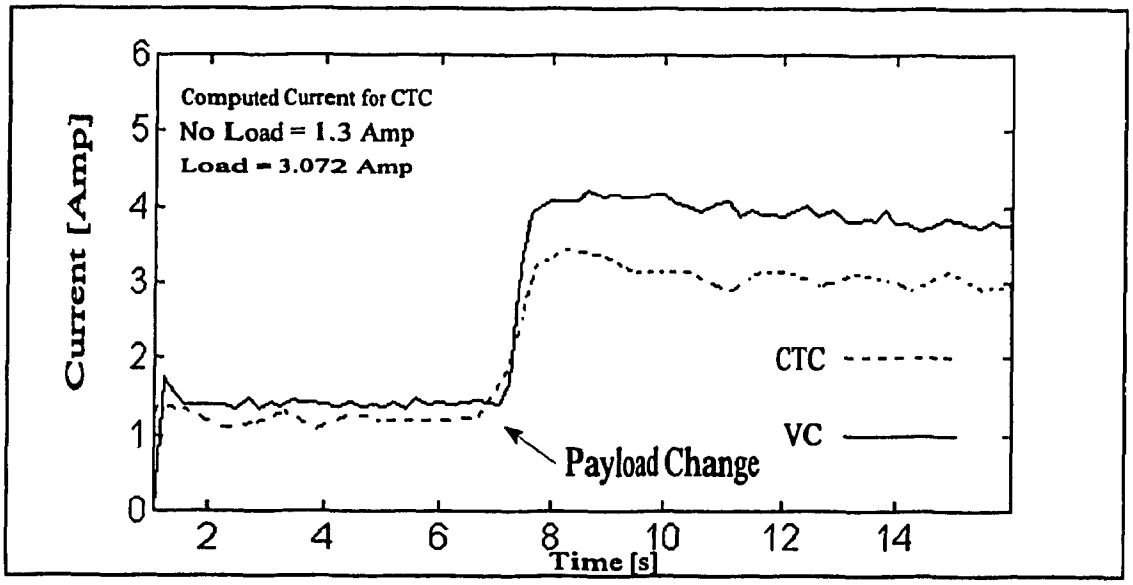

Figure 6.18 Current Drawn by the Motor in Motor Rig Test, Desired Velocity 120 rpm, Payload Increase 10 kg

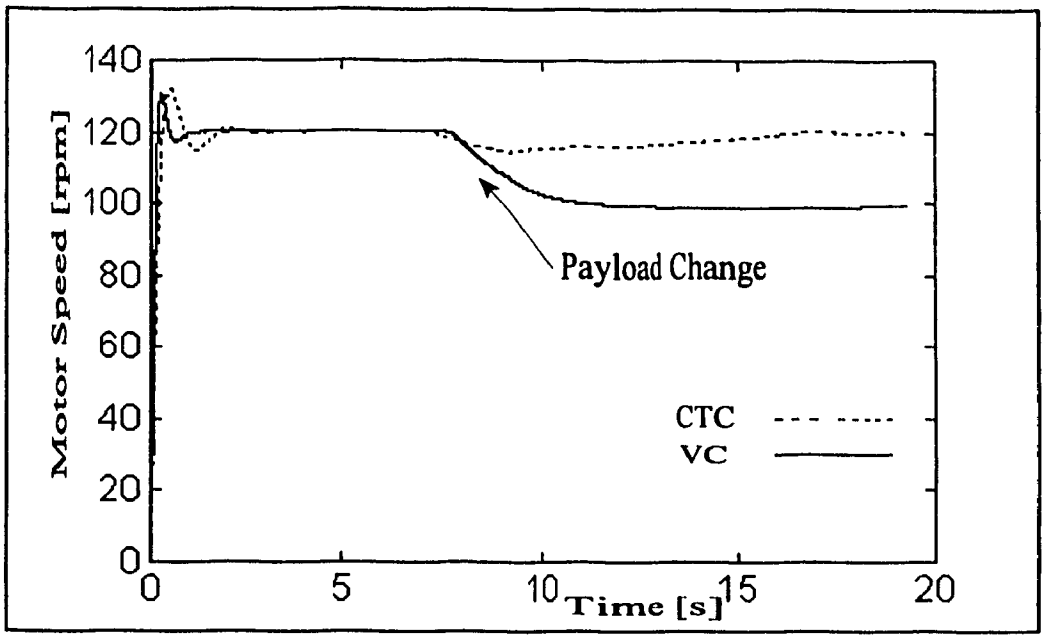

Figure 6.19 Velocity of the Motor in Motor Rig Test, Desired Velocity 120 rpm, Payload Increase 20 kg

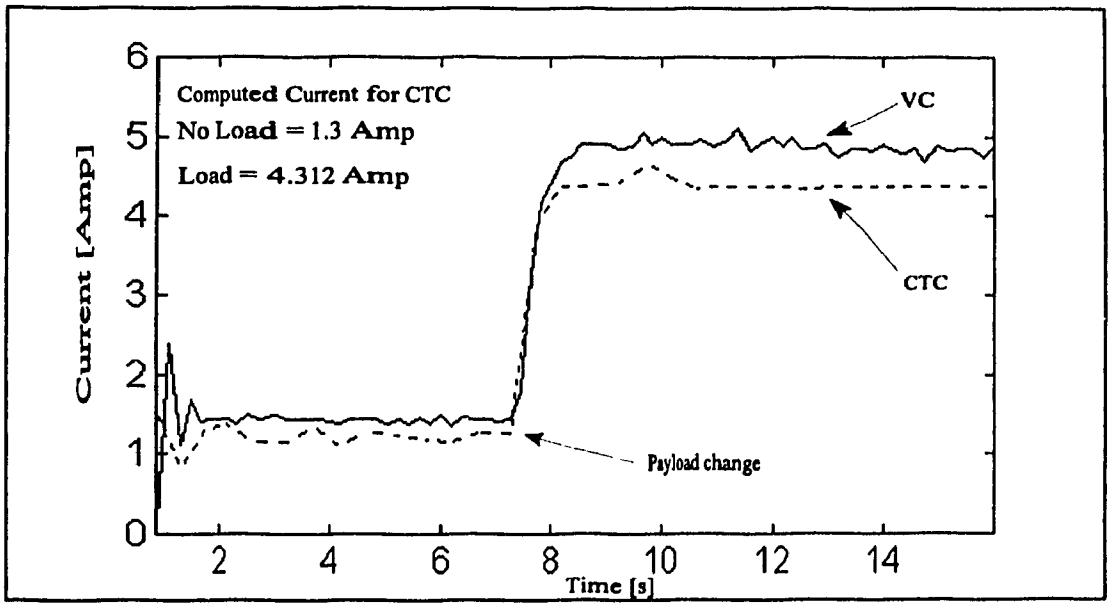

Figure 6.20 Current Drawn by the Motor in Motor Rig Test, Desired Velocity 120 rpm, Payload Increase 20 kg

6.4 Experimental Results Using the CONCIC II AGV

CONCIC II AGV is chosen to perform the tests. A CTC scheme is used to run the vehicle. Further, a Velocity Control (VC) scheme is also used to run the vehicle to compare its performance. The interface card described in Section 6.2.2 is modified and used to control the AGV from a pc.

The layout of the CONCIC II AGV can be found in [1]. Figure 6.21 presents the general layout of the vehicle. The mathematical formulations representing the inverse dynamic model of the vehicle used to form the CTC scheme are presented in Chapter 3.

6.4.1 Control Software

Two separate programs are written and used to run the vehicle under the effect of both CTC and VC schemes. The first program is presented by the flow chart in Figure 6.22. This program is similar in principle and structure to the one presented in Section 6.2.3 for the motor rig test. The program makes use of the inverse dynamic model of the vehicle to calculate the necessary current commands to be sent to the amplifiers. Figure 6.23 presents the flow c. art of the second program to run the vehicle with a conventional VC scheme. This program makes use of the same interface card to communicate with the vehicle components. It uses the DAC and amplifiers models to calculate the commands necessary to control the vehicle.

6.4.2 AGV Tests Results

The AGV is run by both control schemes and is then tested by climbing a ramp. The

ramp has a slope of 3.5 degrees. The velocity of the vehicle is monitored as well as the amplifiers current.

Figures 6.24 to 6.29 present the tests results. Figures 6.24 and 6.25 present the velocity and current drawn by the vehicle motor respectively while moving on a level ground for the sake of comparison with no dynamic changes affecting the vehicle. As can be seen from Figures 6.26 and 6.28, which represent the vehicle velocity while climbing the ramp at different velocities, the VC scheme fails to maintain the desired AGV velocity while climbing the ramp. for a desired velocity of 0.5 m/s, the velocity of the vehicle drops by almost 25% while climbing the ramp for 8 seconds. For a desired velocity of 1 m/s, the velocity of the vehicle does not reach that value on a level ground and drops on the ramp by almost 25% of that value. This is because the same controller gains tuned and used for the case of 0.5 m/s are used in this case also. This indicates clearly that the gains of the PID filter of the control loop need to be changed whenever the desired velocity, or the dynamic parameters are changed. On the other hand, under the CTC scheme, the vehicle attains the desired velocity for all desired speed values and while climbing the ramp, with the same set of gains tuned for running on level ground at a particular speed. Figures 6.27 and 6.29 present the current drawn by the motor when climbing the ramp with a velocity of 0.5 m/s and 1 m/s respectively. As shown by Figures 6.26 and 6.28 the vehicular system experiences a drop in velocity once it meets the ramp. In a period of almost two seconds the CTC scheme brings the system velocity to the desired value while in the case of the Velocity Control scheme the system velocity remains dropping and takes almost the whole test period (8 to 10) seconds to bring the system velocity to a steady value and then start to bring it up

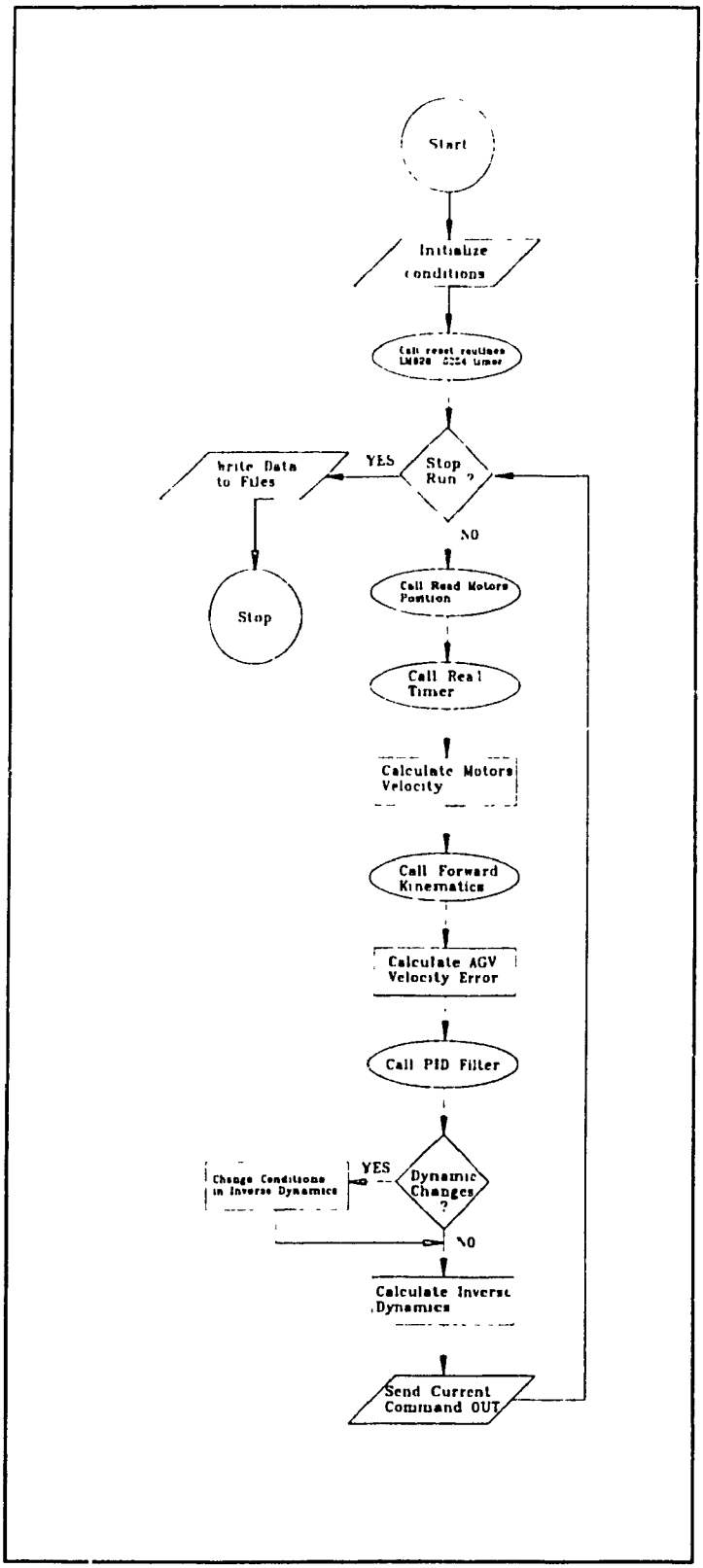

Figure 6.22 Flow Chart of the CTC Scheme Program for the AGV.

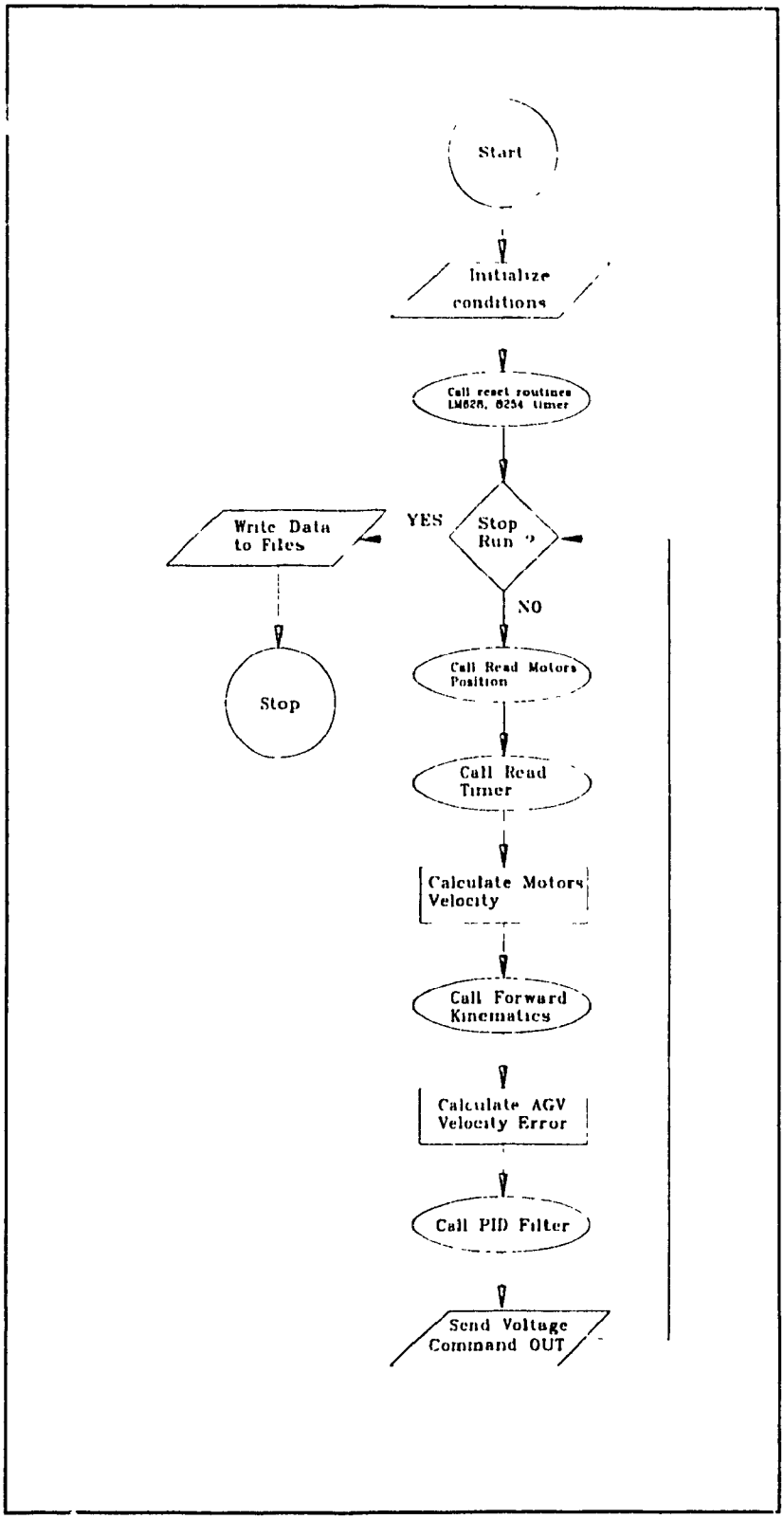

Figure 6.23 Flow Chart of the VC Scheme Program for the AGV

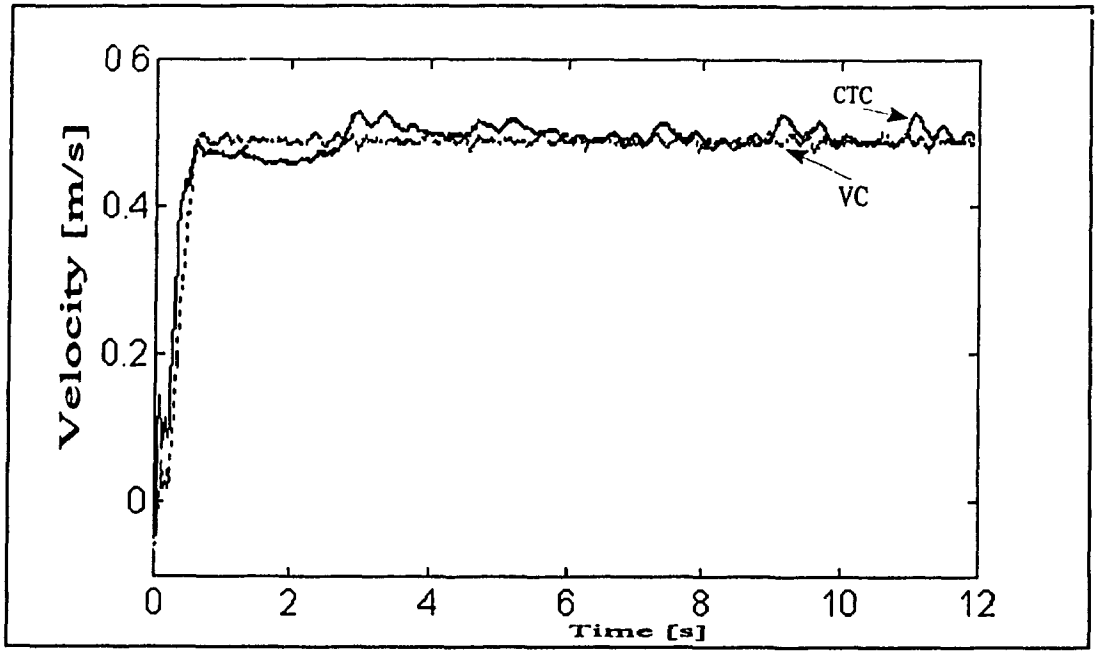

Figure 6.24 AGV Velocity Response On a Flat Surface, Desired Velocity = 0.5 m/s.

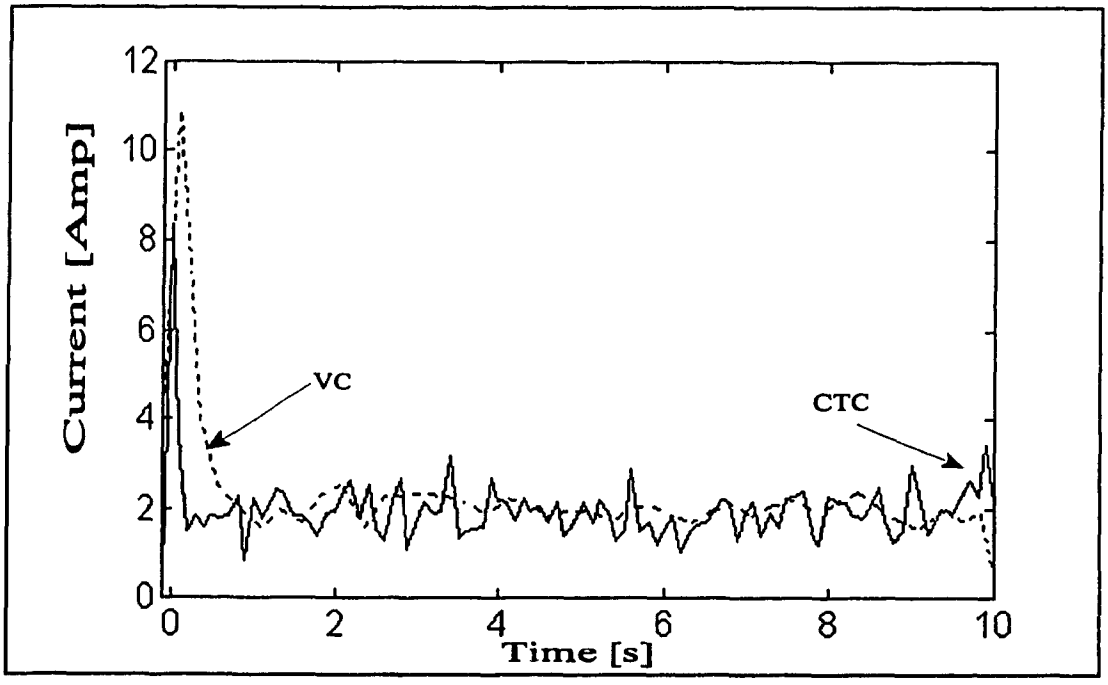

Figure 6.25 Current Drawn by the Motor While the AGV is Moving on a Flat Surface, Desired Velocity = 0.5 m/s.

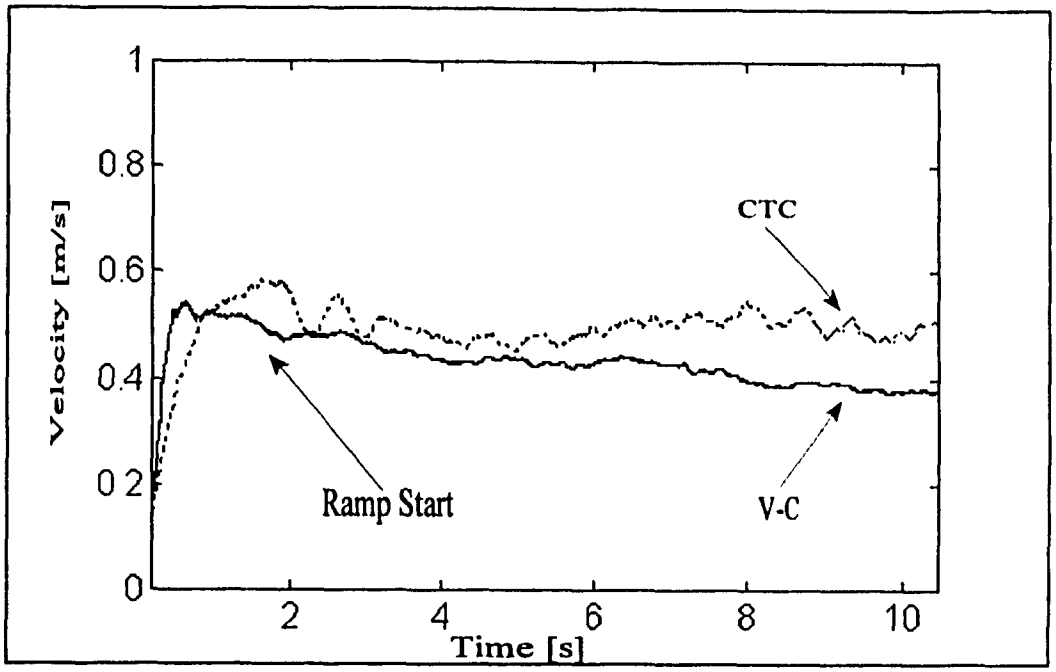

Figure 6.26 AGV Velocity Response While Climbing the Ramp, Desired Velocity = 0.5 m/s

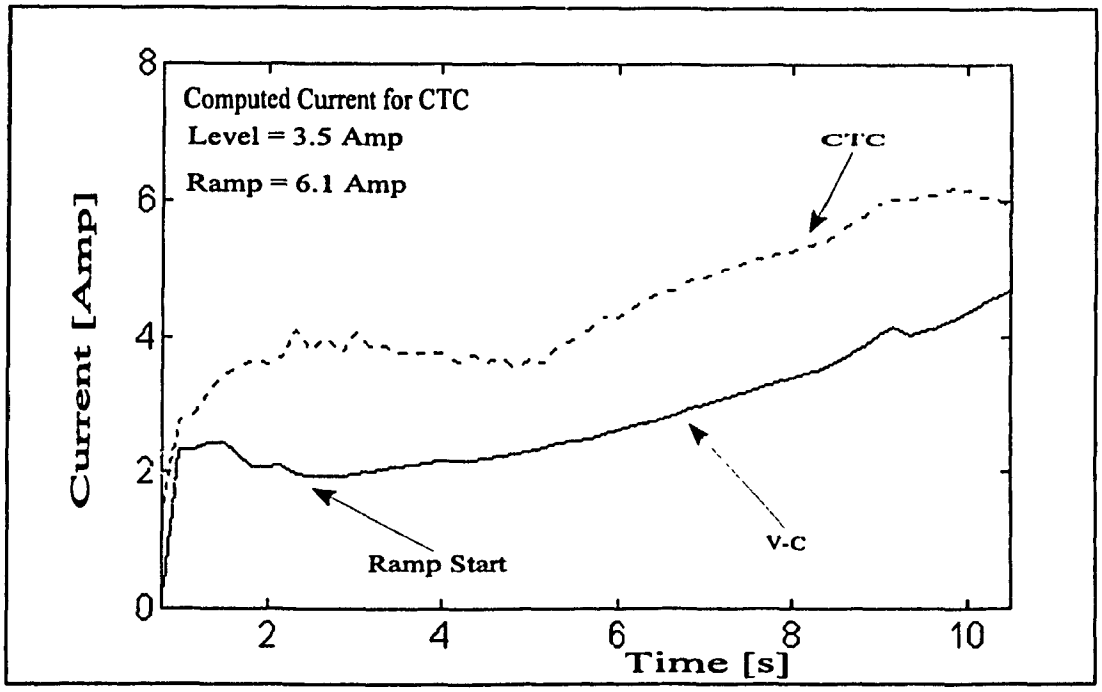

Figure 6.27 Motor Current While the AGV Climbs the Ramp, Desired Velocity = 0.5 m/s

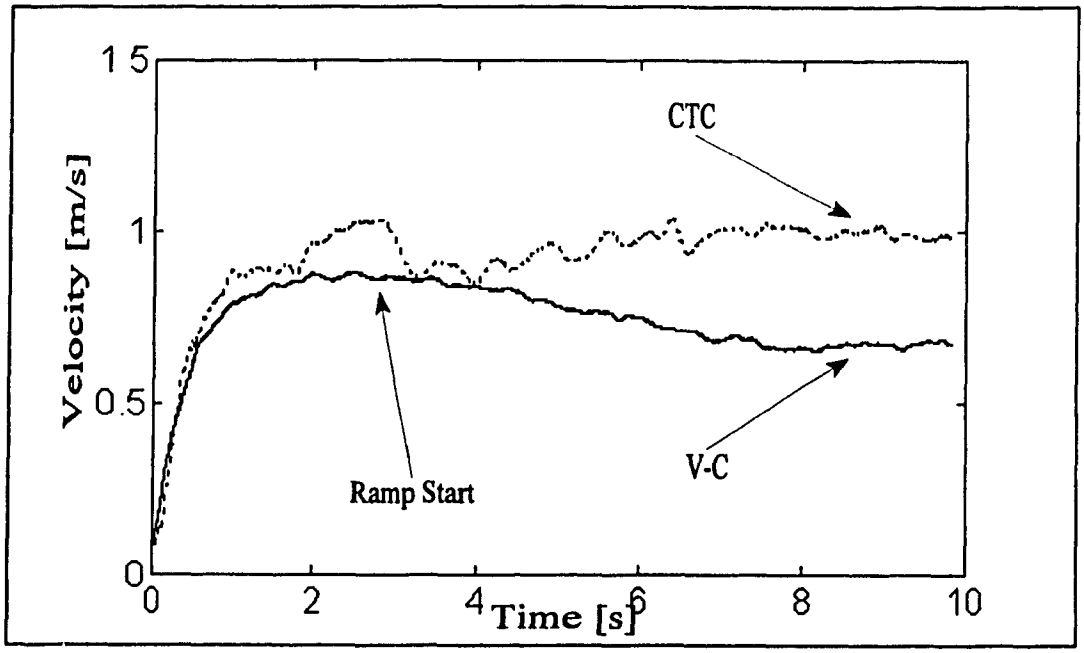

Figure 6.28 AGV Velocity Response While Climbing the Ramp, Desired Velocity = 1 m/s

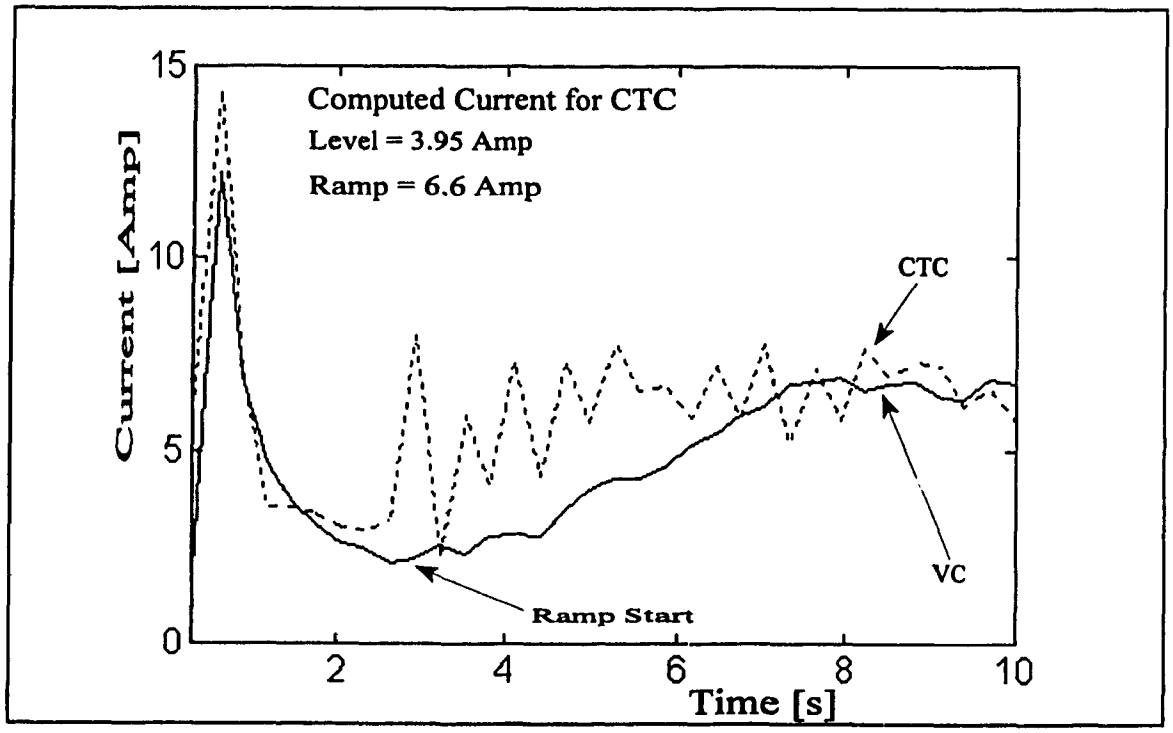

Figure 6.29 Motor Current While the AGV Climbs the Ramp, Desired Velocity = 1 m/s

slowly. It is to be mentioned here that the ramp used to test the vehicle is almost 15 metres in length. At a velocity of 1 m/s the vehicle will start at one end and hit the other end of the ramp in 15 seconds. As per Figures 6.27 and 6.29, higher current values are drawn when the vehicle is controlled by the CTC scheme to overcome the ramp. In the case of the Velocity Control scheme, more time is required for the controller to command the motors to the level of drawing enough current to overcome the ramp. In motor control, adjusting the motor terminal voltage changes the speed while the current demanded by the motor depends on the torque required to overcome the forces and moments acting on the motor. Hence a simple voltage adjustment is not sufficient to meet the power requirements to overcome the effect of changes in the dynamics of the vehicle (forces and moments).

6.5 Summary

Experimental tests have been conducted using two electro-mechanical systems. A motor-test-rig setup was used first to test the response of the system to dynamic changes under a CTC scheme and then a Velocity Control scheme. The dynamic change chosen is the payload on the motor wheel. The second system that is tested is the CONCIC II AGV while climbing a ramp using a CTC scheme and also a Velocity Control scheme. Both are cartesian level control schemes. In the tests carried out the Velocity Control scheme fails to provide the required system performance. On the other hand, the CTC scheme provides the desired performance. The proper current required to run the system at the desired level is calculated by the forward model-based controller and a limit of that value is set by the amplifier. This way the motors are allowed to draw the necessary current and so accelerate or decelerate according to the dynamic changes occurring.

Chapter 7 Conclusions and Recommendations

7.1 Introduction

Modern industry is always seeking means to reduce production costs. One of the means is to automate the production process. Automated Guided vehicles (AGVs) can be used in flexible manufacturing systems (FMS). AGVs help to reduce down-time, provide flexibility, and results in an increase in productivity.

AGVs are considered as part of the robotic systems group. Structure, design and modelling of the robot makes the distinction between AGVs and robot arms. For these systems to operate a control scheme is needed. This is to assure the required performance of the AGV and overcome deviations of that performance. Conventional kinematics-based control schemes perform well in dynamically stable environments as the controller gains are tuned suitably and the acceleration values are chosen appropriately. In a dynamically changing environment these schemes fail to overcome the dynamic changes which reflect on the AGV performance. In such cases the required AGV performance drops or changes considerably. The motivation for this thesis work comes from these factors which indicate the need to develop a dynamic control scheme. A Computed Torque Control (CTC) scheme has been designed and implemented as a feed forward dynamics-based control scheme for the CONCIC II prototype AGV.

7.2 Discussion and Conclusion

The literature has sufficient material on the suitability of CTC scheme for robot arms.

However, the same is not true for AGVs. In this thesis, the suitability of a CTC scheme for the CONCIC II prototype AGV is investigated. The CONCIC II prototype AGV performance is also tested under the effect of a Velocity Control (VC) scheme. This comparative study included simulation and experimental tests. Implementation issues of CTC to electro-mechanical systems are also presented by testing a motor-in-wheel system using a CTC and a VC schemes. Results of this study are presented and discussed in Chapter 6.

Mathematical formulations and analysis of the relevant kinematic and dynamic models of the CONCIC II AGV and the motor testing rig were presented in Chapter 3. Differentially driven vehicles, like the CONCIC II AGV, have advantages such as the invertibility of the kinematic and dynamic models. The inverse dynamic model for this type of vehicles is easy to obtain. Since an inverse is important in developing the CTC scheme loop, differentially driven vehicles such as the CONCIC II AGV are the perfect candidates to apply this control scheme.

Control strategy to apply the CTC scheme and the VC scheme to the CONCIC II AGV in simulation and experimentation is designed and presented in detail in Chapter 4. Control strategy to test the motor rig is also developed and presented in the same chapter. All the controllers operate at the cartesian level. Cartesian level control has advantages over joint level control summarized by: their direct interaction with the task planner in dealing with the task that has to be carried out at the cartesian level and simplicity in planning and development. Cartesian level control major disadvantage is that it is computational demanding. In the literature as mentioned in Chapter 2, task level control is described as a

step towards intelligent control.

The simulation study of the CONCIC II AGV operations under the effect of the CTC scheme and the VC scheme is carried out and presented in Chapter 5. The performance of the vehicle using these control schemes for a variety of changes in the dynamic parameters of the vehicle and the environment has been studied in this thesis. Some of the dynamic changes considered are, (i) payload change on one driving wheel, (ii) payload change on one castor, (iii) load change on all four wheels, (iv) change in coefficient of friction between the wheels and the ground, (v) combinations of the above. It has been demonstrated in this thesis that the CTC scheme provides the required performance compared to the VC scheme with and without a limit on the maximum current available. As an example, for a desired velocity of 1 m/s while the AGV is under the influence of the VC scheme, the drop in velocity is 5 % for a payload increase of 5 times the vehicle mass. If this is combined with an increase in the rolling friction coefficient between the wheels and the ground, the loss or drop becomes 40 % and more. On the other hand, the AGV velocity under the influence of the CTC scheme is kept always at the desired value of 1 m/s for all operating conditions tested above.

Experimental tests have been carried out to investigate the suitability and advantages of implementing the CTC scheme for AGVs. Two steps are followed to achieve this objective. First a motor-in-wheel drive unit is used in a motor-test-rig to conduct experiments. The main purpose of this step is to study the implementation issues and the performance results in the use of CTC scheme for a simple electro-mechanical system. This step is also helpful in realizing the communication requirements between the amplifiers and

the computer and understanding the differences between current and voltage mode settings of the amplifier. The motor performance is different when the amplifier controlling it is set to one of these two modes. This step also assisted in the preparation of the CONCIC II AGV for the second step of experimental work where the CONCIC II AGV is adjusted and tested using the CTC scheme and the VC scheme.

The motor-test-rig setup is tested with each control scheme separately for two different desired velocities and two different payloads increases. Results presented in Chapter 6 show that the VC scheme have failed to maintain the desired velocity of the motor when the payload is increased. As an example, for a desired velocity of 120 rpm and a payload addition of 20 kg to the motor, the drop in velocity is 20 %. On the other hand, using the CTC scheme, the velocity of the motor has been always maintained at the desired value of 120 rpm. In the second experimentation step the CONCIC II AGV is modified and tested for a dynamic change under the influence of the CTC scheme and the VC scheme individually. The dynamic change considered is that of the vehicle going uphill or climbing a ramp. The AGV is tested at two different velocities of 0.5 m/s and 1 m/s. Results are presented in Chapter 6. These results show that the VC scheme fails to maintain the desired velocity of the AGV when climbing the ramp. On the other hand, using the CTC scheme, the AGV velocity maintains the velocity at the desired value while climbing the ramp. For example, when the linear velocity of the vehicle is 0.5 m/s, using the VC scheme the velocity drops by 25% after 8 seconds of operation. In the case of the AGV being controlled by the CTC scheme the velocity is maintained at the desired value.

From these observations, it can be concluded that a kinematic-based control schemes

performs well in dynamically stable environments. In a dynamically changing environment a dynamics-based control scheme like the CTC scheme is necessary to overcome these dynamic changes and attain the AGV performance at the desired level because kinematics based control schemes perform the control task by adjusting the motor terminal voltage to achieve the desired speed. The current demanded by the motor depends on the amount of torque required to overcome the load on the motor. Therefore, voltage adjustment is not sufficient to satisfy the power requirements of the motor which is in turn required to overcome a dynamic change affecting the AGV. Voltage control can change the speed of the motor to achieve the desired vehicular system velocity. In case drastic changes occur, like dynamic parameters of the AGV, this scheme is not sufficient to achieve the control function. This scheme has no control over the current allowed to the motor, and that current is the direct parameter affected by loads on the motor. Henceforth, this scheme has no control on the acceleration of the motor. It is observed also that there is always a need to readjust the system PID filter gains every time a change happens or even when the desired velocity is changed.

Current control allows the calculation of the exact amount of current required by the motor to overcome its own share of the loads on the AGV. Whenever the current is controlled, the acceleration of the vehicle is affected. To bring the vehicular system to the desired velocity the current command to the amplifiers is increased and the motors are allowed to draw the current necessary to achieve an acceleration and hence, reach the desired velocity. If this velocity is to be reduced the current command to the amplifier is reduced and so the motor is allowed to draw less current. Consequently, the motor decelerates until

the desired velocity is reached and maintains that velocity.

Controlling the current using CTC allows the vehicular system to change its acceleration, of which the velocity is a product. The inverse dynamic model of the system works as a predictor in the feed forward path, that makes the controller by far better than the error responsive controllers. Voltage control attempts always to change the velocity of the system, however it fails when the changes are significant (e.g. dynamic) since this controller works in response to error occurrence only.

7.3 Recommendations for Future Work

Dynamic changes were incorporated using the inverse dynamics model for the systems under consideration. This is where this particular model proves to be significant. Future analyses of the dynamic models of the vehicular system should focus on methods to easily and systematically obtain the forward and inverse dynamic model of the AGV under consideration.

Moreover, the dynamic changes applied to the systems under testing were previously stored into the system and that is how it could account for these changes. The future work should focus on means to inform the controller, and in particular the inverse dynamic model, of the occurrence of these changes. A solution would be by installing sensors at points of contact where the vehicle exchanges forces and moments with the environment. This way these changes can be sensed and sent to the controller to adjust the commands accordingly. These sensors can be load cells, strain gages, accelerometers at the suspension points of the AGV, and inclinometers, to name a few. Information consirning whether the vehicle is

going uphill and/or downhill can also be sent back to the controller through the vision system in case that the vision system is capable of analyzing images to this point of accuracy.

The CTC scheme application to an AGV is tested and detailed in this thesis in comparison to a VC scheme. Both schemes work in the cartesian level. More studies and comparisons between the CTC scheme and other controllers like adaptive controllers and / or joint level schemes of control (i.e. low level motion controllers), can contribute more in understanding the physics of this scheme of control and the limitations.

Finally, Adding more safety features to the AGV would allow testing it at higher velocities and for various types of dynamic parameters changes. Moreover, testing this scheme of control on an ATV would allow the tests to be carried out at higher velocities, and hence more significant dynamic changes on the system. The results of carrying out such tests will contribute significantly to the knowledge and understanding of the CTC scheme application to mobile robots in general and to AGVs in particular.

References

1. R. Rajagopalan, "*Guidance Control for Automatic Guided Vehicles Employing Binary Camera Vision*", Ph.D.Thesis, Concordia University, Montreal, Canada, Sept. 1991.

2. R. Rajagopalan, and N. Barakat, "*Model Based Computed Torque Control of a Differentially Driven Automated Vehicle*", Proc. of the 3rd International Conf. on Robotics and Manufacturing, Cancun, Mexico, June 1995.

3. M. G. Mehrabi, "*Path Tracking Control of Automated Vehicles: Theory and Experiment*", Ph.D.Thesis, Dept. of Mechanical Eng., Concordia University, Montreal, Canada, Nov.1993.

4. R. Rajagopalan, and R.M.H. Cheng, "*Computed Torque Control of Autonomous Transit Vehicles*", Proc. of the 27th Int. Symposium on Advanced Transportation Applications (ATT and IVHS), ISATA, Germany, Nov.1994.

5. P. Khosla, "*Choosing a Sampling Rate for Robot Control*", IEEE Proceedings and Transactions, 1987.

6. M. Uebel, I. Minis and K. Cleary, "*Improved Computed Torque Control for Industrial Robots*", Proc. of the 1992 IEEE Int. Conf. on Robotics and Automation, April 1992.

7. T. Tarn, S. Ganguli, A. K. Ramadoria, G. T. Marth, and A. K. Bejczy, "*Experimental Evaluation of the Nonlinear Feedback Robot Controller*", Proceedings of the IEEE, International Conf. on Robotics and Automation, 1991.

8. K. Jankowski and H.Elmaraghy, " *Inverse Dynamics and Feed Forward Controllers*

for High Precision Position/Force Tracking of Flexible Joint Robots", Robotica, Vol. 12, pp. 227-241, 1994.

9. C. Canudas, and R. Roskam, "*Path Following of a 2 DOF Wheeled Mobile Robot under Path and Input Torque Constraints*", Proceedngs of 1991 IEEE Int. Conf. on Robotics and Automation, April 1991.

10. Zhao Fujun, "*The Development of a Model-Based Robotic Controller Using the Transputer Technology*", M.A.Sc. Thesis, Dept. of Mechanical Engineering, Concordia University, Montreal, Quebec, Canada, Nov.1994.

11. M. B. Leahy Jr., "*Industrial Manipulator Control with Feed Forward Dynamic Compensation*", Air force Inst. of Tech., Proc. of the 27th IEEE Con. on Decision and Control, Austin, Texas, Dec. 1988.

12. John J. Craig, "*Introduction to Robotics and Mechanics Control*", Addison Wesley publishing company, 1989.

13. P. F. Muir, and C. P. Neuman, "*Dynamic Modeling of Multibody Robotic Mechanisms*", Proc. of the IEEE Int. Conf. on Robotics and Automation, pp.1546 - 1551, 1988.

14. M. Huang, "*Dynamic Modelling and Simulation of an AGV (CONCIC II)*", M.A.Sc.Thesis. Concordia University, Montreal, Quebec, Canada, 1991

15. R. M. H. Cheng, R. Rajagopalan, "*Binary Camera Vision for the Guidance Control of the Automatic Guided Vehicle*", in "Recent Trends in Mobile Robots", Editor: Prof. Yuan F. Zheng, World Scientific Publishing Co., 1993.

16. Cheng R.M.H., Coubert Y., Surpaceau, Favreau P., and A. Fahim, "*Investigation of*

an Automated Guided Vehicle AGV Driven by Camera Vision", Proc. of the Int. Conf. on Intelligent Autonomous Systems, pp.162-167, Amsterdam, Netherlands, 1986.

17. C. H. An, C. G. Atkinson, J. D. Griffiths and J. M. Hollerbach, *"Experimental Evaluation of Feed Forward and Computed Torque Control"*, IEEE Trans. on Robotics and Automation, Vol. 5, No. 3, June 1989.

18. N. Sarkar, X. Yun, V. Kumar, *"Control of Mechanical systems with Rolling Constraints: Application to Dynamic Control of Mobile Robots"*, The International Journal of Robotics Research. Vol. 13, No. 1, pp. 55-69, Feb. 1994.

19. T. Tarn, S. Ganguli, A. K. Ramadoria, G. T. Marth, and A. K. Bejczy, *"Performance Comparison of Manipulator Servo Schemes"*, Control Systems Magazine, Feb. 1992.

20. R. Simmons, *"Structured Control for Autonomous Robots"*, IEEE Trans. on Robotics and Automation, Vol. 10, No.1, Feb. 1994.

21. Hatwal H. and E. C. Mikulcik, *"An Optimal Control Approach to The Path Tracking Problem for An Automobile"*, Trans. of the CSME. Vol.10, No.4, 1986.

22. H. Seraji, *"Adaptive Control of Robotic Manipulators"*, Jet Propulsion Lab., California Institute of Tech., Pasadina, California, 1986.

23. K. Hashimoto, K. Ohashi, H. Kimura, *"An Implementation of a Parallel Algorithm for Real - Time Model - Based Control on a Network of Microprocessors"*, The Int. Journal of Robotics Research, Vol.9, No.6, Dec. 1990.

24. P. Khosla, *"Some Experimental Results On Model - Based Control Schemes"*, Proceedings of The IEEE, 1988.

25. Sahba M. and D.Mayne, "*Computer - Aided Design of Nonlinear Controllers For Torque Controlled Robot Arms*", IEE Proc., Vol.131, Part D., No. 1, Jan. 1984.

26. T. Hessberg, H. Peng, M. Tomizoka, W. Zhang, E. Kamei, "*An Experimental Study on Lateral Control of a Vehicle*", IEEE Trans. ,1990.

27. Sarkar N., X. Yun, V. Kumar, "*Control of Mechanical systems with Rolling Constraints: Application to Dynamic Control of Mobile Robots*", The Int. Journal of Robotics research, Vol.13, No.1, pp 55-69, Feb. 1994.

28. Sharkey P., "*Transputer Based Real Time Robot Control*", Proc. of the 29th IEEE conf. on Decision and Control. Dec., 1990.

29. An C.H., "*Experimental Evaluation of Feed forward and Computed Torque Control*", IEEE Trans. on Robotics and Automation. Vol.5, No.3, June 1989.

30. M. Leahy Jr., G. Saridis, " *Compensation of Industrial Manipulator Dynamics* ", The International Journal of Robotics Research, Vol.8, No.4, Aug. 1989.

31. M. Uebel, I. Minis, and K. Cleary, "*Improved Computed Torque Control for Industrial Robots*", Proc. of The IEEE Int. Conf. on Robotics and Automation, May, 1992.

32. M. Hashimoto, "*Robot Motion Control Based on Joint Torque Sensing*", Kagoshima Univ., Japan, IEEE Trans. on Robotics and Automation, 1989.

33. Lee S. and J. Williams, "*A Fast Tracking Error Control Method for an Autonomous Mobile Robot*", Robotica, pp. 209-215, Vol.14, 1993.

34. A. M. Bloch and M. Reyhanoglu, "*Control and Stabilization of Nonholonomic Caplygin Dynamic Systems*", Proc. of the 30th Conf. on Decision and Control.

pp.1127-1132, Dec.1991.

35. C. Samson, "*Time-Varying Feed back Stabilization of Car-Like Wheeled Mobile Robots*", The Int. Journal of Robotics Research. Vol.12, No.1, Feb. 1993.

36. S. Jagannathan, F. L. Lewis, and Kai Liu, "*Modeling, Control, and Obstacle avoidance of a Mobile Robot with an Onboard Manipulator*", Proc. of The Int. Symposium on Intelligent Control. Chicago, IL., Aug. 1993.

37. X. Cyril, R.M.H. Cheng, T.S. Sankar, "*Dynamics of Wheeled Mobile Robots (AGVs)*", CIC, Concordia University, Montreal, Quebec, Canada.

38. Thomas P. and W.Forsythe, "*Observations on Control of Automated Guided Vehicles*", Journal of Dynamic Systems, Measurements, and Control.,Vol. 112, Sept. 1990.

39. Lindsay J.F. and V. Ramachandran, "*Modelling and Analysis of Linear Physical Systems*", Weber Systems Inc. 1990.

40. C. H. An, C. G. Atkinson, and J. M. Hollerbach, "*Model-Based Control of A Robot Manipulator*", Massachusettes : The MIT Press, 1988.

41. Muir P.F. and C.P. Neuman, "*Dynamic Modeling of Multibody Robotic Mechanisms*", Proc. of the IEEE Int. Conf. on Robotics and Automation, pp.1546 - 1551, 1988.

42. J.Y. Wong, "*Theory of Ground Vehicles*", New York, John Whily & sons 1978.

43. J.R. Ellis, "*Vehicle Dynamics*", London : Business Books. 1969.

44. Ziegler J.C. and N.B. Nichols, "*Optimum Settings for Automatic Controllers*", Trans. of the ASME. 65, pp. 759-768, 1942.

45. Astrom K.J. and T. Haggland, "*Automatic Tuning of Simple Regulators with Specifications on Phase and Amplitude Margin*", Automatica, 20, No.5, pp.645-651, 1984.

46. LM628/LM629 Precision Motion Controller, National Semiconductor Corporation, Santa Clara, April 1990.

47. R. Rajagopalan, G. Huard, K. Thanjevor, F. Perelli, and N. Barakat, "*Recent Development in Mechatronics Education to Mechanical Engineering Students at Concordia University*", Proc. of the ASME Winter Annual Meeting, Nov. 1995.

48. J. Uffenbeck, "*Microcomputers and Microprocessors*", New Jersy, Prentice Hall Inc. 1991.

49. NI-DAQ Function Reference Manual for PC Compatibles, National Instruments Corporation, Sep. 1994.

50. ESA Series User Manual, Galil Motion Control, Inc., Sunnyvale, CA. Rev (9-90).

51. N. Sinha, "*Control Systems*", New York : The Dryden Press. Saunders college Publishing. 1988.

52. N. Barakat, "*Literature Survey of Computed Torque Control (CTC) Scheme Application to Automatic Guided Vehicles (AGV)*", Internal report No. CIC# 0056, Centre for Industrial Control, Dept. of Mech. Eng., Concordia University, Montreal, Canada, Aug. 1994.

53. Luh J.Y.S., "*On line Computational Scheme for Mechanical Manipulators*", ASME trans. Journal of Dynamical Systems, Measurements and Control. Vol.102, No.2, pp 69-76. 1980.

54. Canudas C. and R. Roskam, "*Path Following of a 2 DOF Wheeled Mobile Robot under Path and Input Torque Constraints*", Proc. of The IEEE Int. Conf. on Robotics and Automation. April 1991.

55. P. Khosla, "*Choosing a Sampling Rate For Robot Control*", IEEE Proceedings and Transactions, 1987.

56. Goldenberg A., "*An Approach to Adaptive Control of Robot Manipulator Using the Computed Torque Technique*", Journal of Dynamic Systems, Measurement and Control., Vol. 111. March, 1989.

58. Sakaki T. and T.Iwakane, "*Impedance Control of a Manipulator Using Torque - Controlled Lightweight Actuators*", IEEE Trans. on Industry Applications. Vol. 28, No.6, Nov.-Dec. 1992.

59. Koshiyama A. and K. Yamafuji, "*Design and Control of an All Direction Steering Type mobile Robot*", The Int. Journal of Robotics Research., Vol.12, No.5, pp. 411 - 419, Oct. 1993.

60. P. Tzenov and R.M.H. Cheng, "*Optimal Vehicle Manoeuvre in Lane Switching*", 2nd International Conf. on Road Vehicle Automation, Bolton, England, Sept. 1995.

APPENDIX - A

Driving Motor Specifications

A.1 Drive Motor Parameters Calculations

From the motor characteristic curves shown in figure A.1, the motor torque constant (K_t) can be calculated as follows :

$$TorqueConstant(K_t) = \frac{2-1}{17.55-9} = \frac{1}{8.55} = 0.116 \quad N.m \ / \ A \qquad (A.1)$$

The relationship between the motor torque and the voltage, and speed are given by :

$$\frac{20.8-21.6}{2-1} = -0.8 \quad Volts/N.m \qquad (A.2)$$

$$\frac{800-1200}{2-1} = -400 \quad rpm/N.m \qquad (A.3)$$

From these relations the velocity constant K_e has been estimated to be :

$$K_e = \frac{-0.8 Volts/N.m}{-400 rpm/N.m} = 0.002 Volts/rpm = 0.00021 Volts/(rad/s) \qquad (A.4)$$

The stall torque (T_s), Static friction torque (T_f) and the no load speed (N_f) of the motor are obtained from figure A.1 as follows :

$$StallTorque = T_s = 4.05 \quad Kg.m^2/s^2 \ (N.m) \tag{A.5}$$

$$FrictionTorque = 0.65 \ N.m \tag{A.6}$$

$$NoLoadSpeed = N_f = 1700 \ rpm = 178.03 \ rad/s \tag{A.7}$$

From the manufacturers specifications, the rotor inertia $J_m = 0.002 \ k_g.m^2$

The mechanical damping coefficient (D_s) and the time constant (τ_m) are evaluated from the mechanical parameters of the motor as follows :

$$Damping = D_s = \frac{T_s}{N_f} = \frac{4.05}{178.03} = 0.0228 \ K_g.m^2/s \tag{A.8}$$

$$MechanicalTimeConstant = \tau_m = \frac{J_m}{D_m} = \frac{0.002}{0.0228} = 0.088s \tag{A.9}$$

Specifications of the driving motor and tire setup are provided in table (A.1).

Table A.1 Characteristics of the driving arrangement.

Specification		**Value**	
Gear ratio of the speed reducer		1 : 9.9	
Maximum Motor Speed		1350	rpm
Maximum Wheel Speed		145	rpm
Maximum Linear Speed		1.2	m/s
Wheel Diameter		150	mm
Tire Width		25	mm
Maximum Axial Load on Tire		200	kg
Tire Material		rubber	
Tire Static Friction Coefficient		0.02	Kg / ton
Rated Voltage	V	24	Volts
Maximum Power Input	P_{in}	198	Watts
Maximum Power Output	P_{out}	130	Watts
Continuous Current	I_c	9.00	Amp
Starting (Peak) Current	I_p	45.5	Amp
Armature Inductance	L_a	4.7	m H
Armature Resistance	R_a	0.602	Ω

APPENDIX - B

Motor - Test - Rig Details

The schematic diagrams following represent the Motor testing rig design blue prints and show in detail the different parts of the rig. It shows also the real dimentions of the rig. This rig was designed and built in CIC for the purpose of testing the driving motor using the different control schemes. Testing a simple system is one way of exploring the reactions and performance before moving to the more complicated dynamic systems. The motor that was tested on this rig is the wheel-in-motor setup described in Appendix-A.

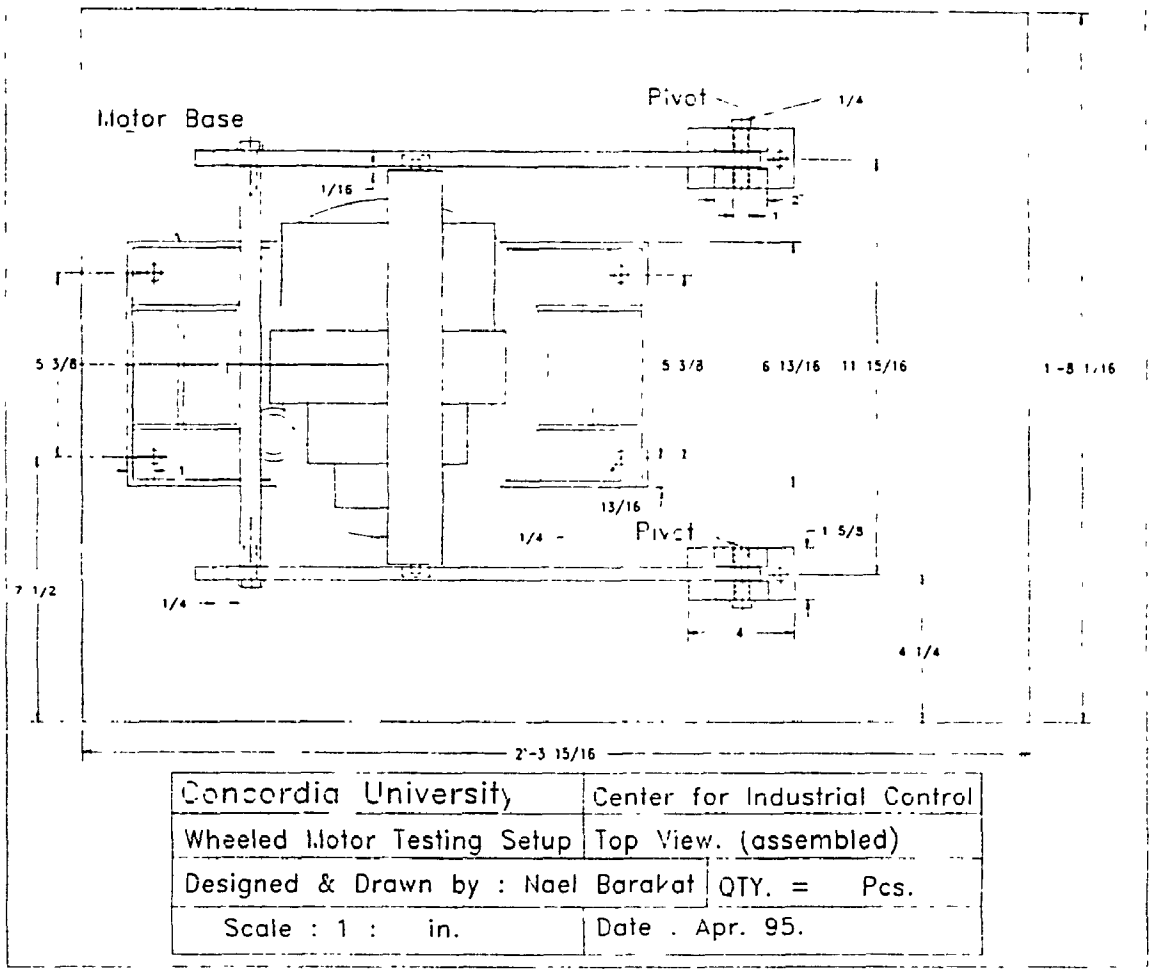

Concordia University	Center for Industrial Control
Wheeled Motor Testing Setup	Top View. (assembled)
Designed & Drawn by : Nael Barakat	QTY. = Pcs.
Scale : 1 : in.	Date . Apr. 95.

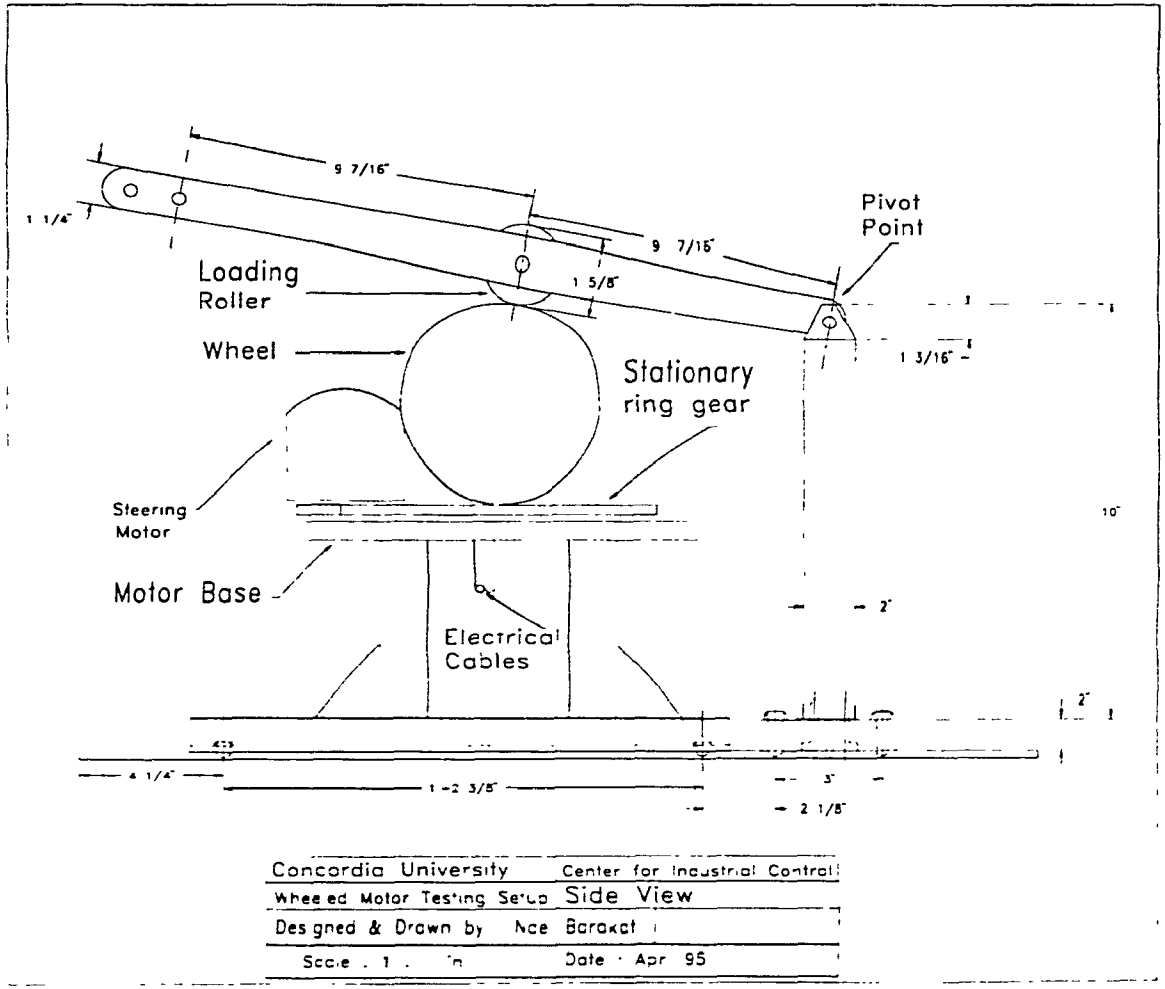

Concordia University	Center for Industrial Control
Wheeled Motor Testing Setup	Side View
Designed & Drawn by Nce Barakat	
Scale . 1 . "n	Date · Apr 95

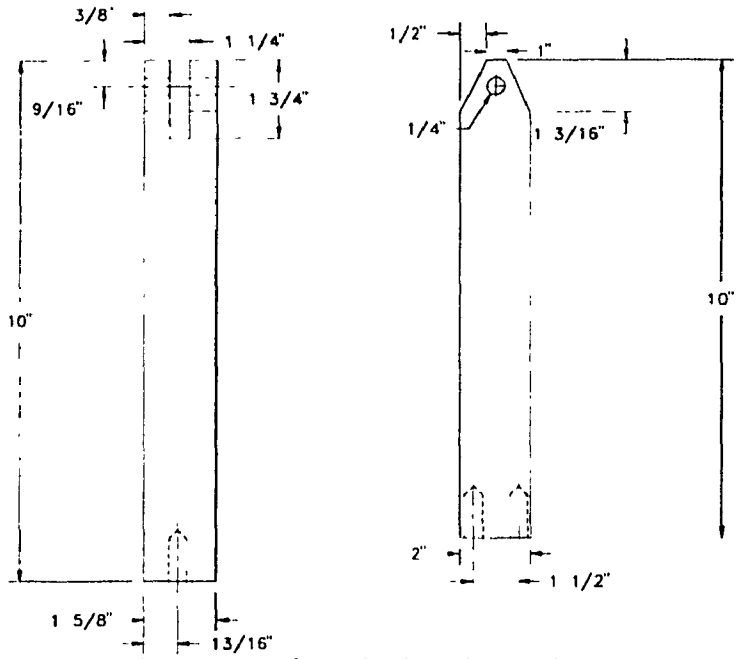

Column front & side view

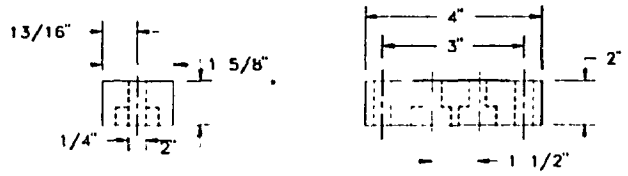

Base front & side views

Concordia University	Center for Industrial Control
Wheeled Motor Testing Setup	Pivot support Columns & base.
Designed & Drawn by : Nael Barakat	Qty.:2 Pcs. of Each
Scale : 1 : in.	Date : Apr. 95.

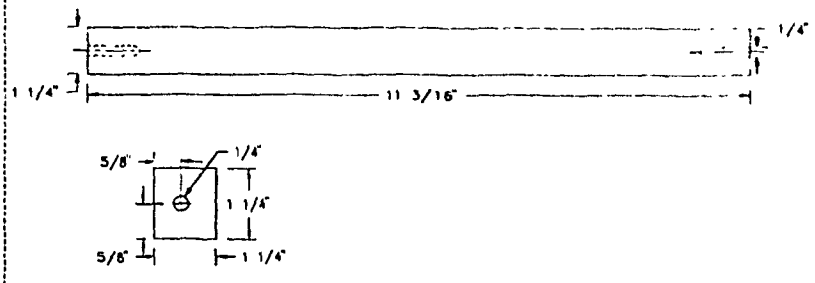

Concordia University	Center for Industrial Control
Wheeled Motor Testing Setup	Links Middle Holder
Designed & Drawn by : Nael Barakat	QTY. = 1 Pcs
Scale : 1 : in.	Date : Apr. 95.

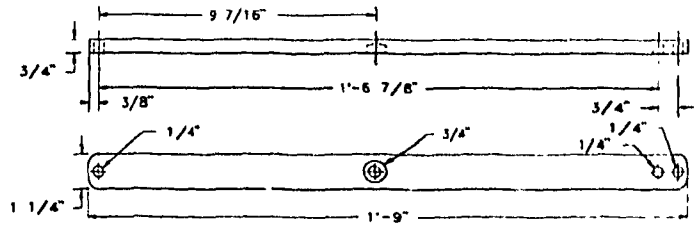

Concordia University	Center for Industrial Control
Wheeled Motor Testing Setup	Side Links
Designed & Drawn by : Nael Barakat	Qty.= 2 Pcs.
Scale : 1 : in.	Date : Apr. 95.